eCAM Evidence-Based Complementary and Alternative Medicine

Bioactives and Traditional Herbal Medicine for the Treatment of Cardiovascular/ Cerebrovascular Diseases 2015

Guest Editors: Joen-Rong Sheu, Pitchairaj Geraldine, and Mao-Hsiung Yen

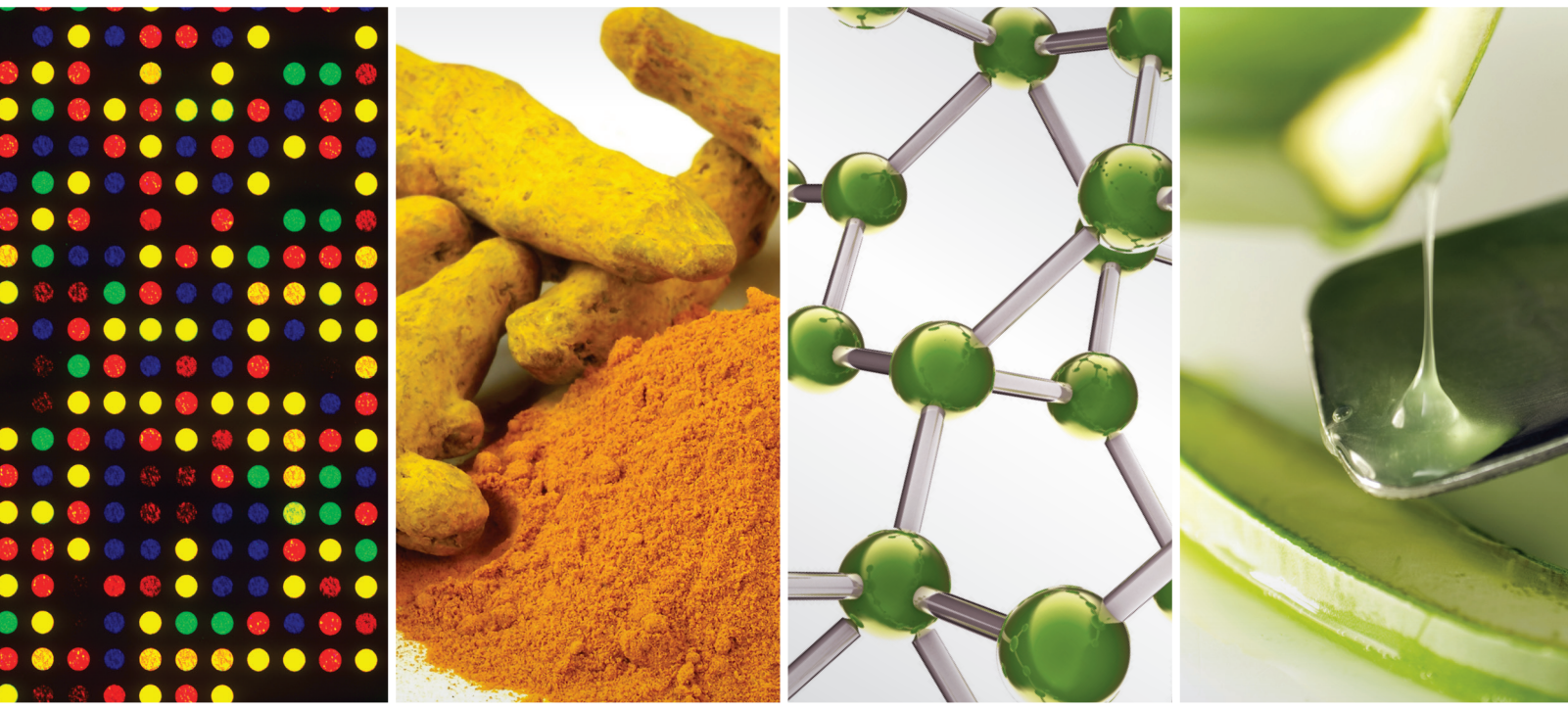

Bioactives and Traditional Herbal Medicine for the Treatment of Cardiovascular/Cerebrovascular Diseases 2015

Evidence-Based Complementary and Alternative Medicine

Bioactives and Traditional Herbal Medicine for the Treatment of Cardiovascular/Cerebrovascular Diseases 2015

Guest Editors: Joen-Rong Sheu, Pitchairaj Geraldine, and Mao-Hsiung Yen

Editorial Board

Contents

Hindawi Publishing Corporation
Evidence-Based Complementary and Alternative Medicine
Volume 2015, Article ID 320545, 2 pages
http://dx.doi.org/10.1155/2015/320545

Editorial

Bioactives and Traditional Herbal Medicine for the Treatment of Cardiovascular/Cerebrovascular Diseases 2015

Joen-Rong Sheu,[1] Pitchairaj Geraldine,[2] and Mao-Hsiung Yen[3]

[1]*Graduate Institute of Medical Sciences, College of Medicine, Taipei Medical University, Taipei 110, Taiwan*
[2]*Department of Animal Science, Bharathidasan University, Tiruchirappalli, Tamil Nadu 620 024, India*
[3]*Department of Pharmacology, National Defense Medical Center, Taipei, Taiwan*

Correspondence should be addressed to Joen-Rong Sheu; sheujr@tmu.edu.tw

Received 8 June 2015; Accepted 8 June 2015

Cardiovascular diseases (CVDs) are still the principal cause of death worldwide. Weakened endothelial function followed by inflammation of the vessel wall hints at atherosclerotic lesion formation that causes myocardial infarction and stroke. Heart failure can arise as consequence of large myocardial infarctions. In its more severe stages, heart failure patients have a life anticipation that is parallel to destructive cancers. Accordingly, the increase in risk factor load by metabolic diseases and age augments the incidence for vascular and cardiac diseases and provides a challenge for developing efficient treatments. There is widespread proof to show that drug treatment of conventional risk factors is effective in reducing cardiovascular events. More effective treatment of CVD with various classes of antihypertensive drugs has been associated with greater benefits, but some recent studies suggest we may be reaching the optimal level of treated blood pressure in some patient groups. Apart from the treatment of cardiovascular risk factors with pharmacological agents and the use of antithrombotic drugs, there is growing awareness of the role of dietary factors and herbal medicines in the prevention of CVD and the possibility of their use in treatment. Investigators from different places of the world like China, Taiwan, Bangladesh, Pakistan, and so forth contributed to this special issue by presenting tremendous papers. These papers deliver an analysis in this field and create innovative contributions concerning the mechanism of action of bioactives and traditional herbal medicine for the treatment of cardiovascular/cerebrovascular diseases.

Some interesting papers in this special issue address the cardioprotective effects of Chinese herbal medicine and natural compounds. For instance, a paper summarized the synergetic cardioprotective potential of herbal combination of four plants, namely, *Terminalia arjuna*, *Cactus grandiflorous*, *Crataegus oxyacantha*, and *Piper nigrum* through curative and preventive mode of treatment analysis and this paper reported preadministration and postadministration of herbal mixture restore the levels of biomarker of cardiotoxicity, which includes cardiac marker enzymes, lipids profile, and antioxidant enzymes. Similarly, another paper in this issue reports the cardioprotective effects of Sundarban honey on cardiac troponin I, cardiac marker enzymes, the lipid profile, lipid peroxidation products, and histoarchitecture of the myocardium against isoproterenol-induced myocardial infarction in Wistar rats. Pinggan Qianyang recipe (PQR), a Chinese medicine recipe, has long been used for calming the liver. It has also been used to treat essential hypertension with satisfactory results. Consistent with this concern, this special issue published a paper that reports PQR exerts its antihypertensive effect through deterioration of the vascular remodeling process. The mechanism might be associated with regulating differentially expressed miRNAs in aorta tissue.

Despite the fact that there are major developments in treating ischemic stroke over the last decade, stroke is still a serious concern for which effective drug therapy is not yet available. In the search for neuroprotective agents from natural sources, a number of plant extracts and several natural products were isolated and reported to provide neuroprotection against ischemic stroke. A few papers in this special issue report the neuroprotective effects of Chinese herbal medicine and natural compounds. For instance, *Antrodia camphorata*

(*A. camphorata*), a fungus generally used in Chinese folk medicine for the treatment of viral hepatitis and cancer, has shown neuroprotective effects in embolic rats. This effect may correlate with the downregulation of the iNOS, HO-1, Bax, and activated caspase-3 and the inhibition of OH° signals. Another study shows alpha-lipoic acid attenuates middle cerebral artery occlusion-induced cerebral ischemia and reperfusion injury via insulin receptor-dependent and PI3K/Akt-dependent inhibition of NADPH oxidase. Moreover, an interesting study in this special issue established the effects of tetramethylpyrazine (TMP) on functional recovery and neuronal dendritic plasticity after experimental stroke. In this study, the authors have shown that enhanced dendritic plasticity contributes to TMP-elicited functional recovery after ischemic stroke.

Hinokitiol is a naturally occurring compound isolated from the wood of *Chamaecyparis taiwanensis*. It is involved in multiple biological activities, including antimicrobial and antitumorigenic activities. Although hinokitiol has been reported to inhibit inflammation, its immunological regulation in lymphocytes remains inadequate. With this context, a well-designed study reported that hinokitiol downregulated cyclin D3, E2F1, and Cdk4 expression and upregulated p21 expression in concanavalin A- (ConA-) stimulated T lymphocytes. It further demonstrated that hinokitiol upregulates p21 expression and attenuates IFN-γ secretion in T lymphocytes from the spleens of mice, thereby arresting the cell cycle in the G0/G1 phase. These authors concluded that hinokitiol provides benefits in treating patients with autoimmune diseases. We expect that this special issue grants inventive awareness to increase the therapeutic value of herbal and/or Chinese medicines for treatment or prevention of cardiovascular and ischemia-reperfusion injury-related disorders.

Joen-Rong Sheu
Pitchairaj Geraldine
Mao-Hsiung Yen

Hindawi Publishing Corporation
Evidence-Based Complementary and Alternative Medicine
Volume 2015, Article ID 394926, 10 pages
http://dx.doi.org/10.1155/2015/394926

Research Article

Effects of Tetramethylpyrazine on Functional Recovery and Neuronal Dendritic Plasticity after Experimental Stroke

Jun-Bin Lin,[1] Chan-Juan Zheng,[1,2] Xuan Zhang,[1] Juan Chen,[3] Wei-Jing Liao,[1] and Qi Wan[3]

[1]*Department of Rehabilitation Medicine, Zhongnan Hospital of Wuhan University, Wuhan 430071, China*
[2]*Department of Rehabilitation Medicine, Center of Brain Department, Hubei Xinhua Hospital, Wuhan 430015, China*
[3]*Department of Physiology, School of Medicine, Wuhan University, Wuhan 430071, China*

Correspondence should be addressed to Wei-Jing Liao; weijingliao@sina.com and Qi Wan; qwan@whu.edu.cn

Received 28 September 2014; Revised 22 December 2014; Accepted 26 December 2014

Academic Editor: Joen-Rong Sheu

The 2,3,5,6-tetramethylpyrazine (TMP) has been widely used in the treatment of ischemic stroke by Chinese doctors. Here, we report the effects of TMP on functional recovery and dendritic plasticity after ischemic stroke. A classical model of middle cerebral artery occlusion (MCAO) was established in this study. The rats were assigned into 3 groups: sham group (sham operated rats treated with saline), model group (MCAO rats treated with saline) and TMP group (MCAO rats treated with 20 mg/kg/d TMP). The neurological function test of animals was evaluated using the modified neurological severity score (mNSS) at 3 d, 7 d, and 14 d after MCAO. Animals were euthanized for immunohistochemical labeling to measure MAP-2 levels in the peri-infarct area. Golgi-Cox staining was performed to test effect of TMP on dendritic plasticity at 14 d after MCAO. TMP significantly improved neurological function at 7 d and 14 d after ischemia, increased MAP-2 level at 14 d after ischemia, and enhanced spine density of basilar dendrites. TMP failed to affect the spine density of apical dendrites and the total dendritic length. Data analyses indicate that there was significant negative correlation between mNSS and plasticity measured at 14 d after MCAO. Thus, enhanced dendritic plasticity contributes to TMP-elicited functional recovery after ischemic stroke.

1. Introduction

Stroke is the leading cause of long-term disability in the western world, which is a severe disease characterized by its high morbidity, mortality, disability, and recurrence [1]. It has become a heavy burden to patients, families, and societies due to the excessive costs of long hospitalizations, nursing care, and rehabilitation [2]. Ischemic stroke accounts for approximately 87% of stroke [3].

2,3,5,6-Tetramethylpyrazine (TMP, Figure 1) is an active ingredient extracted from a traditional Chinese herbal medicine *Ligusticum chuanxiong Hort*. and has been widely used in ischemic stroke by Chinese doctors [4]. TMP exerts pharmacological effects in multiple ways with multiple targets. TMP is reported to protect ischemia reperfusion injury of heart, brain, and kidney via reducing oxidative stress, attenuating Ca^{2+} overload, inhibiting apoptosis, inhibiting inflammatory reaction, and so forth [5–7]. Besides the above-mentioned effects, it is also demonstrated that TMP can inhibit platelet aggregation, depress blood viscosity, and ameliorate microcirculation [8], which could be another important mechanism to treat cardiovascular and cerebrovascular diseases. Recently, it has been found that TMP could protect hepatic fibrosis by modulating multiple signal pathways [9–11]. Furthermore, TMP had a significant therapeutic effect on diabetic nephropathy [12], which could be mediated by downregulated expression of vascular endothelial growth factor in the kidney and reduction of lipoperoxidation [13, 14]. Additionally, TMP has been reported to have beneficial effects in various types of cancer [15–17]. Specific to ischemic stroke, according to previous studies, TMP can play a protective role through the following mechanisms: antiexcitotoxicity [18], inhibiting inflammatory reaction [19], anti-apoptosis [20], antioxidant activity [21], suppression of calcium [21],

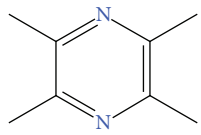

Figure 1: The structure of TMP.

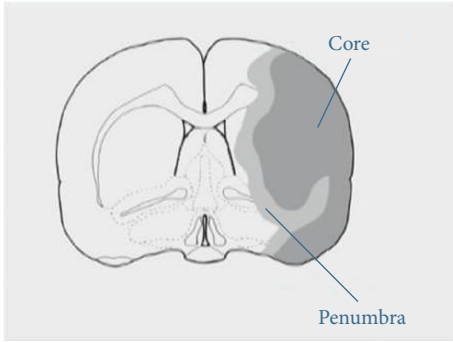

Figure 2: The schematic diagram of ischemic penumbra (IP).

thrombolytic effect [22], enhancing neurogenesis, and cell differentiation [23].

There are at least three processes during recovery after stroke: resolution of acute tissue damage, behavioral compensation, and plasticity [24]. Based on the information above, most studies focus on TMP's inhibitory roles in postischemic cascade process in acute phase. However, the effects and mechanisms of TMP on neuroplasticity are still not clear up to now. The plasticity of dendrites is an important component of plasticity [25, 26]. When challenged by ischemic stroke, dendrites in ischemic penumbra (IP) show a series of changes with morphological modifications [27], which suggest that facilitating or optimizing the plasticity of dendrites is likely to be a promising therapeutic target. Indeed, dendritic changes after ischemic injury could be induced by drugs and rehabilitative trainings.

Ischemic penumbra (IP) was first proposed by Astrup et al. in 1981 [28]. It was defined as a region of reduced cerebral blood flow (CBF) with absent, spontaneous, or induced electrical potentials that still maintained ionic homeostasis and transmembrane electrical potentials. It has the potential for functional recovery if local blood flow can be reestablished within a limited period and is a key target for the treatment of acute stroke [29]. It is located in the peri-infarct area and Figure 2 shows schematic diagram of ischemic core and IP.

In this study, we tested the effects of TMP on functional recovery and dendritic plasticity after ischemic stroke. A classical focal cerebral ischemia reperfusion model was induced by middle cerebral artery occlusion (MCAO) in the rat and we conducted a TTC staining. Firstly, we measured the neurological function performance using the modified neurological severity score (mNSS). In order to measure the dendritic plasticity, after behavioral testing, immunohistochemistry was employed to evaluate the levels of microtubule associated protein-2 (MAP-2, marker of neuronal dendrites) and a modified Golgi-Cox staining was conducted to examine dendritic morphologic plasticity. Finally, correlations analyses between functional outcome and plasticity were performed.

2. Materials and Methods

2.1. Animals. A total of 78 eight-week-old male Sprague Dawley (SD) rats weighing 200–250 g (purchased from Experimental Animal Center of Wuhan University, Wuhan, Hubei, China) were used for this experiment. The rats were acclimated for 3 or more days before the start of any experiments. They were housed in a controlled environment (4 animals per cages, 55 ± 5% relative humidity, 22°C, 12 : 12 h light/dark cycle) and provided with free access to food and water. All experimental procedures involving animals were approved by the Animal Care and Use Committee of Wuhan University Medical School. We made all efforts to minimize the number of animals used and their suffering.

2.2. Model. MCAO was induced using the modified intraluminal filament technique [30]. Briefly, rats were anesthetized with 10% chloral hydrate (400 mg/kg) intraperitoneally and, after a median incision of the neck skin, the right carotid artery (CCA), external carotid artery (ECA), and internal carotid artery (ICA) were carefully isolated. The right MCA was occluded with a monofilament nylon filament (Beijing Cinontech Biotech Co., Ltd., Beijing, China) by inserting it through the right CCA and gently advancing into the ICA up to a point approximately 17 mm distal to the bifurcation of the carotid artery. The filament was fixed in place and the animal was allowed to recover from anesthesia. After 2 h, the filament was withdrawn to permit reperfusion. In sham group, all surgical procedures were the same as above without inserting a nylon filament. A heating pad was used to maintain a rectal temperature of 37.0 ± 0.5°C during the surgical procedure.

6 MCAO rats were anesthetized with an overdose of chloral hydrate and sacrificed by decapitation at 3 d after MCAO. The brains were quickly removed and chilled at −20°C for 10 min. 2 mm coronal slices were cut for each brain and immersed in a PBS solution (pH = 7.4) containing 2% triphenyl tetrazolium chloride (TTC) (Sigma, St. Louis, MO, USA) at 37°C in the dark for 30 min. The stained sections were then fixed in 4% paraformaldehyde for 1 h. All stained sections were scanned and the infarct volumes were analyzed by Image Pro Plus 6.0 (Media Cybernetics Inc., Bethesda, MD, USA). To eliminate the effect of brain edema and differential shrinkage resulting from tissue processing, the percentage of infarct volume was calculated as reported previously [31].

2.3. Grouping and Administration. In this study, the animals were randomly assigned into 3 groups: sham group (sham operated rats treated with saline), model group (MCAO rats treated with saline), and TMP group (MCAO rats treated with 20 mg/kg/d TMP (Aladdin Chemistry Co., Ltd., Shanghai, China)). The first administration was conducted immediately after reperfusion. All injections were conducted through

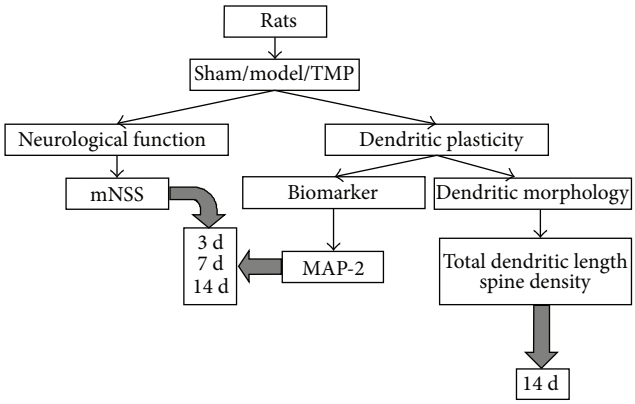

Figure 3: A simple flow-chart of experimental design.

intraperitoneal injection daily and in the volume of 5 mL/kg until the day before they were sacrificed. After neurological function test, 54 rats were sacrificed at 3 d, 7 d, and 14 d after MCAO for immunohistochemistry ($n = 6$ in each group at each time point) and 18 rats for Golgi-Cox staining ($n = 6$ in each group) at 14 d after MCAO. A brief flow diagram is shown in Figure 3.

2.4. Neurological Function Test. Modified neurological severity score (mNSS) test [32] was measured at 3 d, 7 d, and 14 d after MCAO by an observer blinded to experimental groups. The mNSS is a composite of motor, sensory, reflex, and balance tests and is graded on a scale of 0–18 (normal score 0, maximal deficit score 18). In the severity scores of injury, 1 score point is awarded for the inability to perform the test or for the lack of a tested reflex; thus, the higher the score is, the more severe the injury is. It is classified into three levels: 13 to 18 are graded as severe injury, 7 to 12 as moderate injury, and 1 to 6 as mild injury.

2.5. Immunohistochemistry. At 3 d, 7 d, and 14 d after MCAO, rats in each group at each time point ($n = 6$) were anesthetized with an overdose of chloral hydrate and transcardially perfused with 150 mL of 0.9% saline followed by 150 mL of 4% paraformaldehyde. The brains were removed and postfixed in 4% paraformaldehyde overnight. Thereafter, paraffin embedded blocks (bregma: −2 to +2 mm) were obtained and sliced into sections of 6 μm and mounted onto the polylysine-coated slides. Streptavidin-peroxidase (S-P) method [33] was adopted for immunostaining: (1) tissue sections were deparaffinized with xylene and rehydrated in ethanol; (2) they were incubated in endogenous peroxidase blocking solution (Maixin Technology Co., Ltd., Fuzhou, Fujian, China) for 10 min at room temperature; (3) after being incubated with normal rabbit serum (Maixin Technology Co., Ltd., Fuzhou, Fujian, China), the brain sections were incubated overnight with rabbit anti-MAP-2 antibody (1 : 200, Boster, Wuhan, Hubei, China) at 4°C; (4) the sections were incubated with biotin-conjugated second antibody (Maixin Technology Co., Ltd., Fuzhou, Fujian, China) for 15 min; (5) they were incubated with HRP-Streptavidin-Peroxidase (Maixin Technology Co., Ltd., Fuzhou, Fujian, China) for 15 min; (6) the sections were stained with 3, 3′-diaminobenzidine and H_2O_2, washed with tap water, and counterstained with hematoxylin. The sections were rinsed with phosphate-buffered saline (PBS, pH = 7.4) 3 times for 3 min between every procedure of staining. Finally, the sections were dehydrated and coverslipped. To investigate the specificity of the reactions, negative controls were established by replacing the primary antibody with PBS and normal rabbit serum.

For quantitative analysis, three randomly selected sections of each subject and five visual fields (400x) from each section in peri-infarct area were randomly captured under a microscope using a digital camera. Integrated optical density (IOD) was measured using Image Pro Plus 6.0 (Media Cybernetics Inc., Bethesda, MD, USA) for analysis. The analysis procedure was conducted by an investigator in a blind fashion.

2.6. Golgi-Cox Staining Procedure. At 14 d after MCAO, rats in each group ($n = 6$) were injected intraperitoneally with a lethal dose of chloral hydrate to induce anesthesia. Remove the brains as soon as possible without perfusion and rinse tissue in double distilled water for 2-3 seconds to remove blood from the surface. Hito Golgi-Cox OptimStain Kit (Hitobiotec Inc., Wilmington, DE, USA) was applied for tissue preparation and staining procedure. The whole Golgi-Cox staining procedure was conducted in strict accordance with the manufacturer's user manual and material safety data sheet. A series of 100 μm thick coronal sections was sliced from the caudal forelimb region of the motor cortex (approximately from bregma to +2.0 mm from bregma) [34] using a microtome (Leica CM1950 cryostat; Leica Biosystems GmbH, Wetzlar, Germany).

2.7. Selection Criteria for Pyramidal Cells. To be included for analysis, neurons should be selected according to specific criteria [35]: (1) the dendritic trees had to be well impregnated to facilitate accurate observation and analysis; (2) the cell bodies and dendrites had to be in full view and not obscured by other blood vessels, astrocytes, or clustering of dendrites from other pyramidal cells; (3) they also had to appear intact and visible in the plane of section.

2.8. Sholl Analysis. To acquire images for analyzing, layer V pyramidal cells within peri-infarct area were traced at 200x magnification. Pyramidal neurons were readily identified by their characteristic triangular soma-shape, apical dendrites extending toward the pial surface, and numerous dendritic spines [36]. In order to measure the length of dendrites, Sholl analysis [37] was conducted using a Sholl analysis plug-in (available at http://fiji.sc/Sholl_Analysis) for Image J software (National Institutes of Health, Bethesda, MD, USA). The number of intersections of dendrites with a series of concentric rings at 20 μm intervals from the centre of the cell body was counted for each cell. A reflection of total dendritic length can be determined by multiplying the number of

Figure 4: A representative photograph of TTC staining of MCAO rat.

intersections by 20 [38]. Five cells per rat were measured for statistical analysis.

2.9. Measurement of Spine Density. Dendritic spine density was analyzed from layer V pyramidal neurons within peri-infarct area. For each cell, at least 30 μm long segments of terminal basilar densities (third order or greater, $n = 5$) and apical densities (lower half of the apical segments, $n = 5$) on the same cell were traced at 1000x magnification [39]. The number of spines was counted and the exact length of the dendritic segment was calculated to yield spines/10 μm data [39]. We did not make any attempt to correct for spines hidden by the overlying dendrites. Therefore the data may be likely to underestimate the actual density.

2.10. Statistical Analysis. All data was expressed as mean ± standard deviation (SD) and analyzed using SPSS 19.0 software (SPSS Inc., Chicago, IL, USA). Behavior data and immunohistochemical data were analyzed using repeated measures analysis of variance (rANOVA) and when the assumptions of sphericity were violated (Mauchly's test, $P < 0.05$), the Greenhouse-Geisser correction was applied. Post hoc analyses used group designed t-test and Turkey's test. One-way analysis of variance (ANOVA) and Tukey's test were used for analyzing dendritic morphological data. Correlations analysis between functional outcome and plasticity were performed using the Spearman correlation coefficients. $P < 0.05$ was considered statistically significant.

3. Results

3.1. TTC for Model Rats. Figure 4 shows a typical photograph of coronal sections of MCAO rat. The infarct region appeared white, and the normal tissue was red. Rats after MCAO exhibited obvious infarction which was located in cortex and striatum. The infarct volume was 38.42 ± 4.42%.

3.2. Neurological Functional Assessment. As shown in Figure 5, for model group and TMP group, rats showed functional improvement with time going on. Repeated measures analysis of variance showed significant group effects ($F = 11.621$, $P = 0.003$). TMP treatment significantly improved functional recovery, as evidenced by improved mNSS at 7 d (model: 10.92 ± 1.68 versus TMP: 9.33 ± 1.72; $t = 2.281$, $P = 0.033$; decreased 14.56%) and 14 d (model: 8.42 ± 1.38 versus TMP: 6.42 ± 1.16; $t = 3.839$, $P = 0.001$; decreased 23.75%) compared with model group. However, there was no significant difference between the two groups at 3 d after MCAO (model: 12.75 ± 1.66 versus TMP: 11.92 ± 1.24; $t = 1.394$, $P = 0.177$). All rats in sham group performed very well without any neurological deficit.

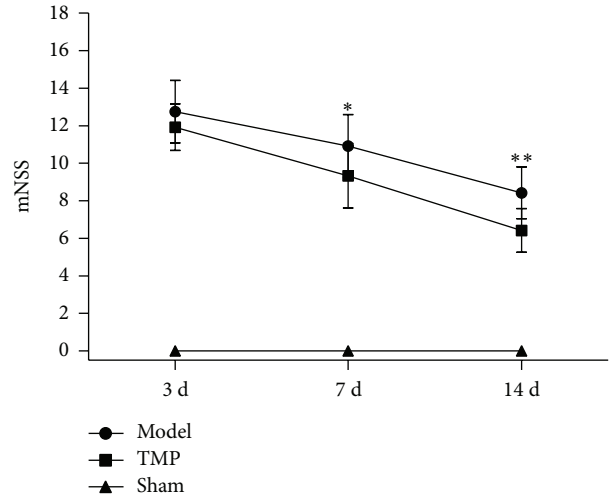

Figure 5: Effect of TMP on neurological status in rats with ischemic cerebral injury. The data were presented as mean ± standard deviation ($n = 12$). $^{*}P < 0.05$ between model group and TMP group; $^{**}P < 0.01$ between model group and TMP group.

3.3. MAP-2 Expression. In this study, IOD values were applied to indicate the expression of MAP-2 (Figure 6). In sham group, obvious MAP-2 immunostaining was observed in the dendrites of the cells. Repeated measures analysis of variance showed there was significant group effects ($F = 77.753$, $P < 0.001$). Post hoc analyses showed that there were significant differences between three groups at 3 d (sham: 38635.39 ± 2649.21 versus model: 17958.93 ± 1244.88 versus TMP: 19128.20 ± 1795.69; $F = 205.913$, $P < 0.001$), 7 d (sham: 38009.15 ± 2715.61 versus model: 22635.95 ± 2102.93 versus TMP: 25521.22 ± 1764.14; $F = 80.61$, $P < 0.001$), and 14 d (sham: 39059.86 ± 2831.29 versus model: 31203.85 ± 2478.53 versus TMP: 37147.30 ± 2168.38; $F = 16.017$, $P < 0.001$). Compared to sham group, rats in model group showed significantly lower expression of MAP-2 (3 d, 7 d, and 14 d all $P < 0.001$; decreased 53.52%, 40.45%, and 20.11%, resp.), although they exhibited an increasing trend from 3 d to 14 d after MCAO. TMP treatment resulted in upregulation in MAP-2 expression in peri-infarct area compared to model group at 14 d ($P = 0.003$; increased 19.05%) after MCAO.

3.4. Dendritic Morphology. The morphological analysis presented here is based on a total of 180 neurons from 18 animals. Golgi-Cox staining clearly filled the dendritic shafts (Figure 7) and the spines of neurons from layer V pyramidal neurons. The total dendritic length and dendritic spine density were obtained for analysis.

3.4.1. Total Dendritic Length. There was no significant difference between three groups at 14 d after MCAO by a one-way

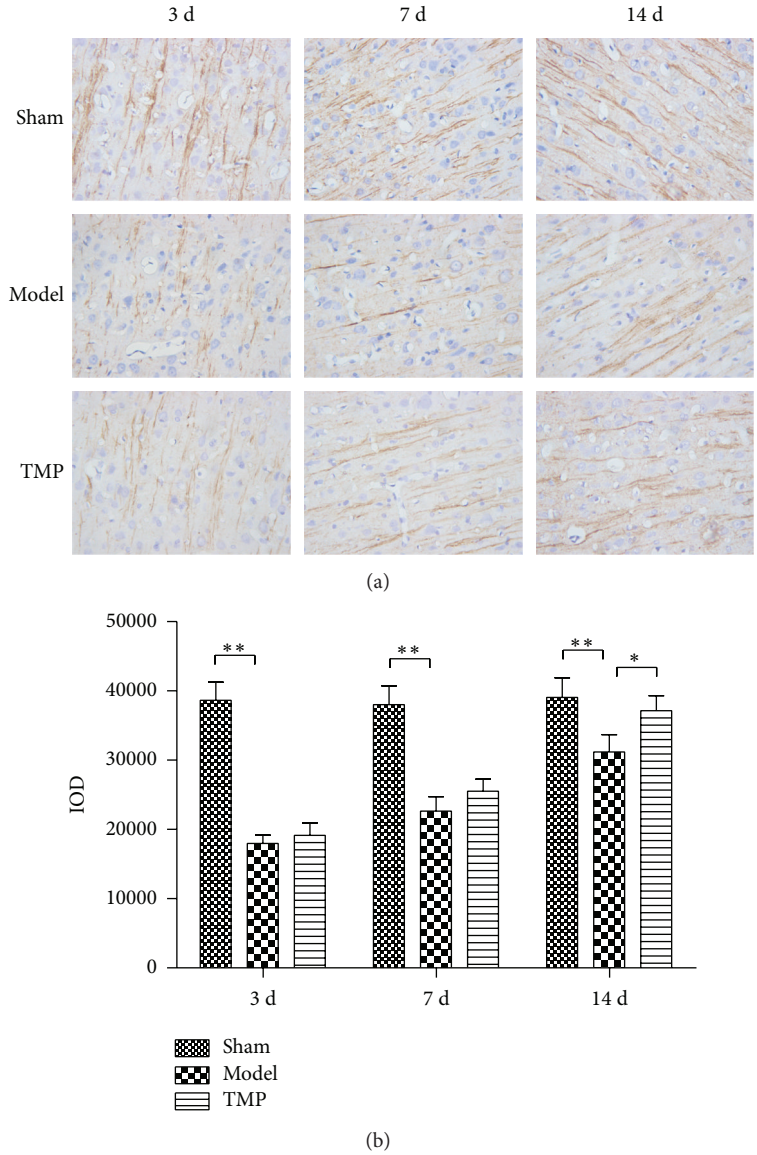

Figure 6: The expression levels of MAP-2 within peri-infarct area of three groups in sham, model, and TMP groups at 3 d, 7 d, and 14 d after MCAO. (a) Immunohistochemical staining of three groups (400x). (b) MAP-2 levels of three groups through measuring the integral optical density (IOD). Data were presented as mean ± standard deviation ($n = 6$). $^{*}P < 0.01$ and $^{**}P < 0.001$.

ANOVA (sham: 1885.67 ± 180.73 versus model: 1786.00 ± 166.02 versus TMP: 1814.67 ± 145.67; $F = 0.582$, $P = 0.571$) (Figure 8).

3.4.2. Spine Density of Basilar Dendrites. For layer V pyramidal neurons, a one-way ANOVA of basilar dendrites spine density found difference between groups at 14 d after MCAO (sham: 9.43±0.85 versus model: 7.70±0.73 versus TMP: 9.07± 0.84; $F = 7.642$, $P = 0.005$) (Figure 9). A following Tukey's test revealed that the dendritic spine density in model group was lower than that of sham group ($P = 0.006$; decreased 18.35%) and TMP treatment increased the dendritic spine density compared to model group ($P = 0.027$; increased 17.79%).

3.4.3. Spine Density of Apical Dendrites. For apical dendrites, a similar trend was observed (Figure 9). A one-way ANOVA of spine density also revealed difference between groups at 14 d after MCAO (sham: 9.73 ± 1.16 versus model: 8.30 ± 0.67 versus TMP: 8.73 ± 0.85; $F = 3.870$, $P = 0.044$). A following Tukey's test showed a decrease in spine density of model group compared to sham group ($P = 0.040$; decreased 14.70%), while no significant increase of density was found after TMP treatment ($P = 0.175$).

3.5. Correlations Analysis. The Spearman correlation coefficients test showed that there were significant negative correlations between mNSS and plasticity measured at 14 d after MCAO (mNSS and MAP-2: $r = -0.619$, $P = 0.032$;

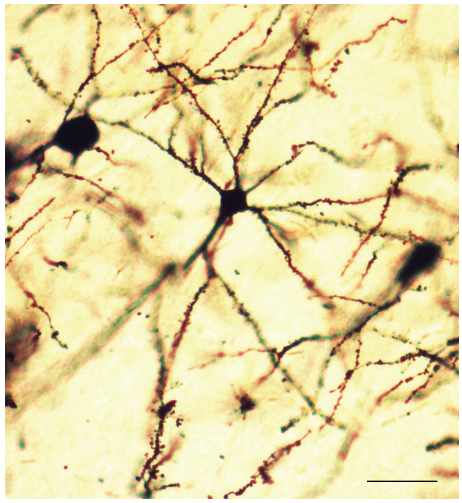

Figure 7: A representative dendritic morphology of layer V pyramidal cells of rats (Golgi-Cox staining). Photomicrograph was viewed at ×200 magnification. Bar = 50 μm.

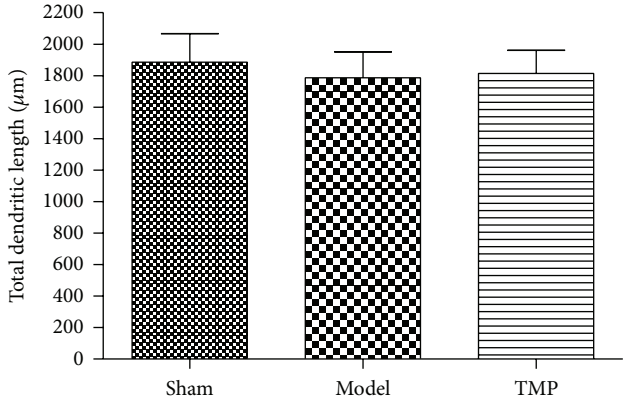

Figure 8: Quantification analysis of effect of TMP on total dendritic length using Sholl analysis. Data were presented as mean ± standard deviation ($n = 6$).

mNSS and total dendritic length: $r = -0.640$, $P = 0.025$; mNSS and spine density of basilar dendrites: $r = -0.705$, $P = 0.010$). But there was no significant correlation between mNSS and spine density of apical dendrites ($r = -0.501$, $P = 0.097$) (Figure 10).

4. Discussion

MCAO model is classical model and produces obvious infarction induced by focal occlusion of middle cerebral artery [40]. TTC staining is a traditional and widely used method for the research of infarct size. In our study, relatively stable and large-sized infarction in cortex and striatum was induced by MCAO in rats in model group, which showed similar results with previous studies [23, 31].

Ischemic stroke often triggers a complex cascade of cellular and molecular events, including excitotoxicity, calcium overload, oxidative stress, and the following apoptosis and neuroinflammation [2]. TMP could block multiple events of the injury cascade to provide protection [19–21]. Up to now, most studies focused on the inhibitory mechanisms of TMP in the early stage of cerebral ischemia injury and only a few studies analyzed the repair mechanisms of TMP [4, 20, 23]. We reported the TMP's effects on dendritic plasticity in a relative late stage, which may provide a new target and a wider therapeutic window.

In our study, neurological score using mNSS showed obvious difference between sham and model group in all time points, which indicates that MCAO induced relative severe neurological function deficits. There must be a natural recovery process after cerebral ischemia reperfusion injury [41, 42], which could be confirmed by our study. TMP is a small molecular weight medicine and reported to have appreciable blood-brain barrier penetrability [43]. According to our data, TMP could improve functional outcome after focal stroke.

MAP-2 is selectively concentrated in the neuron body and dendrites, which plays a key role in maintaining neuroarchitecture, cellular differentiation, and structural and functional plasticity [30]. MAP-2 has an intimate relationship with ischemic cerebral injury and is considered to be an indication of compensatory dendrites reconstruction in remaining neurons [44, 45]. Several studies revealed that the expression of MAP-2 decreased after ischemic cerebral injury [46–48]. In our study, in sham group, MAP-2(+) cells showed staining mainly in the dendrites of the cells; in ischemic animals, we examined the expression of MAP-2 in peri-infarct area at 3 d, 7 d, and 14 d after MCAO; the level of MAP-2 markedly decreased compared to sham group and persistently increased from 3 d to 14 d after stroke, which was consistent with previous study [48]. These results indicated that the expression of MAP-2 showed a dynamic process after stroke (decreasing in early stage and increasing gradually), which may represent degeneration and reconstruction of dendritic structure. Two studies [25, 49] declared there were a peak point and following downtrend during dendrites reconstruction. However, we did not observe this process which may be due to the relatively short period of observation.

Our data showed that treatment of TMP significantly increased MAP-2 expression level in peri-infarct area after stroke and the neurological function was improved meanwhile, indicating that promotion of the reconstruction of dendrites may contribute to the improvements of neurological function. The mechanism is not clear but may be associated with inhibition of calpains. Calpains could be activated by elevated levels of intracellular calcium after ischemic injury [50, 51], causing proteolysis of numerous neuronal cytoskeletal and regulatory proteins. The increase in calpain expression in the ischemic area was accompanied by a loss of its substrate MAP-2 [52]. TMP is a calcium antagonist and could markedly reverse the increased intercellular free calcium concentration [21]. This effect may contribute to upregulation of MAP-2 level. Correlation analysis showed that there was a significant negative correlation between mNSS and expression of MAP-2, indicating that TMP's effect on improvement of neurological function may be the association with upregulation of MAP-2.

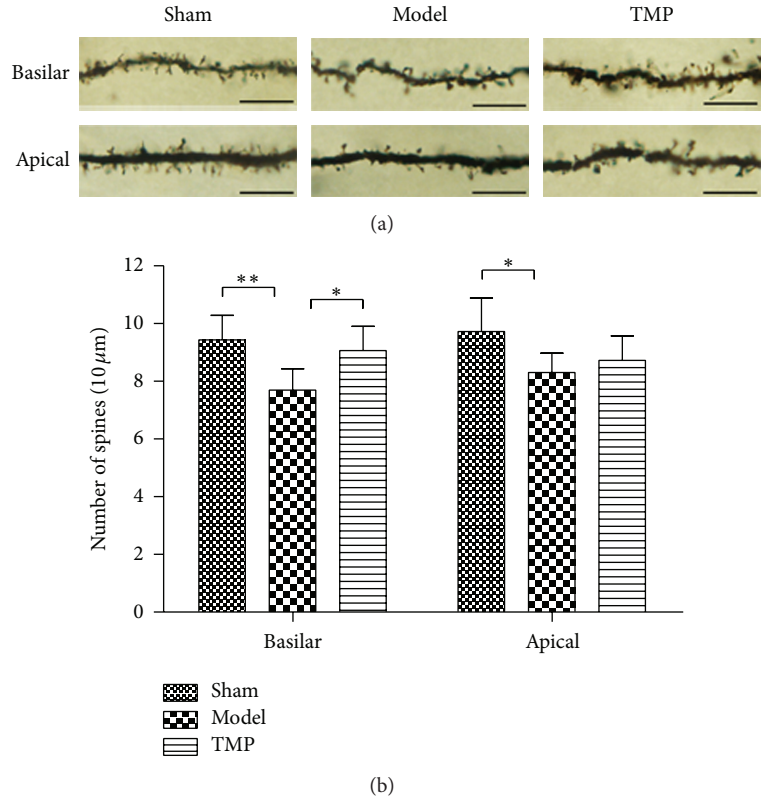

Figure 9: Quantification analyses of effect of TMP on dendritic spine density (basilar dendrites and apical dendrites, resp.). (a) The segments were acquired from layer V pyramidal cells and viewed at ×1000 magnification. Scale bar = 10 μm for all segments. (b) The dendritic spine density was expressed as spines/10 μm and the data were presented as mean ± standard deviation ($n = 6$). $^{*}P < 0.05$ and $^{**}P < 0.01$.

MAP-2 is an indirect marker which can be used for representing dendritic plasticity. However, morphological study is more distinct and more direct for assessments of dendrites. Golgi-Cox staining method has been used broadly for studying morphology of neurites, including quantitative analysis of dendritic length, arborization, and spine density [53], of which spine density is the most important parameter. Dendritic length reflected the total space for synapses and spine density represented the density of excitatory synapses to some extent [54]. Sholl analysis was a classical method for measuring dendritic length, which is an important parameter reflecting dendritic plasticity. We found that the dendritic length of layer V pyramidal cells within peri-infarct area did not change compared to sham group. In fact, the evidence about changes of dendritic length after stroke is controversial; some studies found a shortening of dendrites after cortical lesions [38, 55]; another study found no difference or extension of dendrites in peri-infarct cortex after MCAO [56]. Such paradoxical results are perhaps associated with the absence of a peri-infarct baseline or absence of dynamic study. Brown et al. [57] conducted a longitudinal study and found there was a balance between dendrites extension and retraction after stroke, which may be a mechanism to explain our results. In addition, no obvious alternations of total dendritic length were observed after being treated by TMP, indicating that TMP may fail to affect dendritic length totally at 14 d after stroke. Increasing of dendritic length is good for recovery of stroke, but the result is not good in this regard.

Dendrites and dentritic spines are the primary postsynaptic targets, which receive the majority of excitatory synapses [58]. Previous studies have shown that spine density could be enhanced by drugs [39] or rehabilitative training [59] after experimental stroke, which was likely to play a key role in mediating functional changes that occurred during and after stroke [27]. In our studies, the dentritic spine density of layer V pyramidal neurons decreased significantly in peri-infarct area at 14 d after MCAO, indicating the degeneration of dendrites, which is in accordance with previous study [60]. After chronic treatment with TMP, the spine density of basilar dendrites increased compared to model group; for apical dendrites, there was no significant difference between model group and TMP group. One explanation is that the modifications of basilar dendrites and apical dendrites did not occur at the same time in the recovery period [61]. The degeneration and reorganization of dendritic spines is a complicated process and could be regulated through multiple mechanisms including receptors, scaffolding proteins, and regulators of the cytoskeleton [62, 63]. However, the physiological mechanism responsible for TMP stimulating this increase is unclear in this experiment. Correlation analysis

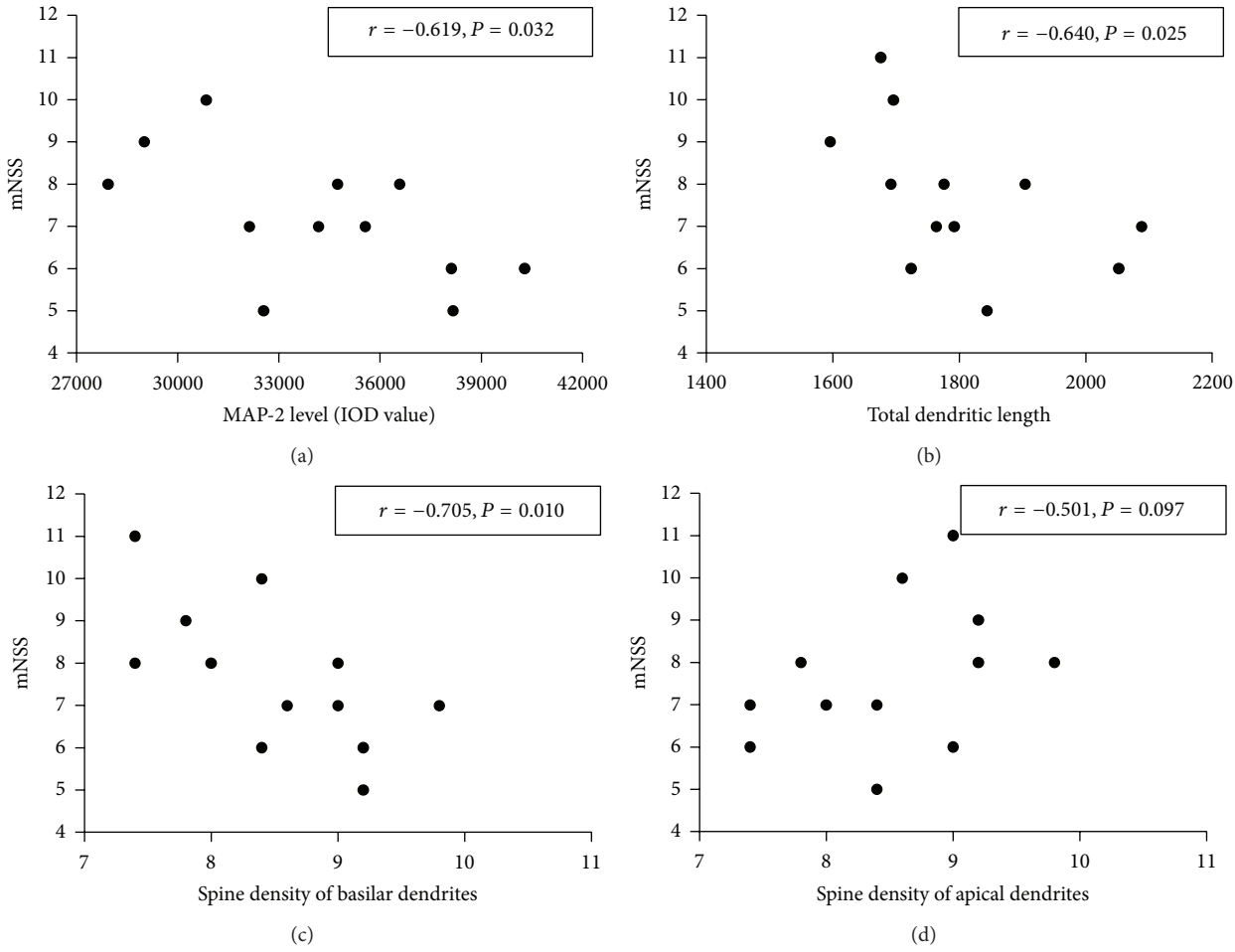

Figure 10: Scatterplots present correlations analysis of mNSS and plasticity measured at 14 d after MCAO. (a) Scatterplots of mNSS and MAP-2 level. (b) Scatterplots of mNSS and total dendritic length. (c) Scatterplots of mNSS and spine density of basilar dendrites. (d) Scatterplots of mNSS and spine density of apical dendrites.

showed that there was a significant negative correlation between mNSS and spine density of basilar dendrites, indicating that TMP's effect on improvement of neurological function may be also the association with increase of spine density of basilar dendrites.

There is a dynamic change of dendrites and dendritic spine after ischemic injury over time [27]. We did not measure the dendritic morphology of other time points, so it is one of limitations that we could not reveal morphological changes during ischemic stroke and recovery.

5. Conclusion

TMP may increase MAP-2 level after cerebral ischemia reperfusion and decrease the alterations of neuronal dendritic spines induced by ischemia, suggesting that TMP may have a potential and specific effect on the neuronal dendritic plasticity in rats with transient focal cerebral ischemia reperfusion. Meanwhile, TMP also improved functional outcome after stroke. Taken together, after cerebral ischemia reperfusion, dendritic plasticity is one of the mechanisms that contributed to functional recovery, which might be regulated by TMP.

Conflict of Interests

The authors declare that there is no conflict of interests regarding the publication of this paper.

Acknowledgment

This study was supported by a research grant from the National Natural Science Foundation of China (no. 81072917).

References

[1] Z.-Q. Lu, Y.-J. Deng, and J.-X. Lu, "Effect of aloe polysaccharide on caspase-3 expression following cerebral ischemia and reperfusion injury in rats," *Molecular Medicine Reports*, vol. 6, no. 2, pp. 371–374, 2012.

[2] E. Candelario-Jalil, "Injury and repair mechanisms in ischemic stroke: considerations for the development of novel neurotherapeutics," *Current Opinion in Investigational Drugs*, vol. 10, no. 7, pp. 644–654, 2009.

[3] D. Lloyd-Jones, R. J. Adams, T. M. Brown et al., "Heart disease and stroke statistics—2010 update: a report from the American Heart Association," *Circulation*, vol. 121, no. 7, pp. e46–e215, 2010.

[4] S.-L. Liao, T.-K. Kao, W.-Y. Chen et al., "Tetramethylpyrazine reduces ischemic brain injury in rats," *Neuroscience Letters*, vol. 372, no. 1-2, pp. 40–45, 2004.

[5] L. Feng, N. Ke, F. Cheng et al., "The protective mechanism of ligustrazine against renal ischemia/reperfusion injury," *The Journal of Surgical Research*, vol. 166, no. 2, pp. 298–305, 2011.

[6] W. Qian, X. Xiong, Z. Fang, H. Lu, and Z. Wang, "Protective effect of tetramethylpyrazine on myocardial ischemia-reperfusion injury," *Evidence-Based Complementary and Alternative Medicine*, vol. 2014, Article ID 107501, 9 pages, 2014.

[7] Y. Chang, G. Hsiao, S. H. Chen et al., "Tetramethylpyrazine suppresses HIF-1alpha, TNF-alpha, and activated caspase-3 expression in middle cerebral artery occlusion-induced brain ischemia in rats," *Acta Pharmacologica Sinica*, vol. 28, no. 3, pp. 327–333, 2007.

[8] X. Cai, Z. Chen, X. Pan et al., "Inhibition of angiogenesis, fibrosis and thrombosis by tetramethylpyrazine: mechanisms contributing to the SDF-1/CXCR4 axis," *PLoS ONE*, vol. 9, no. 2, Article ID e88176, 2014.

[9] X. Zhang, F. Zhang, D. Kong et al., "Tetramethylpyrazine inhibits angiotensin II-induced activation of hepatic stellate cells associated with interference of platelet-derived growth factor β receptor pathways," *FEBS Journal*, vol. 281, no. 12, pp. 2754–2768, 2014.

[10] F. Zhang, Z. Zhang, D. Kong et al., "Tetramethylpyrazine reduces glucose and insulin-induced activation of hepatic stellate cells by inhibiting insulin receptor-mediated PI3K/AKT and ERK pathways," *Molecular and Cellular Endocrinology*, vol. 382, no. 1, pp. 197–204, 2014.

[11] F. Zhang, C. Ni, D. Kong et al., "Ligustrazine attenuates oxidative stress-induced activation of hepatic stellate cells by interrupting platelet-derived growth factor-β receptor-mediated ERK and p38 pathways," *Toxicology and Applied Pharmacology*, vol. 265, no. 1, pp. 51–60, 2012.

[12] B. Wang, Q. Ni, X. Wang, and L. Lin, "Meta-analysis of the clinical effect of ligustrazine on diabetic nephropathy," *The American Journal of Chinese Medicine*, vol. 40, no. 1, pp. 25–37, 2012.

[13] Q.-H. Yang, Y. Liang, Q. Xu, Y. Zhang, L. Xiao, and L.-Y. Si, "Protective effect of *tetramethylpyrazine* isolated from *Ligusticum chuanxiong* on nephropathy in rats with streptozotocin-induced diabetes," *Phytomedicine*, vol. 18, no. 13, pp. 1148–1152, 2011.

[14] L.-M. Lee, C.-F. Liu, and P.-P. Yang, "Effect of *tetramethylpyrazine* on lipid peroxidation in streptozotocin-induced diabetic mice," *The American Journal of Chinese Medicine*, vol. 30, no. 4, pp. 601–608, 2002.

[15] K. Yu, Z. Chen, X. Pan et al., "Tetramethylpyrazine-mediated suppression of C6 gliomas involves inhibition of chemokine receptor CXCR4 expression," *Oncology Reports*, vol. 28, no. 3, pp. 955–960, 2012.

[16] Y. Zhang, X. Liu, T. Zuo, Y. Liu, and J. H. Zhang, "*Tetramethylpyrazine* reverses multidrug resistance in breast cancer cells through regulating the expression and function of P-glycoprotein," *Medical Oncology*, vol. 29, no. 2, pp. 534–538, 2012.

[17] X.-B. Wang, S.-S. Wang, Q.-F. Zhang et al., "Inhibition of *tetramethylpyrazine* on P-gp, MRP2, MRP3 and MRP5 in multidrug resistant human hepatocellular carcinoma cells," *Oncology Reports*, vol. 23, no. 1, pp. 211–215, 2010.

[18] Y.-H. Shih, S.-L. Wu, W.-F. Chiou, H.-H. Ku, T.-L. Ko, and Y.-S. Fu, "Protective effects of *tetramethylpyrazine* on kainate induced excitotoxicity in hippocampal culture," *NeuroReport*, vol. 13, no. 4, pp. 515–519, 2002.

[19] T.-K. Kao, C.-Y. Chang, Y.-C. Ou et al., "*Tetramethylpyrazine* reduces cellular inflammatory response following permanent focal cerebral ischemia in rats," *Experimental Neurology*, vol. 247, pp. 188–201, 2013.

[20] T.-K. Kao, Y.-C. Ou, J.-S. Kuo et al., "Neuroprotection by *tetramethylpyrazine* against ischemic brain injury in rats," *Neurochemistry International*, vol. 48, no. 3, pp. 166–176, 2006.

[21] Q. Tang, R. Han, H. Xiao, J. Shen, Q. Luo, and J. Li, "Neuroprotective effects of tanshinone IIA and/or tetramethylpyrazine in cerebral ischemic injury in vivo and in vitro," *Brain Research*, vol. 1488, pp. 81–91, 2012.

[22] Y. Sun, J. Jiang, Z. Zhang et al., "Antioxidative and thrombolytic TMP nitrone for treatment of ischemic stroke," *Bioorganic & Medicinal Chemistry*, vol. 16, no. 19, pp. 8868–8874, 2008.

[23] X. Xiao, Y. Liu, C. Qi et al., "Neuroprotection and enhanced neurogenesis by *tetramethylpyrazine* in adult rat brain after focal ischemia," *Neurological Research*, vol. 32, no. 5, pp. 547–555, 2010.

[24] S. T. Carmichael, "Plasticity of cortical projections after stroke," *The Neuroscientist*, vol. 9, no. 1, pp. 64–75, 2003.

[25] R. J. Nudo, "Plasticity," *NeuroRx*, vol. 3, no. 4, pp. 420–427, 2006.

[26] B. B. Johansson and P. V. Belichenko, "Neuronal plasticity and dendritic spines: effect of environmental enrichment on intact and postischemic rat brain," *Journal of Cerebral Blood Flow & Metabolism*, vol. 22, no. 1, pp. 89–96, 2002.

[27] C. E. Brown and T. H. Murphy, "Livin' on the edge: imaging dendritic spine turnover in the peri-infarct zone during ischemic stroke and recovery," *The Neuroscientist*, vol. 14, no. 2, pp. 139–146, 2008.

[28] J. Astrup, B. K. Siesjö, and L. Symon, "Thresholds in cerebral ischemia—the ischemic penumbra," *Stroke*, vol. 12, no. 6, pp. 723–725, 1981.

[29] W.-D. Heiss, "The ischemic penumbra: how does tissue injury evolve?" *Annals of the New York Academy of Sciences*, vol. 1268, no. 1, pp. 26–34, 2012.

[30] Q. Zhou, Q. Zhang, X. Zhao et al., "Cortical electrical stimulation alone enhances functional recovery and dendritic structures after focal cerebral ischemia in rats," *Brain Research*, vol. 1311, pp. 148–157, 2010.

[31] Y. M. Zhang, H. Xu, H. Sun, S. H. Chen, and F. M. Wang, "Electroacupuncture treatment improves neurological function associated with regulation of tight junction proteins in rats with cerebral ischemia reperfusion injury,," *Evidence-Based Complementary and Alternative Medicine*, vol. 2014, Article ID 989340, 10 pages, 2014.

[32] J. Chen, Y. Li, L. Wang et al., "Therapeutic benefit of intravenous administration of bone marrow stromal cells after cerebral ischemia in rats," *Stroke*, vol. 32, no. 4, pp. 1005–1011, 2001.

[33] X. Bao, X. Tian, X. Hu, Z. Zhao, Y. Qu, and C. Song, "Discovery of specific tryptophan hydroxylase in the brain of the beetle

Harmonia axyridis," *Brain Research*, vol. 1073-1074, no. 1, pp. 202–208, 2006.

[34] G. Paxinos and C. Watson, *The Rat Brain in Stereotaxic Coordinates*, Elsevier, London, UK, 2007.

[35] C. L. R. Gonzalez, O. A. Gharbawie, P. T. Williams, J. A. Kleim, B. Kolb, and I. Q. Whishaw, "Evidence for bilateral control of skilled movements: ipsilateral skilled forelimb reaching deficits and functional recovery in rats follow motor cortex and lateral frontal cortex lesions," *European Journal of Neuroscience*, vol. 20, no. 12, pp. 3442–3452, 2004.

[36] F. Alcantara-Gonzalez, I. Juarez, O. Solis et al., "Enhanced dendritic spine number of neurons of the prefrontal cortex, hippocampus, and nucleus accumbens in old rats after chronic donepezil administration," *Synapse*, vol. 64, no. 10, pp. 786–793, 2010.

[37] D. A. Sholl, "Dendritic organization in the neurons of the visual and motor cortices of the cat," *Journal of anatomy*, vol. 87, no. 4, pp. 378–406, 1953.

[38] R. L. Gibb, C. L. R. Gonzalez, W. Wegenast, and B. E. Kolb, "Tactile stimulation promotes motor recovery following cortical injury in adult rats," *Behavioural Brain Research*, vol. 214, no. 1, pp. 102–107, 2010.

[39] O. Hurtado, A. Cárdenas, J. M. Pradillo et al., "A chronic treatment with CDP-choline improves functional recovery and increases neuronal plasticity after experimental stroke," *Neurobiology of Disease*, vol. 26, no. 1, pp. 105–111, 2007.

[40] F. Liu and L. D. McCullough, "Middle cerebral artery occlusion model in rodents: methods and potential pitfalls," *Journal of Biomedicine & Biotechnology*, vol. 2011, Article ID 464701, 9 pages, 2011.

[41] D. C. Morris, M. Chopp, L. Zhang, M. Lu, and Z. G. Zhang, "Thymosin β4 improves functional neurological outcome in a rat model of embolic stroke," *Neuroscience*, vol. 169, no. 2, pp. 674–682, 2010.

[42] M. Song, Y.-J. Kim, Y.-H. Kim, J. Roh, S. U. Kim, and B.-W. Yoon, "Effects of duplicate administration of human neural stem cell after focal cerebral ischemia in the rat," *International Journal of Neuroscience*, vol. 121, no. 8, pp. 457–461, 2011.

[43] T.-H. Tsai and C.-C. Liang, "Pharmacokinetics of *tetramethylpyrazine* in rat blood and brain using microdialysis," *International Journal of Pharmaceutics*, vol. 216, no. 1-2, pp. 61–66, 2001.

[44] Y. Li, N. Jiang, C. Powers, and M. Chopp, "Neuronal damage and plasticity identified by microtubule-associated protein 2, growth-associated protein 43, and cyclin D1 immunoreactivity after focal cerebral ischemia in rats," *Stroke*, vol. 29, no. 9, pp. 1972–1980, 1998.

[45] P. C. Garcia, C. C. Real, A. F. B. Ferreira, S. R. Alouche, L. R. G. Britto, and R. S. Pires, "Different protocols of physical exercise produce different effects on synaptic and structural proteins in motor areas of the rat brain," *Brain Research*, vol. 1456, pp. 36–48, 2012.

[46] M. Sun, Y. Zhao, Y. Gu, and C. Xu, "Neuroprotective actions of aminoguanidine involve reduced the activation of calpain and caspase-3 in a rat model of stroke," *Neurochemistry International*, vol. 56, no. 4, pp. 634–641, 2010.

[47] M. Sun, Y. Zhao, Y. Gu, and C. Xu, "Inhibition of nNOS reduces ischemic cell death through down-regulating calpain and caspase-3 after experimental stroke," *Neurochemistry International*, vol. 54, no. 5-6, pp. 339–346, 2009.

[48] F. Wang, Z. Liang, Q. Hou et al., "Nogo-A is involved in secondary axonal degeneration of thalamus in hypertensive rats with focal cortical infarction," *Neuroscience Letters*, vol. 417, no. 3, pp. 255–260, 2007.

[49] T. A. Jones, S. D. Bury, D. L. Adkins-Muir, L. M. Luke, R. P. Allred, and J. T. Sakata, "Importance of behavioral manipulations and measures in rat models of brain damage and brain repair," *ILAR Journal*, vol. 44, no. 2, pp. 144–152, 2003.

[50] B. C. White, J. M. Sullivan, D. J. DeGracia et al., "Brain ischemia and reperfusion: molecular mechanisms of neuronal injury," *Journal of the Neurological Sciences*, vol. 179, no. 1-2, pp. 1–33, 2000.

[51] R. T. Bartus, R. L. Dean, K. Cavanaugh, D. Eveleth, D. L. Carriero, and G. Lynch, "Time-related neuronal changes following middle cerebral artery occlusion: implications for therapeutic intervention and the role of calpain," *Journal of Cerebral Blood Flow & Metabolism*, vol. 15, no. 6, pp. 969–979, 1995.

[52] M. Liebetrau, H. Martens, N. Thomassen et al., "Calpain inhibitor A-558693 in experimental focal cerebral ischemia in rats," *Neurological Research*, vol. 27, no. 5, pp. 466–470, 2005.

[53] R. Gibb and B. Kolb, "A method for vibratome sectioning of Golgi-Cox stained whole rat brain," *Journal of Neuroscience Methods*, vol. 79, no. 1, pp. 1–4, 1998.

[54] B. Kolb, R. Brown, A. Witt-Lajeunesse, and R. Gibb, "Neural compensations after lesion of the cerebral cortex," *Neural Plasticity*, vol. 8, no. 1-2, pp. 1–16, 2001.

[55] R. Mostany and C. Portera-Cailliau, "Absence of large-scale dendritic plasticity of layer 5 pyramidal neurons in peri-infarct cortex," *The Journal of Neuroscience*, vol. 31, no. 5, pp. 1734–1738, 2011.

[56] C. L. R. Gonzalez and B. Kolb, "A comparison of different models of stroke on behaviour and brain morphology," *The European Journal of Neuroscience*, vol. 18, no. 7, pp. 1950–1962, 2003.

[57] C. E. Brown, J. D. Boyd, and T. H. Murphy, "Longitudinal *in vivo* imaging reveals balanced and branch-specific remodeling of mature cortical pyramidal dendritic arbors after stroke," *Journal of Cerebral Blood Flow & Metabolism*, vol. 30, no. 4, pp. 783–791, 2010.

[58] X. Yu and Y. Zuo, "Spine plasticity in the motor cortex," *Current Opinion in Neurobiology*, vol. 21, no. 1, pp. 169–174, 2011.

[59] J. Biernaskie and D. Corbett, "Enriched rehabilitative training promotes improved forelimb motor function and enhanced dendritic growth after focal ischemic injury," *The Journal of Neuroscience*, vol. 21, no. 14, pp. 5272–5280, 2001.

[60] T. Jiang, R. X. Xu, A. W. Zhang et al., "Effects of transcranial direct current stimulation on hemichannel pannexin-1 and neural plasticity in rat model of cerebral infarction," *Neuroscience*, vol. 226, pp. 421–426, 2012.

[61] T. A. Jones and T. Schallert, "Overgrowth and pruning of dendrites in adult rats recovering from neocortical damage," *Brain Research*, vol. 581, no. 1, pp. 156–160, 1992.

[62] J. Lippman and A. Dunaevsky, "Dendritic spine morphogenesis and plasticity," *Journal of Neurobiology*, vol. 64, no. 1, pp. 47–57, 2005.

[63] T. Tada and M. Sheng, "Molecular mechanisms of dendritic spine morphogenesis," *Current Opinion in Neurobiology*, vol. 16, no. 1, pp. 95–101, 2006.

Hindawi Publishing Corporation
Evidence-Based Complementary and Alternative Medicine
Volume 2015, Article ID 734903, 9 pages
http://dx.doi.org/10.1155/2015/734903

Research Article

Cardioprotective Potential of Polyphenolic Rich Green Combination in Catecholamine Induced Myocardial Necrosis in Rabbits

Fatiqa Zafar,[1] Nazish Jahan,[1] Khalil-Ur-Rahman,[2] Ahrar Khan,[3] and Waseem Akram[4]

[1]*Department of Chemistry, University of Agriculture, Faisalabad 38000, Pakistan*
[2]*Department of Biochemistry, University of Agriculture, Faisalabad 38000, Pakistan*
[3]*Department of Pathology, University of Agriculture, Faisalabad 38000, Pakistan*
[4]*Department of Entomology, University of Agriculture, Faisalabad 38000, Pakistan*

Correspondence should be addressed to Nazish Jahan; nazishjahanuaf@yahoo.com

Received 5 February 2015; Revised 13 May 2015; Accepted 21 May 2015

Academic Editor: Joen-Rong Sheu

The present study was designed to develop safer, effective, and viable cardioprotective herbal combination to control oxidative stress related cardiac ailments as new alternatives to synthetic drugs. The synergetic cardioprotective potential of herbal combination of four plants *T. arjuna* (T.A.), *P. nigrum* (P.N), *C. grandiflorus* (C), and *C. oxyacantha* (Cr) was assessed through curative and preventive mode of treatment. In preventive mode of treatment, the cardiac injury was induced with synthetic catecholamine (salbutamol) to pretreated rabbits with the proposed herbal combination for three weeks. In curative mode of treatment, cardiotoxicity/oxidative stress was induced in rabbits with salbutamol prior to treating them with plant mixture. Cardiac marker enzymes, lipids profile, and antioxidant enzymes as biomarker of cardiotoxicity were determined in experimental animals. Rabbits administrated with mere salbutamol showed a significant increase in cardiac marker enzymes and lipid profile and decrease in antioxidant enzymes as compared to normal control indicating cardiotoxicity and myocardial cell necrosis. However, pre- and postadministration of plant mixture appreciably restored the levels of all biomarkers. Histopathological examination confirmed that the said combination was safer cardioprotective product.

1. Introduction

Cardiovascular diseases have become a global threat to life [1] and are major reason of 17.1 million fatalities every year. It is expected that death toll due to cardiac diseases will reach up to 20 million in 2020 [2]. In Pakistan, the condition has become really alarming as cardiac ailments contribute to about 25% of deaths in the country [3]. Diverging to the consistent efforts of medical and pharmaceutical scientists to combat the heart diseases, rather than to minimize the prevalence, the numbers of cardiac patients are increasing [4]. Currently available synthetic cardioprotective medicines have not only been related to a number of side effects but are also very costly [5]. The easy availability, comparatively less side effects, and low cost of medicinal plants make them more attractive therapeutic agents [6].

Medicinal plants enriched with polyphenols, possessing free radical scavenging potential, may reduce the risk of heart diseases because of inverse relationship between cardiovascular diseases and intake of polyphenols [7]. Free radicals are reactive species generated in the body as a result of many endogenous (metabolic pathways) and exogenous (environmental pollution, pesticides, and exposure to radiations) sources [8]. Different environmental factors elevate the level of free radicals and cells become unable to work efficiently against the free radicals leading to accumulation of radicals and oxidative stress which is involved in cell damage, necrosis, and apoptosis and has main causative role in pathogenesis of cardiovascular diseases [9, 10]. Many antioxidants like Vitamins C and E and plant polyphenols are efficient tools in oxidative stress and cardiovascular disorders as potential therapeutic agents [11].

Various medicinal plants possess certain preventive effects regarding heart diseases [12]. Botanical therapeutics with multicomponent has several advantages over single plant extract/isolated compound that may earn them a more prominent place in the field of herbal medicines. Multicomponent therapeutics offer bright prospects for the control of many diseases in a synergistic manner [13].

Mixtures of interacting bioactive compounds produced by plants may provide important combination therapies that simultaneously affect multiple pharmacological targets and provide clinical efficacy beyond the reach of single compound-based drugs. Therefore four medicinal plants were selected to evaluate their combined cardioprotective potential. Medicinal plants *Crataegus oxyacantha* (Cr) exhibit hypotensive, cardiotonic, antispasmodic, diuretic, and sedative properties. It helps to treat heart disease by dilating peripheral and coronary blood vessels and improves the supply of blood to the heart and extenuating symptoms in early period of heart failure [14]. *Cactus grandiflorus* (C) is particularly useful in treating different ailments associated with the heart and is a very good source of polyphenols. It has the ability to reduce the oxidative stress due to its powerful antioxidant activity [15]. *Piper nigrum* (P.N) commonly known as Black Pepper is used to treat cardiac diseases, being a very good combination of antioxidants. *Terminalia arjuna* (T.A) has significant antioxidant properties and is a good heart tonic [16]. Gemmomodified extract of this plant (T.A (g)) is a rich source of bioactive substances. Gemmo preparations (freshly growing parts) of medicinal plants are important as these contain many active substances that start to disappear as plant reaches maturity [17].

Finding ways to screen the synergistic combinations from numerous herbal pharmacological agents is still an ongoing challenge. In the present research work extracts of the above four medicinal plants being used by alternative practitioners and those have known folk medicinal background were used in the ratio of (C : Cr : P.N : T.A (g) = 2 : 1 : 2 : 2) for the assessment of synergetic cardioprotective activity. These plants have been previously analyzed by our research group for their individual antioxidant potential. In the present research, synergistic cardioprotective potential of the combination was evaluated in salbutamol induced cardiotoxicity through animal model.

2. Methodology

2.1. Sample Collection. Freshly growing leaves (gemmo parts) of medicinal plant *Terminalia arjuna* (Arjun) were collected from the Botanical garden, University of Agriculture, Faisalabad, and got identified from plant taxonomist at the Department of Botany, University of Agriculture, Faisalabad, Pakistan. *Piper nigrum* (Black pepper) was bought from market and ground into fine powder. Ethanolic extracts of medicinal plants *Cactus grandiflorus* and *Crataegus* were purchased from a branded company of Germany "Schwabe" from Homoeopathic Medical store.

2.2. Sample Preparation. Freshly growing leaves (gemmo parts) of *Terminalia arjuna* were washed with cold water to remove dirt and were used in the form of gemmomodified extract. *Piper nigrum* was purchased from herbal store and was ground into fine powder, whereas prepared ethanolic extracts of Cactus and Crataegus were used.

2.3. Preparation of Plant Extracts. Gemmomodified extract of *Terminalia arjuna* was prepared by maceration process. The fresh plant material was blended in a mixture of alcohol and glycerin having 2 : 1 ratio for 21 days [17]. Aqueous extract of *Piper nigrum* was prepared by boiling the plant material with water for ten minutes and filtrate was used.

2.4. Determination of Phenolics by HPLC. For the determination of phenolic contents by HPLC, method of Pak-Dek et al. [18] was followed. Plant extract (50 mg) was dissolved in 24 mL methanol and homogenized, and then distilled water (16 mL) and HCl (10 mL, 6 M) were added. This mixture was thermostated for 2 h at 95°C. The final solution was filtered using a 0.45 μm nylon membrane filter and High Performance Liquid Chromatography (HPLC) analysis was carried out. The conditions used for the HPLC analysis are given in Table 1.

2.5. Preparation of Herbal Combinations. Herbal combination was prepared by appropriately mixing the extracts of Cactus, Crataegus, Arjuna, and *Piper nigrum* in the ratio of 2 : 1 : 2 : 2. These plant extracts were individually analyzed by our research group for their total polyphenolic contents, antioxidant activity, and cardioprotective potential. Present study was planned to evaluate their synergistic cardioprotective potential.

2.6. Animals. Male albino rabbits weighing 1–1.5 kg were selected for this study. Rabbits were kept under standard conditions of environment in the department of Clinical Medicine and Surgery (CMS), University of Agriculture, Faisalabad, Pakistan, and were allowed free access to standard diet and water. All international ethical considerations about animal studies were monitored during the experiment.

2.7. Experimental Protocol. Rabbits were kept for one week acclimatization period and then randomly divided into different groups. Each group comprised three rabbits.

Group I (Normal Controls). Rabbits were given standard diet only.

Group II (Salbutamol Control Group). Salbutamol was ingested to the rabbits (60 mg/Kg b.wt.) for two consecutive days to induce oxidative stress/myocardial cell necrosis.

Group III (Baseline Group). Herbal combination (100 mg/kg b.wt) was given orally to rabbits of this group once daily for three weeks.

Group IV (Preventive Group). Rabbits of this group were pretreated with plant combination 100 mg/kg b.wt. once daily for three weeks and then treated with two consecutive doses

Table 1: Conditions used for HPLC analysis.

Column	Shim-Pack CLC-ODS (C-18), 25 cm × 4.6 mm, 5 μm
Mobile phase	Gradient: A (H_2O : AA—94 : 6, pH = 2.27), B (CAN 100%), 0–15 min = 15% B, 15–30 = 45% B, 30–45 = 100% B
Flow rate	1 mL/min
Detector	UV-visible detector. 280 nm
Temperature	RT
Range	Bipolar, 1250 mV, 10 samples per sec.
Detection	Gradient

of salbutamol (60 mg/kg) orally. Blood samples were taken to evaluate any effect of herbal combination.

Group V (Curative Groups). Rabbits were treated with salbutamol (60 mg/kg) for two days to induce cardiotoxicity. Then these cardiointoxicated rabbits were treated with 200 mg/kg b.wt of plant combination once daily for five days and blood samples were collected daily to check the posttreatment effect of herbal mixture.

Group VI (Standard Curative Group (Synthetic Drug)). Rabbits were treated orally with salbutamol (60 mg/kg) for two days to induce cardiotoxicity. Then these cardiointoxicated rabbits were treated with a standard drug (Norvasc and Capoten) once daily for five days and blood samples were collected daily.

3. Biochemical Assessment

3.1. Estimation of Cardiac Biomarkers. Blood samples were taken from the jugular vein of rabbits and serum was separated for analysis of different cardiac biomarkers like lactate dehydrogenase (LDH), creatine kinase-MB fraction (CK-MB), aspartate transaminase (AST), and alanine transaminase (ALT). Among lipids total cholesterol, triglyceride, low density lipoprotein (LDL), and high density lipoprotein (HDL) were also estimated. All these analyses were performed with commercially available kits using chemistry analyzer (Semar S 1000-elite).

3.2. Estimation of Antioxidant Enzymes in Heart Tissues. After experimental period animals were slaughtered and heart tissues were separated and washed with isotonic saline. The tissues were homogenized in 10% ice cold phosphate buffer (pH = 7). Then this mixture was centrifuged and supernatant was collected for analysis of antioxidant enzymes like SOD, CAT, and GPx by following the method of Hameed et al. [19].

4. Toxicological Studies

4.1. Gross Pathology of Experimental Animal. Gross pathology of experimental animals was performed under the supervision of a veterinary doctor. Changes in weight and structure of heart, kidneys, liver, stomach, and lungs were noted.

4.2. Histopathological Analysis. Histopathological analysis was performed on the apical portion of the heart, lungs, kidney, and liver. Fresh tissues of these organs were excised and fixed in 10% formalin for 24 hours. Sections were cut into 5 μm thickness and stained with hematoxylin and eosin. The sections were mounted and observed under light microscope with magnification of 200x for histological changes.

4.3. Statistical Analysis. The results were expressed as mean ± standard error of mean for three rabbits in each group. The statistical analysis was performed using Minitab 16.0. Analysis was made using one-way analysis of variance (ANOVA) followed by Tukey's comparison test. P value of <0.05 was considered statistically significant.

5. Results

5.1. HPLC Profile of Polyphenolic Contents. The amount of polyphenols identified in different medicinal plants has been shown in Figure 1.

Highest amount of caffeic acid was present in gemmo Arjun (4.352 mg/100 g of plant extract) followed by Crataegus (2.326 mg/100 g), Black Pepper (1.851 mg/100 g), and Cactus (1.361 mg/100 g).

Highest amount of Chlorogenic Acid was found in *Cactus grandiflorus* (Cactus) that was 11.429 mg/100 g of plant extract, while the concentration of Chlorogenic Acid was 9.118 mg/100 g in Black Pepper, 5.816 mg/100 g in gemmo Arjun, and 2.409 mg/100 g in Crataegus. Maximum amount of Ferulic acid was present in Crataegus (9.328 mg/100 g) followed by Cactus and Black Pepper in which the amount of Ferulic acid was 9.067 mg/100 g and 6.935 mg/100 g of plant extract, respectively. *P*-Coumaric acid acid was only present in Crataegus (1.568 mg/100 g) and was absent in all other plants.

5.2. Effect of Herbal Combination on Cardiac Markers (Enzyme) and Lipids. Cardioprotective potential of herbal combination was assessed through curative and preventive modes of treatment.

5.3. Preventive Cardioprotective Potential. In preventive mode of treatment herbal combination was fed orally for three weeks to experimental animals. After that, salbutamol was given (60 mg/kg b.wt.) for two consecutive days to induce oxidative stress which could untimely lead to cell necrosis, ventricular arrhythmia, and myocardial infarction that was confirmed by positive troponin test. Troponins are structural proteins of cardiac muscles which are secreted into blood with myocardial injury and are good markers for myocardial cell necrosis and myocardial infarction.

Salbutamol significantly ($p < 0.05$) increased the level of cardiac biomarker enzymes (CK-MB, AST, ALT, and LDH) in salbutamol induced control group as compared to animals of normal control. Increased level of these enzymes was due

Table 2: Preventive cardioprotective effect of herbal combination on cardiac enzymes in different experimental groups.

Groups	CK-MB (IU/L)	LDH (IU/L)	AST (IU/L)	ALT (IU/L)
Normal control	35.5 ± 0.32	545.8 ± 2.24	37.26 ± 0.37	45.6 ± 0.41
Salbutamol control group	80.4 ± 0.47*	859.5 ± 3.57*	113.5 ± 0.83*	140.7 ± 0.63*
Base line group	22.8 ± 0.27#	539.7 ± 4.01#	36.8 ± 0.54#	49.5 ± 0.84#
Herbal mixture + (salbutamol)	38.2 ± 0.48#	551.5 ± 2.07#	39.7 ± 0.55#	62.4 ± 1.05#

Results are expressed as Mean ± Standard Error of Mean (SEM) for $n = 3$.
*Significantly different from normal control.
#Significantly different from salbutamol control.

Table 3: Preventive cardioprotective effect of herbal combination on lipid profile in different experimental groups.

Groups	Cholesterol (mg/dL)	Triglyceride (mg/dL)	LDL (mg/dL)	HDL (mg/dL)
Normal control group	42 ± 0.45	118.5 ± 1.43	26 ± 0.34	45.6 ± 0.47
Salbutamol control group	86.2 ± 0.39*	342.4 ± 1.64*	57.6 ± 0.63*	32.4 ± 0.36*
Base line group	49.5 ± 0.63#	164 ± 1.83#	19 ± 0.14#	55 ± 0.48#
Herbal mixture + salbutamol	55.5 ± 0.83#	203.8 ± 0.54#	29.5 ± 0.47#	43.7 ± 0.31#

Results are expressed as Mean ± Standard Error of Mean (SEM) for $n = 3$.
*Significantly different from normal control.
#Significantly different from salbutamol control.

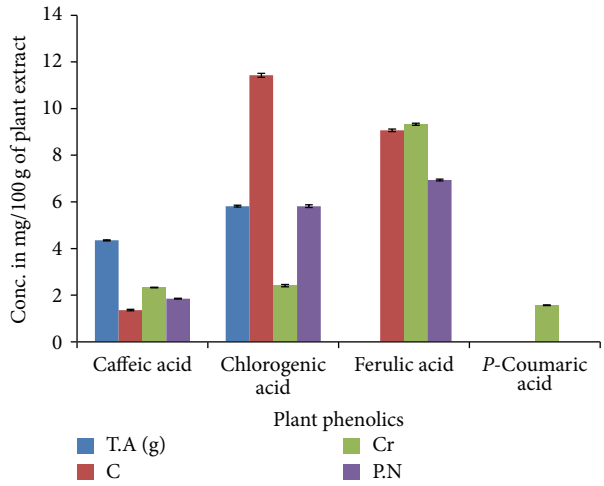

Figure 1: HPLC analysis of polyphenolic contents of four medicinal plants.

to the oxidative stress and myocardial cell necrosis caused by salbutamol. Prior administration of herbal mixture at the dose of 100 mg/kg significantly ($p < 0.05$) maintained the salbutamol induced elevated level of cardiac enzymes. A significant ($p < 0.05$) increase was observed in the levels of lipid profile (LDL, cholesterol, and triglycerides) in salbutamol induced control group as compared to normal control indicating hyperlipidemia, while level of HDL was decreased in salbutamol induced control group. Herbal combination prevented the increase of lipids in preventive group showing the lipid lowering effect of herbal supernatant. Herbal mixture also restored level of HDL, whereas rabbits of base line group showed nonsignificant changes in the level of cardiac biomarkers (Tables 2 and 3).

5.4. Curative Cardioprotective Potential. In curative mode of treatment, oxidative cardiotoxicity (myocardial cell necrosis) was induced in rabbits by giving orally two consecutive doses of salbutamol, which significantly ($p < 0.05$) increased the level of cardiac biomarkers (CK-MB, LDH, AST, and ALT) and lipids of experimental animals. This increased level was then subsequently decreased gradually by treating the animals with herbal mixture. After five days treatment animals were almost completely recovered, indicating the cardioprotective potential of herbal combination. The cardioprotective potential of herbal combination was comparable with synthetic standard drug. Five days treatment of cardio intoxicated rabbits with herbal combination also maintained salbutamol induced elevated level of lipids. Herbal combination restored the lipid level better than synthetic cardioprotective drug (Tables 4 and 5).

5.5. Effect of Herbal Mixture on Myocardial Antioxidants Enzymes. Results of antioxidant enzymes demonstrated that the level of all the three enzymes superoxide dismutase (SOD), catalase, and glutathione peroxidase was decreased significantly ($p < 0.05$) in salbutamol induced control group as compared to the animals of normal control group indicating high oxidative stress. Treatment of rabbits with herbal mixture restored the level of antioxidant enzymes. Polyphenolics rich herbal combination exhibited better potential in curative mode of treatment (Table 6).

6. Toxicological Studies

Toxicological study was performed through gross pathology and histopathological examination.

6.1. Gross Pathology. Results of gross pathology of various organs of different experimental groups of rabbits are given in Tables 7 and 8. These results demonstrated that the weight of different body organs of salbutamol induced control group was increased remarkably ($p < 0.05$) as compared to animals

Table 4: Curative cardioprotective effect of herbal combination on cardiac marker (enzymes) in different experimental groups.

Enzyme	Day	Normal control	Salbutamol control	Salbutamol + herbal mixture	Standard drug
CK-MB (IU/L)	1	35.3 ± 0.50	80.3 ± 1.32*	59.3 ± 0.49#	67.8 ± 1.06
	2	34.5 ± 0.35	81.5 ± 1.42*	57.67 ± 0.54#	61.2 ± 1.67
	3	36.1 ± 0.54	83.7 ± 2.12*	48.3 ± 0.76#	57.3 ± 2.32#
	4	32.7 ± 0.62	85.2 ± 1.37*	39.25 ± 0.53#	49.8 ± 2.10#
	5	33.8 ± 0.47	82.8 ± 1.02*	37.6 ± 0.67#	42.7 ± 1.84#
AST (IU/L)	1	37 ± 0.43	113.6 ± 0.86*	95.3 ± 0.96	101.7 ± 2.5
	2	35.67 ± 0.70	114.1 ± 0.74*	51.33 ± 1.76#	97.25 ± 2.47
	3	36.8 ± 0.23	113.7 ± 0.97*	45.0 ± 1.65#	66.34 ± 3.10#
	4	35.1 ± 0.87	113.5 ± 0.75*	41.67 ± 1.45#	61.9 ± 2.95#
	5	37.2 ± 0.56	114.3 ± 1.02*	39.4 ± 2.01#	54.3 ± 1.95#
ALT (IU/L)	1	45 ± 1.43	142.4 ± 1.23*	139 ± 1.87	147.3 ± 3.10
	2	43.3 ± 1.62	142.9 ± 1.54*	136 ± 2.43	135.6 ± 2.73
	3	42.7 ± 1.45	143.7 ± 3.02*	93.3 ± 2.56#	133.8 ± 2.74
	4	45.5 ± 1.56	141.8 ± 2.31*	83.67 ± 2.12#	113 ± 2.43
	5	47.3 ± 1.76	144.2 ± 2.13*	60.33 ± 1.98#	69.8 ± 3.45#
LDH (IU/L)	1	545.2 ± 2.43	859.2 ± 4.35*	747.6 ± 4.71	810.5 ± 7.23
	2	549.5 ± 2.87	859.6 ± 3.84*	609.7 ± 2.54#	771.5 ± 6.34
	3	542.8 ± 2.61	857.3 ± 4.71*	588 ± 3.78#	634 ± 9.33
	4	547.2 ± 3.54	855.1 ± 3.42*	567 ± 9.32#	588.5 ± 7.83#
	5	541.3 ± 2.69	860.3 ± 5.67*	549.6 ± 5.43#	552.7 ± 5.99#

Results are expressed as Mean ± Standard Error of Mean (SEM) for $n = 3$.
*Significantly different from normal control.
#Significantly different from salbutamol control.

Table 5: Curative cardioprotective effect of herbal combination on lipids in different experimental groups.

Enzyme	Day	Normal control	Salbutamol control	Salbutamol + herbal mixture	Standard drug
Cholesterol (mg/dL)	1	42.3 ± 0.73	102.0 ± 3.45*	98.7 ± 1.33	104 ± 0.64
	2	42.7 ± 0.43	102.8 ± 3.87*	86.3 ± 1.06#	101 ± 0.71
	3	45.3 ± 0.56	101.3 ± 2.56*	80.0 ± 1.43#	76.5 ± 0.48#
	4	43.5 ± 0.37	100.8 ± 2.76*	67.8 ± 1.01#	69.7 ± 0.82#
	5	44.25 ± 0.92	103.1 ± 1.99*	53.4 ± 0.43#	56.4 ± 0.58#
Triglyceride (mg/dL)	1	118.7 ± 1.56	342.6 ± 3.07*	326.7 ± 1.47	340.7 ± 1.19
	2	117.9 ± 2.62	341.8 ± 2.25*	305.2 ± 1.94	338.8 ± 1.35
	3	118.1 ± 3.27	343.6 ± 2.52*	273.8 ± 1.54#	321.4 ± 1.39
	4	119.1 ± 2.97	342.1 ± 2.87*	236.5 ± 1.43#	212.3 ± 1.09#
	5	116.6 ± 3.11	340.2 ± 3.67*	147.7 ± 1.65#	192.7 ± 1.62#
LDL (mg/dL)	1	26.1 ± 1.96	57.0 ± 0.38*	51.67 ± 0.23	55.4 ± 1.26
	2	26.8 ± 1.62	56.8 ± 0.87*	48.3 ± 0.27	49.4 ± 1.33
	3	23.6 ± 1.68	57.7 ± 0.59*	47.7 ± 0.34	43.8 ± 1.93
	4	22.9 ± 0.99	55.9 ± 0.48*	36.67 ± 0.41#	36.6 ± 1.35#
	5	24.1 ± 0.57	55.4 ± 0.79*	25.33 ± 0.22#	35.8 ± 1.29#
HDL (mg/dL)	1	45.7 ± 1.66	31.5 ± 1.32*	31.33 ± 0.43	33.3 ± 1.37
	2	43.9 ± 1.59	33.2 ± 1.61*	33.5 ± 0.97	35.6 ± 1.40
	3	44.3 ± 1.39	32.4 ± 0.99*	38.3 ± 0.68	38.33 ± 0.9
	4	42.8 ± 2.56	31.8 ± 2.01*	42.1 ± 1.3	40.2 ± 0.86
	5	43.1 ± 1.84	32.4 ± 1.03*	43.3 ± 1.04	41.5 ± 0.37

Results are expressed as Mean ± Standard Error of Mean (SEM) for $n = 3$.
*Significantly different from normal control.
#Significantly different from salbutamol control.

Table 6: Level of antioxidant enzymes (Units/g of wt.) in different experimental groups of rabbit.

Antioxidant enzyme	Control	Salbutamol control	Herbal mixture + salbutamol (preventive)	Salbutamol + herbal mixture (curative)	Standard drug
Superoxide dismutase (SOD)	95.42 ± 0.54	49.73 ± 0.64*	66.45 ± 0.69#	99.68 ± 0.86#	44 .54 ± 0.47
Catalase	403.07 ± 0.87	61.00 ± 0.58*	62.00 ± 0.47	400.00 ± 1.74#	937.43 ± 1.46#
Peroxidase	810.3 ± 1.32	730 ± 1.04*	1800 ± 1.76#	600 ± 1.26#	1205.7 ± 1.73#

Results are expressed as Mean ± Standard Error of Mean (SEM) for $n = 3$.
*Significantly different from normal control.
#Significantly different from salbutamol control.

Table 7: Weight of different body organs of different experimental groups.

Groups	Heart	Liver	Lungs	Kidney	
				Right	Left
Normal control	2.5	20.6	4.7	5	5.1
Salbutamol control	5.1*	34.2*	11*	7.2*	8.1*
Preventive group	2.5#	20.2#	5.1#	4.8#	4.9#
Curative group	3.3	33.8	7.5	5.2	4.4#
Standard drug	2.8#	41.1	9.1	5#	5.3

Results are expressed as Mean ± Standard Error of Mean (SEM) for $n = 3$.
*Significantly different from normal control.
#Significantly different from salbutamol control.

of normal control. The weight of body organs was normal in rabbits treated with herbal combination.

6.2. Histopathological Examination of Cardiac Tissues. The histopathological architecture of heart from different experimental groups showed series of variations (Figure 2). In the normal control group, myocardial fibers were arranged regularly with clear striation. No apparent degeneration or necrosis was observed (Figure 2(a)). Histological section of salbutamol treated heart showed severe necrotic and degenerative changes and hyperchromatic and pyknotic nuclei as well as fibroblastic hyperplasia and thick connective tissue proliferation (Figure 2(b)). Heart tissues were normal in rabbits treated with herbal combination. Mild necrotic changes in cardiomyocytes were observed in curative mode of treatment (Figure 2(c)). An insignificant necrosis was examined in the heart of preventive group (Figure 2(d)). Rabbits of base line group also showed normal results.

7. Discussion

The present study revealed both imperative curative and preventive ways of cardioprotective potential. It explained the cardioprotective potential of herbal mixture of four plants in widely used catechol amine-induced model of myocardial cell necrosis in rabbits. In the present research a significant ($p < 0.05$) increase was observed in the level of cardiac enzymes (CK-MB, LDH, AST, and ALT) in salbutamol (catechol amine) induced control group as compared to animals of normal control group. Salbutamol, which has structural similarities with Isoproterenol (ISO), is a synthetic catecholamine and β- adrenergic receptor agonist. At high dose it has the ability to destruct myocardial cells and produce cardiotoxicity in experimental animals, as a result of disturbance in physiological balance between production of free radicals and antioxidant defense system [20]. Increases in the level of these enzymes were due to their leakage from the damaged heart tissues into the blood stream during myocardial necrosis because of myofibril degeneration and myocyte necrosis [21, 22]. It also caused cardiac dysfunction and increased lipid peroxidation along with an increase in the level of myocardial lipids and altered activities of the cardiac markers and antioxidant enzymes [23, 24].

Treatment of different groups of rabbits with herbal mixture significantly reduced the salbutamol-induced secretion of all cardiac diagnostic marker enzymes (CK-MB, LDH, AST, and ALT). This decreased level or reduction in the secretion of enzymes could be of enzymes could be due to repairing and maintenance of the myocardial cells membrane. Curative and preventive treatment of rabbits with polyphenolic enriched herbal combination significantly decreased the elevated cardiac enzyme. Polyphenols are potent antioxidant, neutralizing lipid free radicals and prevent decomposition of hydroperoxides into free radicals [25, 26]. Their cardioprotective potential may be due to scavenging of highly oxidized metabolites produced by salbutamol and stabilization of heart membrane by herbal combination with a consequent decrease in the leakage of these markers [21]. The tendency of these cardiac markers to become near the normal levels in prior and posttreated group is a clear manifestation of the cardioprotective potential of the herbal combination.

Significant ($p < 0.05$) elevated levels of total cholesterol, triglycerides, and low density lipoproteins (LDL) were observed in salbutamol induced control group indicating salbutamol induced hyperlipidemia. Highly oxidative metabolites of catecholamines lead lipid peroxidation which is the major destructive reaction in cellular mechanism of the myocardial ischemia. Highly oxidative metabolite of catecholamines like isoproterenol and salbutamol accelerates rate of peroxidation in membrane phospholipids and releases free fatty acids into plasma by the action of phospholipase A2 and it is a main causative aspect of salbutamol-induced hyperlipidemia [20]. The treatment of experimental animals with herbal mixture decreased salbutamol induced high level of lipids. With both ways of treatment the (preventive and

Table 8: Gross pathology of different groups of experimental rabbits.

Groups	Heart	Liver	Lungs	Kidney	
				Right	Left
Normal control	Normal	Normal	Normal	Normal	Normal
Salbutamol control	Enlarged, hard, and necrosis	Normal	Congested	Slight necrosis congested	Hemorrhage and congested
Preventive	Normal	Normal	Normal	Normal	Normal
Curative	Slightly congested	Normal	Normal	Normal	Normal
Standard drug	Normal	Normal	Congested	Normal	Slight necrosis

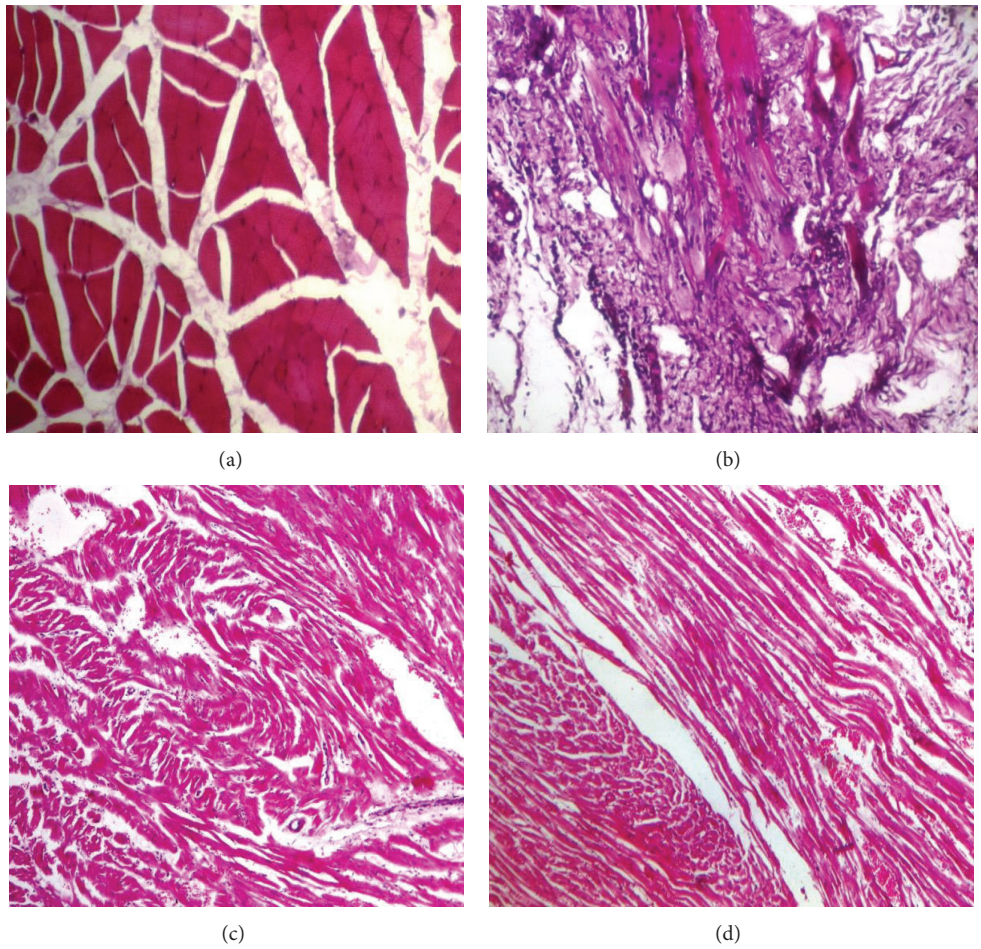

Figure 2: Histopathological architecture of heart of different experimental groups.

curative) the levels of lipid profile reduced closer to the normal level because of the remedial action of herbal combination. The level of HDL was decreased in salbutamol control group indicating the reduction of good cholesterol, but in both curative and preventive group the HDL level increased significantly ($p < 0.05$) which is comparable with the normal control. It is hypothesized that HDL can eradicate cholesterol, from atheroma within arteries, and transfer it back to the liver for excretion or reutilization. That is why HDL-bound cholesterol is sometimes called "good cholesterol." A high level of HDL-C protects against cardiovascular diseases, and low HDL cholesterol levels increase the risk of heart diseases [27]. Same trend of lipid profile was observed in many previous findings [16, 23, 28–31]. It is also obvious from the present findings that the prepared herbal combination gave overall better results as compared to the standard drugs because of its powerful antioxidant and nontoxic nature.

Level of antioxidant enzymes was significantly ($p < 0.05$) lower in salbutamol induced control group. Antioxidant enzymes are biomarker of oxidative stress. Production of highly reactive free radical species inhibited the activities of antioxidant enzymes [32]. Glutathione antioxidant system plays a fundamental role in cellular defense against reactive free radicals and other oxidant species. It protects the myocardial cellular membrane against oxidative damage by regulating the redox status of proteins in the cell surface membrane [4, 22]. In the present case decreased superoxide dismutase (SOD) activity in salbutamol control group may be due to

excessive formation of superoxide anions or the decreased removal of superoxide anion, which can be harmful to the myocardium. The activities of H_2O_2 scavenging enzymes (CAT and peroxidase) also decreased significantly ($p < 0.05$) after the induction of salbutamol to the experimental rabbits. The activities of these enzymes can be explained by the fact that excessive superoxide anion may inactivate SOD, thus resulting in activation of H_2O_2 scavenging enzymes [4, 28]. Pretreatment of rabbits with herbal combination restored the level of endogenous antioxidant enzymes SOD, CAT, and peroxidase. Posttreatment of experimental animals with herbal mixture helped to regain the level of these enzymes near to normal. This can be correlated to the free radical scavenging potential of the herbal combination which protected the rabbits from reactive oxygen species. Several studies have reported the increase of endogenous antioxidants by herbal formulation or plants extracts in cardiovascular diseases [33, 34].

Gross/histopathological examination of different body organs such as heart, liver, lungs, and kidney proved the safe cardioprotective potential of herbal combination. Results of histopathological analysis are in line with many previous studies [35–39] and illustrated the cardioprotective potential and nontoxic nature of herbal combination.

8. Conclusion

The herbal combination prepared by mixing the appropriate ratio of four medicinal plants was administered to the rabbits suffering from salbutamol induced myocardial cell necrosis through both preventive and curative mode of treatments. All these four plants have been already evaluated individually, by our research group, for the cardioprotective potential. In the present study the green combination of the medicinal plants was made which showed better synergistic cardioprotective potential. Bioactive compounds present in different plants exert synergistic biofunctionalities in combination by interacting with one another, rather than acting alone. This herbal combination can be used as an alternative effective drug for the treatment of cardiovascular diseases because of its enriched polyphenolic contents and synergic cardioprotective potential.

Conflict of Interests

The authors do not have any conflict of interests with other people or organizations.

Acknowledgment

The authors are grateful to Higher Education Commission of Pakistan for all financial support (no. PM-IPFP/HRD/HEC/2012/4009) of this study.

References

[1] R. K. Srivastav, H. H. Siddiqui, T. Mahmood, and F. Ahsan, "Evaluation of cardioprotective effect of silk cocoon (Abresham) on isoprenaline-induced myocardial infarction in rats," *Avicenna Journal of Phytomedicine*, vol. 3, no. 3, pp. 216–223, 2013.

[2] A. Upaganlawar, H. Gandhi, and R. Balaraman, "Isoproterenol induced myocardial infarction: protective role of natural products," *Journal of Pharmacology and Toxicology*, vol. 6, no. 1, pp. 1–17, 2011.

[3] N. Jahan, K. U. Rahman, and S. Ali, "Cardioprotective and antilipidemic potential of *Cyperus rotundus* in chemically induced cardiotoxicity," *International Journal of Agriculture and Biology*, vol. 14, no. 6, pp. 989–992, 2012.

[4] S. Ojha, J. Bhatia, S. Arora, M. Golechha, S. Kumari, and D. S. Arya, "Cardioprotective effects of *Commiphora mukul* against isoprenaline-induced cardiotoxicity: a biochemical and histopathological evaluation," *Journal of Environmental Biology*, vol. 32, no. 6, pp. 731–738, 2011.

[5] W. Kchaou, F. Abbès, H. Attia, and S. Besbes, "In vitro antioxidant activities of three selected dates from Tunisia (*Phoenix dactylifera* L.)," *Journal of Chemistry*, vol. 2014, Article ID 367681, 8 pages, 2014.

[6] J. Liu, K. Peter, D. Shi et al., "Anti-inflammatory effects of the chinese herbal formula sini tang in myocardial infarction rats," *Evidence-based Complementary and Alternative Medicine*, vol. 2014, Article ID 309378, 10 pages, 2014.

[7] M. Quiñones, M. Miguel, and A. Aleixandre, "Beneficial effects of polyphenols on cardiovascular disease," *Pharmacological Research*, vol. 68, no. 1, pp. 125–131, 2013.

[8] E. Souri, G. Amin, H. Farsam, and M. B. Tehrani, "Screening of antioxidant activity and phenolic content of 24 medicinal plant extracts," *Daru*, vol. 16, no. 2, pp. 83–87, 2008.

[9] I. Mohanty, S. K. Gupta, and D. S. Arya, "Antiapoptotic and cardioprotective effects of a herbal combination in rats with experimental myocardial infarction," *International Journal of Integrative Biology*, vol. 1, no. 3, pp. 178–188, 2007.

[10] T. S. Zima, L. Fialová, O. Mestek et al., "Oxidative stress, metabolism of ethanol and alcohol-related diseases," *Journal of Biomedical Science*, vol. 8, no. 1, pp. 59–70, 2001.

[11] S. V. kumar, G. Saritha, and M. Fareedullah, "Role of antioxidants and oxidative stress in cardiovascular diseases," *Annals of Biological Research*, vol. 1, no. 3, pp. 158–173, 2010.

[12] F. Ahsan, H. H. Siddiqui, T. Mahmood, R. K. Srivastav, and A. Nayeem, "Evaluation of cardioprotective effect of *Coleus forskohlii* against isoprenaline induced myocardial infarction in rats," *Indian Journal of Pharmaceutical and Biological Research*, vol. 2, no. 1, pp. 17–25, 2014.

[13] X. L. Wang, "Potential herb-drug interaction in the prevention of cardiovascular diseases during integrated traditional and western medicine treatment," *Chinese Journal of Integrative Medicine*, vol. 21, no. 1, pp. 3–9, 2015.

[14] S. K. Verma, V. Jain, D. Verma, and R. Khamesra, "Crataegus oxyacantha—a cardioprotective herb," *Journal of Herbal Medicine and Toxicology*, vol. 1, no. 1, pp. 65–71, 2007.

[15] R. K. Verma, S. E. Haque, and K. K. Pillai, "*Cactus grandiflorus*, a homeopathic preparation has protective effect against doxorubicin induced cardiomyopathy in rats," *International Journal of Phytopharmacology*, vol. 3, no. 3, pp. 281–290, 2012.

[16] N. Jahan, K. U. Rehman, S. Ali, and I. A. Bhatti, "Antioxidant activity of gemmo therapeutically treated indiginous medicinal plants," *Asian Journal of Chemistry*, vol. 23, no. 8, pp. 3461–3470, 2011.

[17] F. Khursheed, K. U. Rehman, M. S. Akhtar, M. Z. U. H. Dogar, and B. Khalil, "Comparative antilipidemic effects of native and gemmo-treated *Withania somnifera* (Asghand) extracts," *Journal of Applied Pharmaceutical Science*, vol. 1, no. 2, pp. 47–59, 2010.

[18] M. S. Pak-Dek, A. Osman, N. G. Sahib et al., "Effects of extraction techniques on phenolic components and antioxidant activity of *Mengkudu* (*Morinda citrifolia* L.) leaf extracts," *Journal of Medicinal Plants Research*, vol. 5, no. 20, pp. 5050–5057, 2011.

[19] A. Hameed, T. M. Shah, B. M. Atta, M. A. Haq, and H. Sayed, "Gamma irradiation effects on seed germination and growth, protein content, peroxidase and protease activity, lipid peroxidation in desi and kabuli chickpea," *Pakistan Journal of Botany*, vol. 40, no. 3, pp. 1033–1041, 2008.

[20] V. S. Panda and S. R. Naik, "Evaluation of cardioprotective activity of *Ginkgo biloba* and *Ocimum sanctum* in rodents," *Alternative Medicine Review*, vol. 14, no. 2, pp. 161–171, 2009.

[21] A. G. Beaulah, M. A. Sadiq, V. Sivakumar, and J. R. Santhi, "Cardioprotective activity of methanolic extract of *Croton sparcifloruson* isoproterenol induced myocardial infarcted wistar albino rats," *Journal of Medicinal Plants Studies*, vol. 2, no. 6, pp. 1–8, 2014.

[22] K. H. Sabeena Farvin, R. Anandan, S. H. S. Kumar, K. S. Shiny, T. V. Sankar, and T. K. Thankappan, "Effect of squalene on tissue defense system in isoproterenol-induced myocardial infarction in rats," *Pharmacological Research*, vol. 50, no. 3, pp. 231–236, 2004.

[23] M. Murugesan, M. Ragunath, S. Nadanasabapathy, R. Revathi, and V. Manju, "Protective role of fenugreek on isoproterenol induced myocardial infarction in rats," *International Research Journal of Pharmacy*, vol. 3, no. 2, pp. 211–216, 2012.

[24] S. Ittagi, V. K. Merugumolu, and R. S. Siddamsetty, "Cardioprotective effect of hydroalcoholic extract of *Tecoma stans* flowers against isoproterenol induced myocardial infarction in rats," *Asian Pacific Journal of Tropical Disease*, vol. 4, no. 1, pp. S378–S384, 2014.

[25] H.-Y. Li, Z.-B. Hao, X.-L. Wang, L. Huang, and J.-P. Li, "Antioxidant activities of extracts and fractions from Lysimachia foenum-graecum Hance," *Bioresource Technology*, vol. 100, no. 2, pp. 970–974, 2009.

[26] A. Rohman, S. Riyanto, N. Yuniarti, W. R. Saputra, R. Utami, and W. Mulatsih, "Antioxidant activity, total phenolic, and total flavaonoid of extracts and fractions of red fruit (*Pandanus conoideus Lam*)," *International Food Research Journal*, vol. 17, no. 1, pp. 97–106, 2010.

[27] O. I. Oyewole, I. G. Adanlawo, and R. O. Arise, "Serum and tissue lipid profile in wistar rats administered leaf extract of *Ficusexasperata*," *Annals of Biological Research*, vol. 4, pp. 288–291, 2013.

[28] F. Kousar, N. Jahan, K. U. Rehman, and S. Nosheen, "Cardioprotective potential of *Coriandrum sativum*," *Plant Science Journal*, vol. 1, no. 1, pp. 1–6, 2012.

[29] R. Sivakumar, R. Rajesh, S. Budhan et al., "Antilipideimic effect of chitosan against experimentally induced myocardial infarction in rats," *Journal of Cell and Animal Biology*, vol. 1, no. 4, pp. 71–77, 2007.

[30] M. A. Kareem, G. S. Krushna, S. A. Hussain, and K. L. Devi, "Effect of aqueous extract of nutmeg on hyperglycaemia, hyperlipidaemia and cardiac histology associated with isoproterenol-induced myocardial infarction in rats," *Tropical Journal of Pharmaceutical Research*, vol. 8, no. 4, pp. 337–344, 2009.

[31] K. Adi, K. Metowogo, A. Mouzou et al., "Evaluation of cardioprotective effects of *Parkia biglobosa* (Jacq.Benth) mimosaceae stem bark," *Journal of Applied Pharmaceutical Science*, vol. 3, no. 2, pp. 60–64, 2013.

[32] M. Eshaghi, S. Zare, N. Banihabib, V. Nejati, F. Farokhi, and P. Mikaili, "Cardioprotective effect of Cornus mas fruit extract against carbon tetrachloride induced-cardiotoxicity in albino rats," *Journal of Basic and Applied Scientific Research*, vol. 2, no. 11, pp. 11106–11114, 2012.

[33] I. Mohanty, D. S. Arya, A. Dinda, K. K. Talwar, S. Joshi, and S. K. Gupta, "Mechanisms of cardioprotective effect of *Withania somnifera* in experimentally induced myocardial infarction," *Basic and Clinical Pharmacology & Toxicology*, vol. 94, no. 4, pp. 184–189, 2004.

[34] S. N. Goyal, S. Arora, A. K. Sharma et al., "Preventive effect of crocin of *Crocus sativus* on hemodynamic, biochemical, histopathological and ultrastuctural alterations in isoproterenol-induced cardiotoxicity in rats," *Phytomedicine*, vol. 17, no. 3-4, pp. 227–232, 2010.

[35] F. Fathiazad, A. Matlobi, A. Khorrami et al., "Phytochemical screening and evaluation of cardioprotective activity of ethanolic extract of *Ocimum basilicum* L. (basil) against isoproterenol induced myocardial infarction in rats," *DARU Journal of Pharmaceutical Sciences*, vol. 20, no. 1, article 87, 2012.

[36] I. R. Mohanty, S. K. Gupta, D. S. Arya, N. Mohanty, and Y. Deshmukh, "Medicinal herbs can play significant role in attenuation of ischemia and reperfusion injury," *Journal of Homeopathy and Ayurvedic Medicine*, vol. 3, pp. 2–5, 2013.

[37] S. Sahreen, M. R. Khan, and R. A. Khan, "Hepatoprotective effects of methanol extract of *Carissa opaca* leaves on CCl_4-induced damage in rat," *BMC Complementary & Alternative Medicine*, vol. 11, article 48, 2011.

[38] K. Yousefi, F. Fathiazad, H. Soraya, M. Rameshrad, N. Maleki-Dizaji, and A. Garjani, "*Marrubium vulgare* L. methanolic extract inhibits inflammatory response and prevents cardiomyocyte fibrosis in isoproterenol-induced acute myocardial infarction in rats," *BioImpacts*, vol. 4, no. 1, pp. 21–27, 2014.

[39] S. Hina, K. Rehman, Z. H. Dogar et al., "Cardioprotective effect of gemmotherapeutically treated *Withania somnifera* against chemically induced myocardial injury," *Pakistan Journal of Botany*, vol. 42, no. 3, pp. 1487–1499, 2010.

Hindawi Publishing Corporation
Evidence-Based Complementary and Alternative Medicine
Volume 2015, Article ID 595824, 8 pages
http://dx.doi.org/10.1155/2015/595824

Research Article

Hinokitiol Negatively Regulates Immune Responses through Cell Cycle Arrest in Concanavalin A-Activated Lymphocytes

Chi-Li Chung,[1,2] Kam-Wing Leung,[3] Wan-Jung Lu,[4] Ting-Lin Yen,[4] Chia-Fu He,[4] Joen-Rong Sheu,[4] Kuan-Hung Lin,[4,5] and Li-Ming Lien[6,7]

[1]*Division of Pulmonary Medicine, Department of Internal Medicine, Taipei Medical University Hospital, Taipei 110, Taiwan*
[2]*School of Respiratory Therapy, College of Medicine, Taipei Medical University, Taipei 110, Taiwan*
[3]*Department of Dentistry, Yuan's General Hospital, Kaohsiung 802, Taiwan*
[4]*Department of Pharmacology and Graduate Institute of Medical Sciences, College of Medicine, Taipei Medical University, Taipei 110, Taiwan*
[5]*Central Laboratory, Shin Kong Wu Ho-Su Memorial Hospital, Taipei 111, Taiwan*
[6]*School of Medicine, College of Medicine, Taipei Medical University, Taipei 110, Taiwan*
[7]*Department of Neurology, Shin Kong Wu Ho-Su Memorial Hospital, Taipei 111, Taiwan*

Correspondence should be addressed to Kuan-Hung Lin; d102092002@tmu.edu.tw and Li-Ming Lien; m002177@ms.skh.org.tw

Received 30 September 2014; Revised 12 February 2015; Accepted 16 February 2015

Academic Editor: Attila Hunyadi

Autoimmune diseases are a group of chronic inflammatory diseases that arise from inappropriate inflammatory responses. Hinokitiol, isolated from the wood of *Chamaecyparis taiwanensis*, engages in multiple biological activities. Although hinokitiol has been reported to inhibit inflammation, its immunological regulation in lymphocytes remains incomplete. Thus, we determined the effects of hinokitiol on concanavalin A- (ConA-) stimulated T lymphocytes from the spleens of mice. In the present study, the MTT assay revealed that hinokitiol (1–5 μM) alone did not affect cell viability of lymphocytes, but at the concentration of 5 μM it could reduce ConA-stimulated T lymphocyte proliferation. Moreover, propidium iodide (PI) staining revealed that hinokitiol arrested cell cycle of T lymphocytes at the G0/G1 phase. Hinokitiol also reduced interferon gamma (IFN-γ) secretion from ConA-activated T lymphocytes, as detected by an ELISA assay. In addition, hinokitiol also downregulated cyclin D3, E2F1, and Cdk4 expression and upregulated p21 expression. These results revealed that hinokitiol may regulate immune responses. In conclusion, we for the first time demonstrated that hinokitiol upregulates p21 expression and attenuates IFN-γ secretion in ConA-stimulated T lymphocytes, thereby arresting cell cycle at the G0/G1 phase. In addition, our findings also indicated that hinokitiol may provide benefits to treating patients with autoimmune diseases.

1. Introduction

Mature lymphocytes must proliferate intensely and repeatedly to provide a rapid immune response and generate immunological memory [1]. Cell proliferation is a mandatory process for immune-system function. However, unregulated or excessive immune responses may cause immune-mediated inflammatory diseases (IMIDs) such as rheumatoid arthritis, Crohn's disease, systemic lupus erythematosus (SLE), and multiple sclerosis [2, 3]. These diseases are commonly T lymphocyte-mediated disorders. Although the pathogenic mechanisms underlying the development of these diseases are not entirely clear, studies have proposed that increased lymphocyte cycling or defective apoptosis may cause breakdown of immune tolerance and autoimmunity as well as lymphoma generation [1–3]. Thus, controlling the cell cycle of lymphocytes may be an effective therapeutic strategy for treating patients with IMIDs.

The cell cycle inhibitor p21, which belongs to the Cip/Kip family, interferes with cycling by inhibiting all cyclin-dependent kinases (CDKs) involved in the G1/S phase, thereby controlling cell proliferation and tumorigenesis in

various cell types [4]. In addition, p21 deficiency was reported to enhance T lymphocyte activation and proliferation and to induce autoimmune manifestations [5]. Suppression of p21 promotes malignant T lymphocyte proliferation in malignant $CD30^+$ T lymphocytes [6]. Thus, p21 may play a critical role in autoimmune diseases and tumorigenesis by regulating T lymphocyte activation and proliferation.

Hinokitiol is a naturally occurring compound isolated from the wood of *Chamaecyparis taiwanensis* [7]. Hinokitiol has been used in hair tonics, tooth pastes, cosmetics, and food as an antimicrobial agent [8]. Moreover, hinokitiol engages in multiple biological activities, including anticancer and anti-inflammatory activities [9, 10]. Studies have reported that hinokitiol suppresses tumor growth by inhibiting cell proliferation and inducing apoptosis or autophagy in various cancer cell lines [9, 11–13]. It was also reported to suppress tumor necrosis factor α production by inhibiting NF-κB activity in lipopolysaccharide-stimulated macrophages [10]. In our previous study, we demonstrated that hinokitiol exhibits potent antiplatelet activity [14].

Although hinokitiol has been reported to engage in multiple biological activities, the regulation of lymphocytes by hinokitiol has not been fully investigated. In our preliminary study, we determined that hinokitiol can arrest the cell cycle of T lymphocytes. Thus, we evaluated the effects of hinokitiol in concanavalin A- (ConA-) activated T lymphocytes isolated from the spleens of mice.

2. Materials and Methods

2.1. Materials. Hinokitiol was purchased from Sigma (St. Louis, MO). The anticyclin D3, anti-E2F1, anti-Cdk4, and anti-GAPDH polyclonal antibodies (pAbs) and anti-p21 monoclonal antibody (mAb) were purchased from GeneTex (Irvine, CA). The PI-annexin V-FITC kit was purchased from BioLegend (San Diego, CA). The Mouse Interferon Gamma (IFN-γ) ELISA Ready-SET-Go kit was purchased from eBioscience (San Diego, CA). The Hybond-P polyvinylidene difluoride membrane, an enhanced chemiluminescence (ECL) western blotting detection reagent and analysis system, the horseradish peroxidase- (HRP-) conjugated donkey anti-rabbit immunoglobulin G (IgG), and the sheep anti-mouse IgG were purchased from Amersham (Buckinghamshire, UK). Hinokitiol was dissolved in 0.5% dimethyl sulfoxide (DMSO) and stored at 4°C until used.

2.2. Mice. The protocols conformed to the Guide for the Care and Use of Laboratory Animals (NIH publication number 85–23, 1996). Briefly, male BALB/c mice (6–8 weeks old, approximately 20–25 g) were purchased from BioLASCO Taiwan Co. Ltd. and fed in the animal house of Taipei Medical University.

2.3. Lymphocyte Preparation. The spleen was aseptically removed from each mouse and placed in a sterile petri dish containing the RPMI 1640 medium. Single-cell suspensions were prepared by gently disrupting the spleen on a sterile wire mesh. The cell suspensions were centrifuged at 300 g for 5 min, and red blood cells were then lysed using the ACK (ammonium-chloride-potassium) lysis buffer (15 mL) and, subsequently, 1x phosphate buffered saline (PBS; 20 mL). The lymphocyte pellets were collected through centrifugation at 300 g for 5 min and suspended with RPMI containing 5% heat-inactivated fetal bovine serum (Gibco). The cell viability was determined according to trypan blue exclusion. The cells were prepared at an appropriate density depending on the scale of each experiment.

2.4. Cell Viability. Cell proliferation was evaluated using a colorimetric assay. Cell viability was measured by conducting a 3-(4,5-dimethylthiazol-2-yl)-2,5-diphenyl tetrazolium bromide (MTT) assay. In brief, cells (3×10^5 cells/well) were cultured in 96-well plates and incubated with a vehicle or hinokitiol (1, 2, or 5 μM) for 24 or 48 h. MTT (5 mg/mL) was added and the cells were incubated for an additional 1 h. The cells were then lysed in 400 μL of DMSO. The absorbance was measured at 570 nm by using a microplate reader. Each experiment was performed in triplicate and repeated at least three times.

2.5. Cytokine Secretion according to ELISA Assay. The amounts of secreted IFN-γ protein were quantified using the Mouse IFN-γ ELISA Ready-SET-Go kit (eBioscience, San Diego, CA). Recombinant IFN-γ was used to generate a standard curve, which was employed in calculating the IFN-γ concentrations of all samples. All procedures were performed according to the manufacturer's instructions (eBioscience).

2.6. Flow Cytometric Analysis. Cells were cultured in 24-well plates. After reaching 80% confluence, the cells were treated with a vehicle or hinokitiol (1, 2, or 5 μM) for 48 h. The cells were washed twice with PBS, detached, and centrifuged. The cells (1×10^6) were then resuspended with 0.5 mL of PBS and then added to propidium iodide (PI, 50 μg/mL) for 15 min at room temperature in the dark before flow cytometric analysis was conducted. Finally, the cells were filtered on a nylon mesh filter. The samples were analyzed using a flow cytometer (Becton Dickinson, FACScan Syst., San Jose, CA). Each experiment was repeated at least three times.

2.7. Immunoblotting. Cells (1×10^7) were cultured in 6-well plates. After reaching 80% confluence, the cells were treated with a vehicle or hinokitiol (1, 2, or 5 μM) for 24 h. After the reactions, the cells were collected and lysed with 70 μL of a lysis buffer. Samples containing 40 μg of protein were separated by conducting sodium dodecyl sulfate polyacrylamide gel electrophoresis. The proteins were electrotransferred by a Bio-Rad semidry transfer (Hercules, CA). The membranes were blocked with TBST (10 mM Tris-base, 100 mM NaCl, and 0.01% Tween 20) containing 5% BSA for 1 h and then probed with various primary antibodies. Membranes were incubated with the HRP-linked anti-mouse IgG or anti-rabbit IgG (diluted 1 : 3000 in TBST) for 1 h. Immunoreactive bands were detected using an ECL system. Semiquantitative results were obtained by scanning reactive bands and quantifying the optical density of each band by using videodensitometry

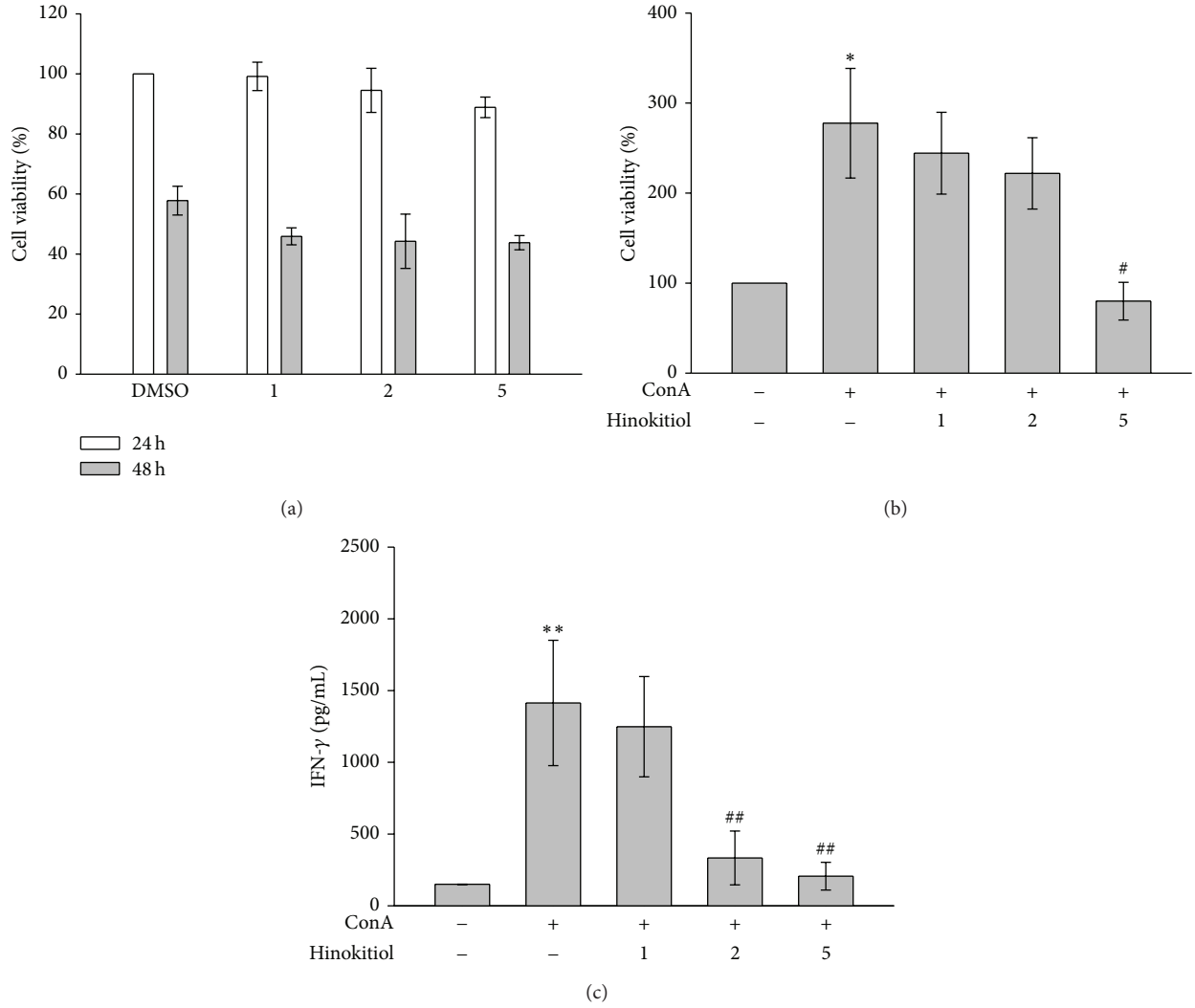

Figure 1: Effects of hinokitiol on cell viability and interferon gamma (IFN-γ) secretion in ConA-activated T lymphocytes. Cells were treated with hinokitiol (1–5 μM) in the absence or presence of ConA (10 μg/mL) for 24 or 48 h. (a, b) Cell viability was determined using a MTT assay ($n = 4$). (c) The level of IFN-γ was measured by an ELISA assay ($n = 3$). Data (b, c) are presented as the mean ± SEM ($^{*}P < 0.05$ and $^{**}P < 0.01$ compared with solvent control (DMSO); $^{\#}P < 0.05$ and $^{\#\#}P < 0.01$ compared with the ConA-treated group).

(Bio-profil; Biolight Windows Application V2000.01; Vilber Lourmat, France).

2.8. Data Analysis. The experimental results are expressed as the mean ± SEM and are accompanied by the number of observations. The data were assessed by conducting an analysis of variance. When this analysis indicated significant differences among the group means, further comparisons were made using the Newman-Keuls method. $P < 0.05$ indicated statistical significance.

3. Results

3.1. Hinokitiol Reduces the Viability and Cytokine Secretion of Lymphocytes. In the present study, an MTT assay was used to evaluate the cell viability and proliferation of lymphocytes. As shown in Figure 1(a), hinokitiol at the concentrations of 1, 2, and 5 μM did not affect the viability of lymphocytes after treatment for 24 and 48 h, indicating that hinokitiol (≤5 μM) did not exhibit cytotoxicity to lymphocytes. Figure 1(b) shows that ConA treatment (10 μg/mL) for 24 h induced lymphocyte proliferation, which was reversed by 5 μM hinokitiol, indicating that hinokitiol inhibits ConA-induced cell proliferation of lymphocytes. In addition, we determined the influence of hinokitiol on the levels of IFN-γ secreted from ConA-stimulated T lymphocytes (Figure 1(c)).

3.2. Hinokitiol Arrests the Cell Cycle at the G0/G1 Phase. PI staining was used to determine the effect of hinokitiol on the cell cycle in ConA-activated lymphocytes. Following ConA stimulation for 48 h, quiescent lymphocytes (G0) began cycling. The population of the G0/G1 phase decreased 22.9% and the population of the S and G2/M phases increased 23.1% upon ConA treatment compared with nontreatment

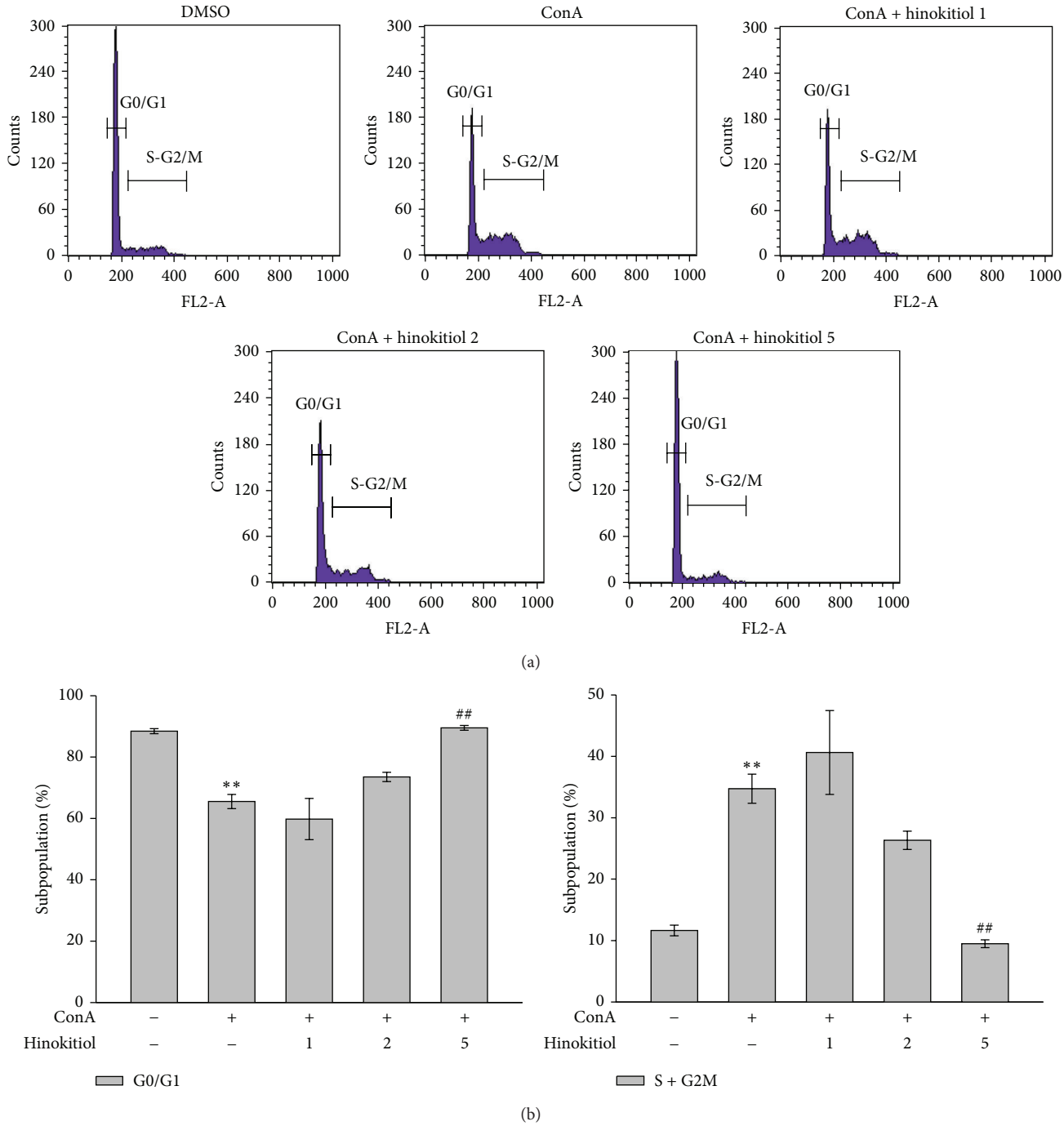

Figure 2: Effects of hinokitiol on the cell cycle in ConA-activated T lymphocytes. Cells were treated with hinokitiol (1–5 μM) in the absence or presence of ConA (10 μg/mL) for 48 h. (a) Cell cycle was determined by PI staining under a flow cytometry. (b) The panel shows the population of the G0/G1 and S-G2/M phases. Data (b) are presented as the mean ± SEM ($n = 3$; $^{**}P < 0.01$ compared with solvent control (DMSO); $^{\#\#}P < 0.01$ compared with the ConA-treated group).

(resting); these changes were reversed by 5 μM hinokitiol (Figures 2(a) and 2(b)). Hinokitiol markedly arrested the cell cycle at the G0/G1 phase in ConA-stimulated lymphocytes (Figure 2(a)). Compared with ConA treatment, 5 μM hinokitiol treatment increased the population of the G0/G1 phase by 24% and reduced the population of the S and G2/M phases by 25.2% (Figures 2(a) and 2(b)).

3.3. Hinokitiol Downregulates the Expression of the Cyclin D3, Cdk4, and E2F1 Proteins and Upregulates the Expression of the p21 Protein. The processes of cell cycling are complex and involve positive regulators such as cyclin D3, Cdk4, and E2F1 and negative regulators such as p21. These proteins were determined in this study. Our data revealed that 5 μM hinokitiol significantly inhibited ConA-induced

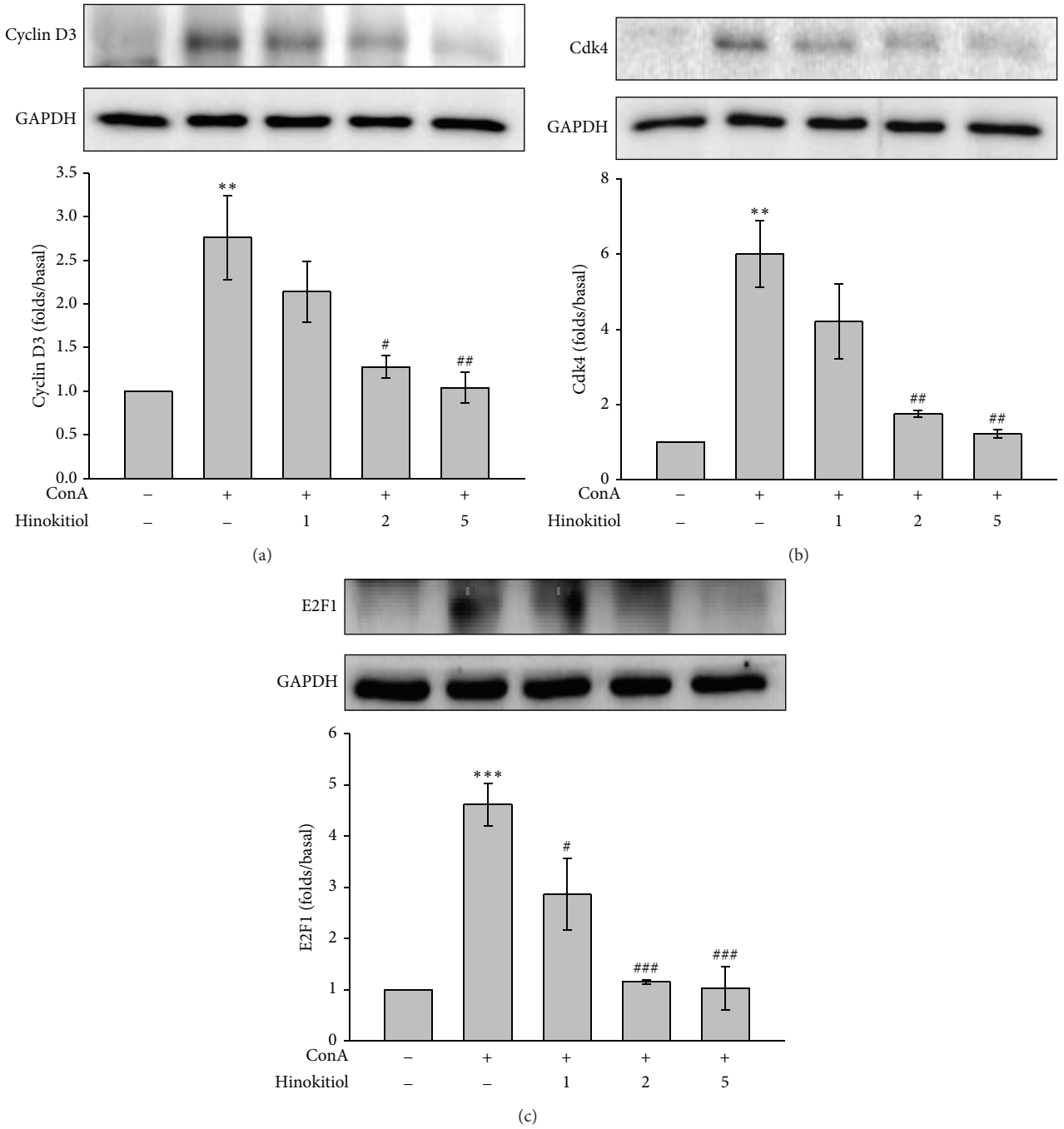

Figure 3: Effects of hinokitiol on positive regulators of the cell cycle. Cells were treated with hinokitiol (1–5 μM) in the absence or presence of ConA (10 μg/mL) for 24 h. The specific antibodies were used to detect (a) cyclin D3, (b) Cdk4, and (c) E2F1. Data (a–c) are presented as the mean ± SEM ($n = 3$; $^{**}P < 0.01$ and $^{***}P < 0.001$ compared with solvent control (DMSO); $^{\#}P < 0.05$, $^{\#\#}P < 0.01$, and $^{\#\#\#}P < 0.001$ compared with the ConA-treated group).

cyclin D3 and Cdk4 expression (Figures 3(a) and 3(b)) and downregulated the transcriptional factor E2F1 (Figure 3(c)). In addition, hinokitiol upregulated the cell cycle inhibitor p21 (Figure 4(a)).

4. Discussion

In the present study, we, for the first time, demonstrated that hinokitiol negatively regulates immune responses by arresting the G0/G1 phase of the cell cycle in ConA-activated

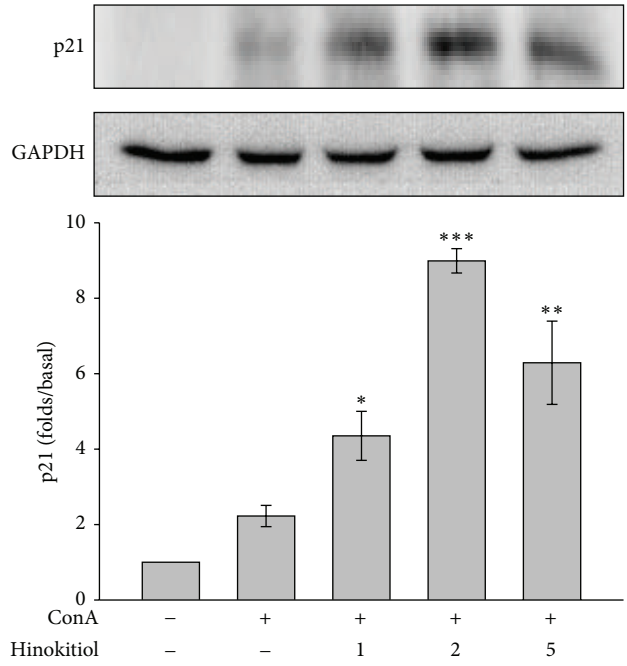

(a)

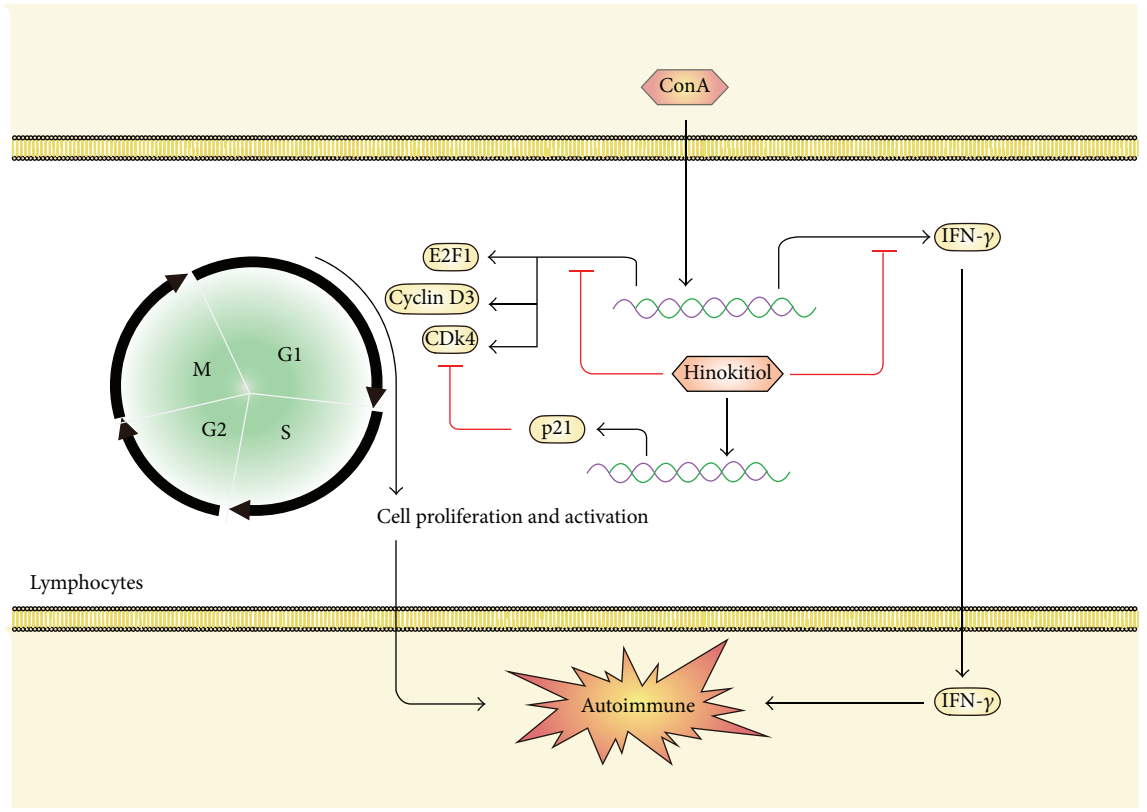

(b)

FIGURE 4: Effects of hinokitiol on negative regulators of the cell cycle. (a) Cells were treated with hinokitiol (1–5 μM) in the presence of ConA (10 μg/mL) for 24 h. The specific antibody was used to detect p21. Data are presented as the mean ± SEM ($n = 3$; $^{*}P < 0.05$, $^{**}P < 0.01$, and $^{***}P < 0.001$ compared with the ConA (alone)-treated group). (b) Schematic illustration of hinokitiol-mediated inhibition of immune responses in ConA-activated T lymphocytes. Hinokitiol downregulates cyclin D3, Cdk4, and E2F1 expression and upregulates p21 expression and subsequently arrests the cell cycle at the G0/G1 phase. Hinokitiol also attenuates IFN-γ secretion. Finally, hinokitiol negatively regulates immune responses.

T lymphocytes. Hinokitiol, a tropolone-related compound found in heartwood cupressaceous plants, exhibits multiple biological activities, including anti-inflammatory, antitumorigenic, and antiplatelet activities [9, 10, 14]. However, the regulation of lymphocytes by hinokitiol has not been fully investigated. Thus, in the present study, we examined the mechanisms underlying the regulation of T lymphocytes by hinokitiol. The lectin ConA from the jack bean (*Canavalia ensiformis*) has been used widely as a T lymphocytes-specific mitogen and to induce the proliferation of lymphocytes [15]. Thus, we used this model to investigate the effect of hinokitiol on T lymphocytes in response to ConA.

Dysregulation of the immune system may lead to various chronic diseases such as autoimmune diseases. Most of the damage inflicted by autoimmune diseases is the result of inappropriate inflammatory responses [16]. Failure of self-tolerance is the fundamental cause of autoimmunity. The principal mechanisms of peripheral tolerance are anergy (functional unresponsiveness), deletion (apoptotic cell death), and suppression by regulatory T cells [17]. A previous study reported that increased cell cycling or defective apoptosis of lymphocytes may lead to a break of tolerance and autoimmunity [1]. The cell cycle is a complex process that involves positive regulators such as cyclins and CDKs and negative regulators such as CDK inhibitors. CDK inhibitors are classified into two families, INK4 and Cip/Kip. During the G1-S transition, cyclins (D2 and D3) and CDKs (4 and 6) are upregulated. By contrast, the cell cycle inhibitor p21, which belongs to the Cip/Kip family, interferes with cycling by inhibiting all CDKs involved in the G1/S phase [1].

In the present study, we observed that hinokitiol arrested the cell cycle of T lymphocytes by suppressing cyclin D3, Cdk4, and E2F1 expression and upregulating p21 expression. A study reported that p21 controls T lymphocyte proliferation [18], and Trivedi et al. indicated that NK cells inhibit T lymphocyte proliferation by upregulating p21, resulting in cell cycle arrest at the G0/G1 phase [19]. The findings of these studies are consistent with our findings that p21 upregulation by hinokitiol leads to G0/G1 arrest. In addition to negatively regulating the cell cycle, p21 was reported be associated with tolerance and systemic autoimmune disease. Loss of tolerance was observed in $p21^{-/-}$ mice, of which the T lymphocytes became more proliferative in response to stimulation. These mice also exhibited an SLE-like syndrome characterized by the development of anti-DNA antibodies and glomerulonephritis [18, 20]. These observations suggest that hinokitiol prevents autoimmune responses by upregulating p21.

In addition, IFN-γ is crucial for immunity to pathogens. IFN-γ is mainly produced in T lymphocytes, NKT cells, NK cells, and B cells [21]. T lymphocytes are the major sources of IFN-γ in adaptive immune responses [21]. Studies have reported that increased IFN-γ production is associated with greater antibacterial and antiviral effects [22, 23]. However, aberrant IFN-γ expression has been associated with inflammatory diseases. Jaruga et al. demonstrated that IFN-γ plays a vital role in ConA-activated T cell hepatitis by enabling leucocytes to infiltrate the liver [24]. Moreover, excess IFN-γ has been associated with chronic autoimmune diseases, including inflammatory bowel disease, multiple sclerosis, diabetes mellitus, and SLE [25, 26]. Thus, we determined the effect of hinokitiol on IFN-γ expression in ConA-stimulated T lymphocytes and observed that hinokitiol significantly prevented IFN-γ expression.

In clinical practice, therapies for autoimmune diseases primarily involve using powerful agents, chemicals, or biologics (corticosteroids, thiopurines, methotrexate, cyclosporine, and antitumor necrosis factor agents) [27]. Such agents suppress the global immune system but frequently cause undesirable side effects. Certain studies have reported that immunosuppressive drugs can increase the risk of cancer and infectious complications [28–31]. Regarding this part, we demonstrated that hinokitiol exerts immunosuppressive effects. Moreover, previous studies have proved that hinokitiol engages in antitumor and antibacterial activities. Whether these beneficial effects of hinokitiol reduce the incidence of side effects associated with immune suppression warrants investigation.

In summary, we observed that hinokitiol inhibits the activation and proliferation of T lymphocytes by arresting the cell cycle at the G0/G1 phase, upregulating p21 expression, and preventing IFN-γ production (Figure 4(b)). Because it engages in multiple biological activities, especially anti-inflammatory and antitumorigenic activities, hinokitiol may reduce the unexpected occurrence of side effects during the treatment of patients with autoimmune diseases. Thus, the results of our study suggest that hinokitiol provides benefits in treating autoimmune diseases.

Conflict of Interests

The authors declare that they have no conflict of interests.

Acknowledgments

This work was supported by grants from the National Science Council, Taiwan (NSC102-2320-B-341-001-MY3, NSC100-2320-B-038-021-MY3, MOST103-2811-B-038-023, and NSC101-2314-B-038-044-MY3), Yuan's General Hospital and Taipei Medical University (103-YGH-TMU-01-1), and the Shin Kong Wu Ho-Su Memorial Hospital (SKH-8302-101-DR-12, SKH-8302-102-DR-15, SKH-8302-103-NDR-05, and SKH-8302-104-NDR-08). Dr. Chi-Li Chung and Dr. Kam-Wing Leung contributed equally to this work.

References

[1] D. Balomenos and A. C. Martinez, "Cell-cycle regulation in immunity, tolerance and autoimmunity," *Immunology Today*, vol. 21, no. 11, pp. 551–555, 2000.

[2] R. Beyaert, L. Beaugerie, G. van Assche et al., "Cancer risk in immune-mediated inflammatory diseases (IMID)," *Molecular Cancer*, vol. 12, no. 1, article 98, 2013.

[3] A. Kuek, B. L. Hazleman, and A. J. K. Östör, "Immune-mediated inflammatory diseases (IMIDs) and biologic therapy: a medical revolution," *Postgraduate Medical Journal*, vol. 83, no. 978, pp. 251–260, 2007.

[4] C. J. Sherr and J. M. Roberts, "CDK inhibitors: positive and negative regulators of G1-phase progression," *Genes and Development*, vol. 13, no. 12, pp. 1501–1512, 1999.

[5] M.-L. Santiago-Raber, B. R. Lawson, W. Dummer et al., "Role of cyclin kinase inhibitor p21 in systemic autoimmunity," *The Journal of Immunology*, vol. 167, no. 7, pp. 4067–4074, 2001.

[6] Y. Wang, X. Gu, G. Zhang et al., "SATB1 overexpression promotes malignant T-cell proliferation in cutaneous $CD30^+$ lymphoproliferative disease by repressing p21," *Blood*, vol. 123, no. 22, pp. 3452–3461, 2014.

[7] H. Suzuki, T. Ueda, I. Juránek et al., "Hinokitiol, a selective inhibitor of the platelet-type isozyme of arachidonate 12-lipoxygenase," *Biochemical and Biophysical Research Communications*, vol. 275, no. 3, pp. 885–889, 2000.

[8] Y. Saeki, Y. Ito, M. Shibata, Y. Sato, K. Okuda, and I. Takazoe, "Antimicrobial action of natural substances on oral bacteria," *The Bulletin of Tokyo Dental College*, vol. 30, no. 3, pp. 129–135, 1989.

[9] L. H. Li, P. Wu, J. Y. Lee et al., "Hinokitiol induces DNA damage and autophagy followed by cell cycle arrest and senescence in gefitinib-resistant lung adenocarcinoma cells," *PLoS ONE*, vol. 9, no. 8, Article ID e104203, 2014.

[10] S. E. Byeon, Y. C. Lee, J.-C. Kim, J. G. Han, H. Y. Lee, and J. Y. Cho, "Hinokitiol, a natural tropolone derivative, inhibits TNF-α production in LPS-activated macrophages via suppression of NF-κB," *Planta Medica*, vol. 74, no. 8, pp. 828–833, 2008.

[11] W.-K. Wang, S.-T. Lin, W.-W. Chang et al., "Hinokitiol induces autophagy in murine breast and colorectal cancer cells," *Environmental Toxicology*, 2014.

[12] S. Liu and H. Yamauchi, "p27-Associated G1 arrest induced by hinokitiol in human malignant melanoma cells is mediated via down-regulation of pRb, Skp2 ubiquitin ligase, and impairment of Cdk2 function," *Cancer Letters*, vol. 286, no. 2, pp. 240–249, 2009.

[13] Y. Ido, N. Muto, A. Inada et al., "Induction of apoptosis by hinokitiol, a potent iron chelator, in teratocarcinoma F9 cells is mediated through the activation of caspase-3," *Cell Proliferation*, vol. 32, no. 1, pp. 63–73, 1999.

[14] K. H. Lin, J. R. Kuo, W. J. Lu et al., "Hinokitiol inhibits platelet activation ex vivo and thrombus formation in vivo," *Biochemical Pharmacology*, vol. 85, no. 10, pp. 1478–1485, 2013.

[15] N. Sharon, "Lectin receptors as lymphocyte surface markers," *Advances in Immunology*, vol. 34, pp. 213–298, 1983.

[16] I. R. Cohen, "Activation of benign autoimmunity as both tumor and autoimmune disease immunotherapy: a comprehensive review," *Journal of Autoimmunity*, vol. 54, pp. 112–117, 2014.

[17] J. D. Rioux and A. K. Abbas, "Paths to understanding the genetic basis of autoimmune disease," *Nature*, vol. 435, no. 7042, pp. 584–589, 2005.

[18] D. Balomenos, J. Martín-Caballero, M. I. García et al., "The cell cycle inhibitor p21 controls T-cell proliferation and sex-linked lupus development," *Nature Medicine*, vol. 6, no. 2, pp. 171–176, 2000.

[19] P. P. Trivedi, P. C. Roberts, N. A. Wolf, and R. H. Swanborg, "NK cells inhibit T cell proliferation via p21-mediated cell cycle arrest," *Journal of Immunology*, vol. 174, no. 8, pp. 4590–4597, 2005.

[20] C. F. Arias, A. Ballesteros-Tato, M. I. García et al., "p21CIP1/WAF1 controls proliferation of activated/memory T cells and affects homeostasis and memory T cell responses," *Journal of Immunology*, vol. 178, no. 4, pp. 2296–2306, 2007.

[21] K. Schroder, P. J. Hertzog, T. Ravasi, and D. A. Hume, "Interferon-gamma: An overview of signals, mechanisms and functions," *Journal of Leukocyte Biology*, vol. 75, no. 2, pp. 163–189, 2004.

[22] I. B. Autenrieth, M. Beer, E. Bohn, S. H. E. Kaufmann, and J. Heesemann, "Immune responses to Yersinia enterocolitica in susceptible BALB/c and resistant C57BL/6 mice: an essential role for gamma interferon," *Infection and Immunity*, vol. 62, no. 6, pp. 2590–2599, 1994.

[23] A. S. Major and C. F. Cuff, "Effects of the route of infection on immunoglobulin G subclasses and specificity of the reovirus-specific humoral immune response," *Journal of Virology*, vol. 70, no. 9, pp. 5068–5974, 1996.

[24] B. Jaruga, F. Hong, W.-H. Kim, and B. Gao, "IFN-γ/STAT1 acts as a proinflammatory signal in T cell-mediated hepatitis via induction of multiple chemokines and adhesion molecules: a critical role of IRF-1," *The American Journal of Physiology—Gastrointestinal and Liver Physiology*, vol. 287, no. 5, pp. G1044–G1052, 2004.

[25] J. R. Schoenborn and C. B. Wilson, "Regulation of interferon-gamma during innate and adaptive immune responses," *Advances in Immunology*, vol. 96, pp. 41–101, 2007.

[26] D. Balomenos, R. Rumold, and A. N. Theofilopoulos, "Interferon-gamma is required for lupus-like disease and lymphoaccumulation in MRL-lpr mice," *The Journal of Clinical Investigation*, vol. 101, no. 2, pp. 364–371, 1998.

[27] K. Orlicka, E. Barnes, and E. L. Culver, "Prevention of infection caused by immunosuppressive drugs in gastroenterology," *Therapeutic Advances in Chronic Disease*, vol. 4, no. 4, pp. 167–185, 2013.

[28] T. Hino-Arinaga, T. Ide, R. Kuromatsu et al., "Risk factors for hepatocellular carcinoma in Japanese patients with autoimmune hepatitis type 1," *Journal of Gastroenterology*, vol. 47, no. 5, pp. 569–576, 2012.

[29] R. Das, P. Feuerstadt, and L. J. Brandt, "Glucocorticoids are associated with increased risk of short-term mortality in hospitalized patients with clostridium difficile-associated disease," *The American Journal of Gastroenterology*, vol. 105, no. 9, pp. 2040–2049, 2010.

[30] W. G. Dixon, K. L. Hyrich, K. D. Watson et al., "Drug-specific risk of tuberculosis in patients with rheumatoid arthritis treated with anti-TNF therapy: results from the British Society for Rheumatology Biologics Register (BSRBR)," *Annals of the Rheumatic Diseases*, vol. 69, no. 3, pp. 522–528, 2010.

[31] S. D. Dojcinov, G. Venkataraman, M. Raffeld, S. Pittaluga, and E. S. Jaffe, "EBV positive mucocutaneous ulcer—a study of 26 cases associated with various sources of immunosuppression," *The American Journal of Surgical Pathology*, vol. 34, no. 3, pp. 405–417, 2010.

Hindawi Publishing Corporation
Evidence-Based Complementary and Alternative Medicine
Volume 2015, Article ID 154691, 10 pages
http://dx.doi.org/10.1155/2015/154691

Research Article

Effects of the Pinggan Qianyang Recipe on MicroRNA Gene Expression in the Aortic Tissue of Spontaneously Hypertensive Rats

Guangwei Zhong,[1] Xia Fang,[2] Dongsheng Wang,[1] Qiong Chen,[2] and Tao Tang[2]

[1]*Institute of Integrated Traditional Chinese and Western Medicine, Xiangya Hospital, Central South University, Changsha 410008, China*
[2]*Department of Geriatrics, Xiangya Hospital, Central South University, Changsha 410008, China*

Correspondence should be addressed to Qiong Chen; qiongch@163.com

Received 9 September 2014; Revised 24 January 2015; Accepted 28 January 2015

Academic Editor: Joen-Rong Sheu

The present study aimed to investigate the relationship between miRNAs and in spontaneously hypertensive rats (SHR) vascular remodeling and analyze the impact of the Pinggan Qianyang recipe (PQR) on miRNAs. Mammalian miRNA microarrays containing 509 miRNA genes were employed to analyze the differentially expressed miRNAs in the three groups. MiRNAs were considered to be up- or downregulated when the fluorescent intensity ratio between the two groups was over 4-fold. Validation of those miRNAs changed in SHR after PQR treatment was used by real-time quantitative RT-PCR (qRT-PCR). Compared with the normal group, a total of 32 miRNAs were differentially expressed by more than twofold; among these, 18 were upregulated and 14 were downregulated in the model group. Compared with the normal group, there were a number of 17 miRNAs which were significantly expressed by more than twofold in the different expressions of 32 miRNAs; among these, 10 were downregulated and 7 were upregulated in the PQR group. qRT-PCR verified that miR-20a, miR-145, miR-30, and miR-98 were significantly expressed in the three groups. These data show that PQR could exert its antihypertensive effect through deterioration of the vascular remodeling process. The mechanism might be associated with regulating differentially expressed miRNAs in aorta tissue.

1. Introduction

Hypertension, a lifelong condition, is one of the most common cardiovascular diseases. Among patients treated by the authors, the prevalence of hypertension in 15 to 69-year-old patients is 23.4%, greater than the current estimate of patients with hypertension in China [1]. Because hypertension is an important risk factor for coronary heart disease and stroke, damage to the vital organs such as the heart, brain, and kidneys can be avoided or minimized by preventing and controlling high blood pressure [2]. A Chinese medicine scholar has successfully explored the pathogenesis of spontaneous hypertension and various therapy approaches, including the Pinggan Qianyang recipe (PQR), a Chinese medicine recipe for calming the liver and suppressing yang [3]. PQR, which originated from the use of Tianma Guoteng beverages, has been used to treat essential hypertension with satisfactory results [4]. Recent research has found that Chinese herbal medicines that involve PQR have a beneficial effect on reducing blood pressure and recovering circadian rhythm in essential hypertension patients [5, 6]. However, the underlying mechanism of these therapeutic effects remains unknown.

miRNAs are a class of highly conserved, noncoding, small-molecule RNAs, consisting of about 22 nucleotides each. They adjust protein levels by promoting mRNA degradation or inhibiting mRNA translation. miRNAs thus participate in many important biological processes throughout the body [7, 8]. miRNAs are involved in cell proliferation, differentiation, migration, and apoptosis [9, 10]. Cordes et al. found that reducing miRNA-143 levels could inhibit adipocyte differentiation in vitro, suggesting that miRNAs may play

a significant role in the renin-angiotensin system (RAAS)—an important modulator of systemic blood pressure [11]. Some miRNAs, including miR-1, miR-145, miR-122, miR-221, and miR-222, have been linked to vascular endothelial dysfunction [12]. Others have been linked to the regulation of vascular smooth muscle cells; these include miR-145, let-7d, miR-24, miR-26a, and miR-146 [13]. The miRNAs miR-1, miR-155, and miR-208 have significant effects on the RAAS [14]. Therefore, a new strategy for hypertension treatment might involve maintenance and restoration of stability by targeting corresponding miRNA expression in the organ of interest.

To elucidate the association between miRNA expression and PQR treatment for essential hypertension, we carried out analysis of miRNA gene expression in aortic tissue from SHR that had received PQR intervention. We tested the hypothesis that PQR plays an antihypertensive role by regulating miRNA expression in rat aortic tissue. This research may also provide new insights into potential therapeutic targets to prevent and treat hypertension.

2. Materials and Methods

2.1. Animals and Drugs. Forty 16-week-old male spontaneously hypertensive rats (SHR) and 20 male Wistar (WKY) rats (Vital River Laboratory Animal Technology Co., Ltd., Beijing, China) of the same age were housed in a sterile environment at a temperature of 21 ± 1°C and a relative humidity of 50% ± 10% in a 12-hour day-night cycle. Both groups of rats had been fed standard rat chow and water until they were 16 weeks old. All animal study protocols were approved by the Animal Care and Use Committee of Central South University (201303117) and followed the animal management rules set out by the Ministry of Health, China, and the US National Institutes of Health Guide for the Care and Use of Laboratory Animals. The PQR medication recipe was composed of Rhizoma Gastrodiae, Ramulus Uncariae cum Uncis, Concha Haliotidia, Concha Ostreae, and Radix Achyranthis Bidentatae; all components were purchased from the Department of Pharmacy, Xiangya Hospital, Central South University. One gram of extract was equal to 4.25 g of crude material.

2.2. Animal Groupings and Treatments. The WKY rats and SHR were arbitrarily separated into three groups: the normal group ($n = 20$), the model group ($n = 20$), and the PQR group ($n = 20$). Rats in the PQR group were administered PQR at a dose of 5.0 $mg \cdot kg^{-1} \cdot d^{-1}$ by gastrogavage. The others were given an equal volume of distilled water. For all groups, the administration course lasted 4 weeks. All animals were used for the miRNA analysis and verification study. Forty SHR were randomly divided into two groups and were given 5.0 mg/kg of PQR by gastrogavage once daily for 4 weeks; normal saline was given as the negative control.

2.3. Blood Pressure Detection. Systolic blood pressure (SBP) was measured in all rats as previously described [15]. Tail-cuff plethysmography (TCP) with a rat tail blood pressure monitor was used. The SBP of each rat was measured five times—once before treatment and 1, 2, 3, and 4 weeks after treatment. At every time point, the mean of the lowest three values within 5 mmHg was regarded as the SBP value.

2.4. Histological and Morphological Assay. Rats were anesthetized with 10% chloral hydrate (400 mg/kg, intraperitoneal injection) at the end of each week of whole-day drug administration. The thoracic aorta below the aortic arch of each rat was stripped and clipped. A portion was fixed in 8% neutral formaldehyde, embedded in paraffin, sectioned at 5 μm, and stained with the hematoxylin-eosin (HE) and Masson methods [16]. Light microscopy was used to image each cross-sectional slice, of which there were five per rat. Each vascular ring in the perpendicular position and the vessel media wall were observed. The images were observed under a Leica imaging system (Leica Microsystems GmbH, Wetzlar, Germany). The media thickness (MT) and inner diameter (LD) were measured, and the ratio of media thickness to inner diameter (MT/LD) was calculated. Other parts of the thoracic aorta were removed from the adventitia and were promptly refrigerated at −80°C for miRNA assay.

2.5. RNA Microarray and Hybridization

RNA Extraction. Total RNA was extracted by a one-step method using TRIzol (Invitrogen, USA) following the manufacturer protocol, concentrated using isopropanol precipitation, and quantified using a spectrophotometer and agarose gel electrophoresis. The polyethylene glycol (PEG) method was used to isolate and purify 50 μg of total RNA.

Fluorescently Labeled miRNA. miRCURY LNA array labeling kit (Exiqon, Denmark) was used. Total RNA (10 μg) was added to 2 μL of Hy_3 fluorescent label solution and 2 μL of labeling enzyme, mixed by pipetting, and then incubated at 65°C for 15 min to terminate the labeling process.

miRNA Microarray Hybridization. A miRCURY LNA array labeling kit using Macro Kit (ID # 208000V7.1) and hybrid box II (ID # 40080) was purchased from Exiqon. Biochip slides and cover slips were purchased from Ambion, Inc. (USA). miRNA microarray hybridization was performed according to the miRCURY LNA array kit instructions: 10 μL of total RNA was added to 10 μL of 2x hybridization buffer and incubated for 3–5 min at 95°C. Then, 20 μL of the hybridization solution was placed on a microarray slide and completely covered with a Bioarray Lifter Slip coverslip. The microarray slide was placed into the Hybridization Chamber II in a horizontal orientation and bathed at 60°C for 16 h. Following incubation, hybridization samples were removed from the microarray slides with a wash solution. Each of 509 miRNAs was detected by three replicate probe spots on each microarray slide, for a total of six measurements per miRNA per sample after repeated fluorescence exchange.

Image Acquisition and Quantification. Each microarray (chip) was rinsed and immediately dried, then illuminated by a single 635 nm beam and scanned by a GenePix 4000B dual laser scanner (Molecular Devices, LLC, USA). Image files were

saved in TIFF format. The data were analyzed by GenePix Pro 6.0 software (Molecular Devices, LLC, USA). After preprocessing, the data were normalized to the same interchip global mean. Finally, the differentially expressed genes were analyzed by SAM (Significance Analysis of Microarrays, version 2.1). We used the following screening conditions: false discovery rate of <5%, and expression differences of ≥2-fold.

2.6. Target Prediction Methods. Predicted miRNA target genes were determined by four software programs: miRanda (http://www.microrna.org/), miRBase Target Database (http://microrna.sanger.ac.uk), and Target Scan (http://www.targetscan.org/) [17]. Outputs varied among the programs. Genes predicted by at least two programs were selected as predicted miRNA target genes.

2.7. Quantitative RT-PCR. Differentially expressed miRNAs, selected according to ≥2-fold upregulation or downregulation by microarray analysis, were measured by qRT-PCR using RNA-tailing and primer extension. Briefly, 2 μg of RNA was added to 2.5 U/μL of poly (A) polymerase and 1 mmol/L of ATP and incubated in water for 30 min at 37°C. PCR primers were designed according to miRNA sequences indicated by the aforementioned online software programs (2.6). U6 small nuclear RNA in the rats was used as an internal control gene. Real-time PCR reactions were amplified in a 96-well PCR fluorescence analyzer (MJ real-time PCR instrument, Bio-Rad Laboratories, Inc., USA). Samples were predenatured for 5 min at 95°C, denatured for 20 s at 94°C, annealed for 20 s at 58°C, and extended for 30 s at 72°C, for a total of 40 cycles, with each sample analyzed in triplicate. The specific product in each PCR reaction was confirmed by the amplification curve. Quantification of relative gene expression was determined by the standard $2^{-\Delta\Delta Ct}$ method: relative gene expression = $2^{-(\Delta Ctsample - \Delta Ctcontrol)}$.

2.8. Statistical Analysis. All results are presented as the mean ± standard deviation. All experiments were repeated three times. An independent sample t-test was applied when only two groups were compared, whereas comparisons between more than two groups were made by analysis of variance (ANOVA) followed by a Bonferroni posttest. Differences were considered significant at the level of $P < 0.05$.

3. Results

3.1. PQR Significantly Decreased SBP. At the beginning of treatment, SBP was 126 ± 11 mmHg in the normal group and 208 ± 14 mmHg in the model and PQR groups ($P < 0.01$). However, a decrease in SBP was observed in the PQR group after 2 weeks of treatment ($P < 0.05$). After 4 weeks of treatment, the SBP of the PQR group was approximately 45 mmHg lower than at the beginning of treatment (Figure 1).

3.2. Morphology and Histology of Vascular Tissue Changes. Masson and HE staining showed that the aortic tunica media of the model group was thicker than that of normal group, and the aortic tunica media of PQR-treated rats was thinner

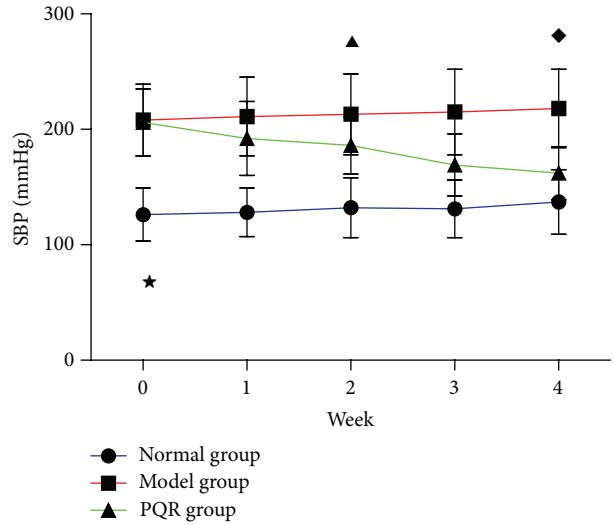

Figure 1: SBP changes in WKY rats or SHR receiving an i.a. of PQR or distilled water at various times. Data are shown as the mean ± SD for twenty rats of each group. P values for statistical significance were as $^{\star}P < 0.01$, compared with the model group; $^{\blacktriangle}P < 0.05$, and $^{\blacklozenge}P < 0.01$, compared with the PQR group, respectively.

Table 1: A260, A280, and A260/A280 ratios, and miRNA concentrations.

Group	A260	A280	Ratio of A260/A280	Concentration (μg/uL)
Normal group	0.57	0.28	1.96	0.183
Model group	1.06	0.51	2.08	0.295
PQR group	0.92	0.47	1.95	0.266

than that of control rats in the model group (Figures 2(a) and 2(b)). As shown in Figures 2(c) and 2(d), both MT and MT/LD were higher in the model group than in the normal group (MT: 126.7 ± 11.6 μm versus 84.3 ± 8.3 μm, resp., $P = 0.02$; MT/LD: 1.92 ± 0.19 versus 1.23 ± 0.21, resp., $P = 0.009$). However, both MT and MT/LD were significantly lower in the PQR group than in the model group (MT: 102.4 ± 9.4 μm versus 126.7 ± 11.6 μm, resp., $P = 0.04$; MT/LD: 1.45 ± 0.22 versus 1.92 ± 0.19, resp., $P = 0.03$).

3.3. Quality Assessment of Total RNA. We extracted total RNA from the aortic tissues of all rats. The purity of the total RNA was high, as indicated by the A260/A280 ratio being greater than 1.90. Quality assessment indicated that the total RNA met the quality requirement of the miRNA microarray analysis (Figure 3 and Table 1).

3.4. Aberrant Expression of miRNAs in SHR Aortic Tissue. To determine which miRNAs are potentially involved in the underlying mechanism of PQR treatment for essential hypertension, we tested miRNA levels in all rats by microarray analysis. We found that miRNA expression was remarkably aberrant in the model group compared with that of the normal group. In the model group, 32 of the 509 rat aortic

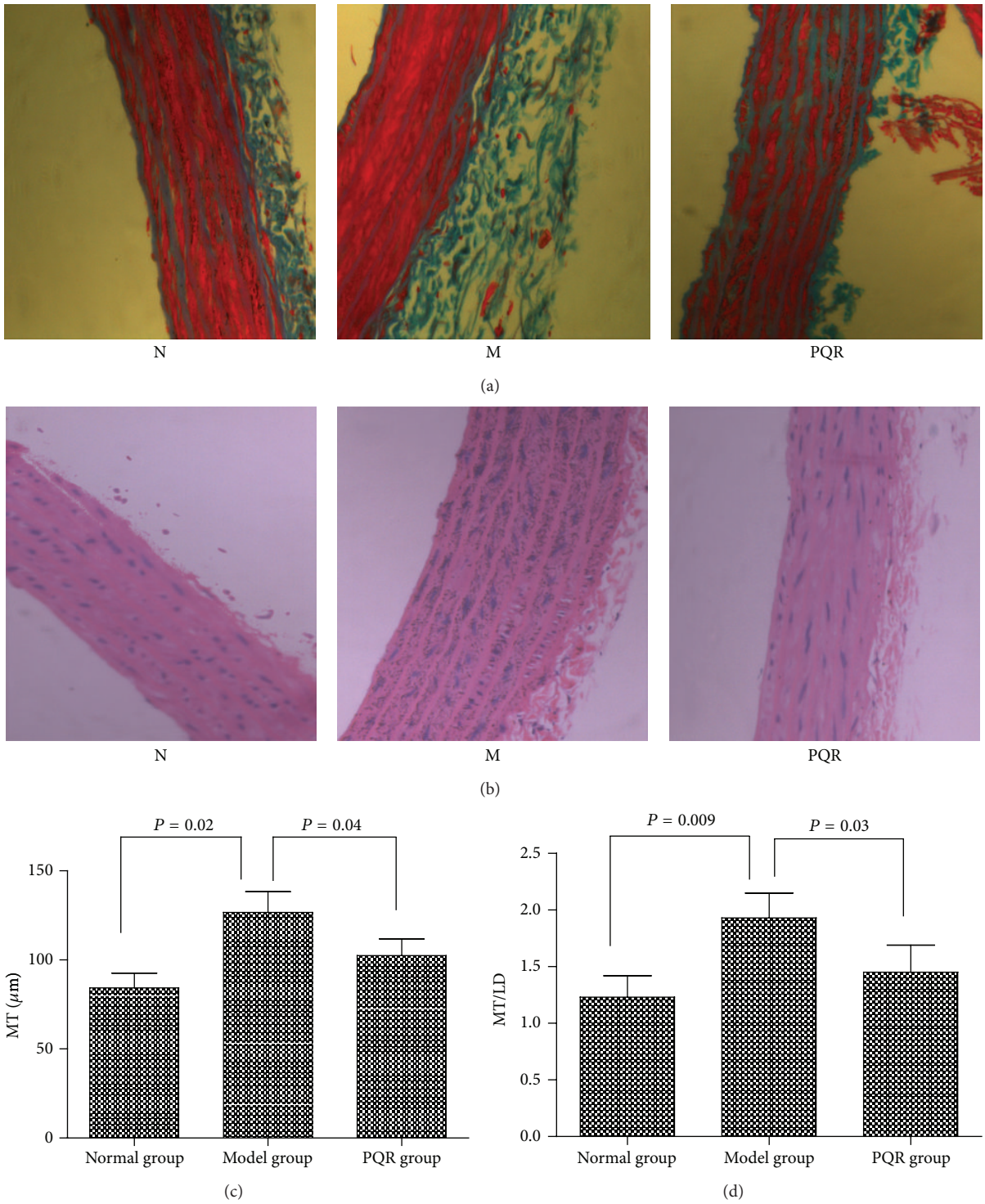

Figure 2: (a) Masson staining of vascular tissue in each group (400x magnification). (b) HE staining of vascular tissue in each group (400x magnification). (c) MT. (d) MT/LD. N: normal group; M: model group; PQR: PQR group. MT: medial thickness; LD: luminal diameter.

miRNAs analyzed were differentially expressed ($P < 0.01$), with 18 miRNAs upregulated and 14 miRNAs downregulated. After 4 weeks of PQR treatment, we found that 17 of the 32 aortic miRNAs were differentially expressed; seven were upregulated and 10 were downregulated. Significant time course changes of miRNA expression were observed in the aortic tissue; more than 46.8% miRNAs were dysregulated (down- or upregulated) after PQR treatment (Figure 2(a)). All differential expression levels of miRNAs at three time points are listed in Figure 4 and Table 2. These data indicate

Table 2: Significantly upregulated and downregulated miRNAs in three groups.

miRNA	Expression level			Model/normal	PQR/model
	Normal group	Model group	PQR group		
rno-miRNA-1	36.3	82.4	68.7	2.27	0.83
rno-miRNA-10a/b	8.5	21.2	11.8	2.49	0.56
rno-miRNA-17-5p	12.1	93.3	28.9	7.71	0.31
rno-miRNA-20a	32.7	621.6	121.5	19.01	0.19
rno-miRNA-96	43.2	753.7	211.3	17.45	0.29
rno-miRNA-126-5p	9.3	32.3	35.6	3.47	1.10
rno-miRNA-139	19.7	42.8	33.4	2.17	0.78
rno-miRNA-145	12.8	78.6	23.5	6.14	0.30
rno-miRNA-153	6.8	105.9	35.1	15.57	0.33
rno-miRNA-186a	35.5	213.6	178.8	6.52	0.84
rno-miRNA-187	26.4	136.6	33.4	5.17	0.24
rno-miRNA-196a/b	45.1	209.7	61.2	4.65	0.29
rno-miRNA-210	25.3	198.8	38.6	7.86	0.19
rno-miRNA-218	19.4	79.3	54.8	4.09	0.61
rno-miRNA-221	22.5	89.5	29.8	3.98	0.33
rno-miRNA-378	14.8	125.3	38.7	8.47	0.31
rno-miRNA-451	34.5	76.4	59.8	2.21	0.78
rno-miRNA-486	7.1	23.5	22.8	3.31	0.97
rno-miRNA-556	12.4	61.7	23.5	4.97	0.38
rno-miRNA-15b	164.3	23.8	28.9	0.14	1.21
rno-miRNA-26a/b	87.4	15.6	47.9	0.18	3.13
rno-miRNA-30	79.5	32.3	94.8	0.41	2.93
rno-miRNA-23a/b	23.5	6.8	5.7	0.29	0.84
rno-miRNA-29b	256.2	45.9	138.2	0.18	3.01
rno-miRNA-98	135.1	6.6	52.7	0.05	7.98
rno-miRNA-122	120.6	19.7	78.6	0.16	3.99
rno-miRNA-125b	378.6	113.4	178.2	0.29	1.57
rno-miRNA-142-3p	99.6	48.7	46.9	0.49	0.96
rno-miRNA-158	132.8	29.8	34.2	0.22	1.15
rno-miRNA-21	56.6	10.3	142.7	0.18	13.85
rno-miRNA-330	322.5	80.9	118.6	0.25	1.47
rno-let-7b/c	78.6	17.4	15.2	0.22	0.87

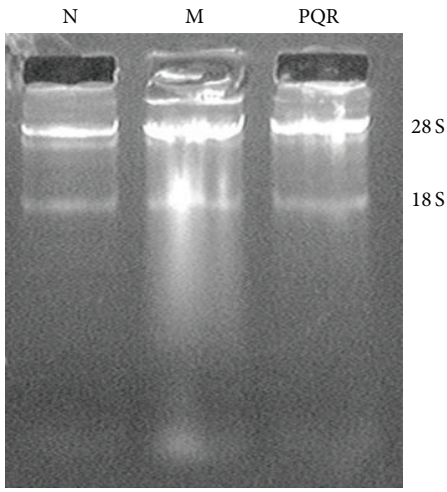

Figure 3: Electrophoresis of total RNA. N: normal group; M: model group; PQR: PQR group.

that the development of essential hypertension involves a wave of expression of sequential classes of miRNAs. The temporal regulation of these miRNAs indicates that they might play an important role in PQR treatment of essential hypertension.

3.5. Validation of miRNA Microarray Results Using qRT-PCR. qRT-PCR is a quantitative and specific method that can be used to distinguish a single nucleotide difference between miRNAs. Thus, involution was obtained by miChip analysis for four selected miRNAs that showed either high (*miR-145*) or low (*miR-30*) signal intensities, or high (*miR-20a*) or low (*miRNA-98*) differential expression values among the three groups. The results of qRT-PCR analysis were often more reliable than those of the microarray analysis. qRT-PCR showed that *miR-145* and *miR-20a* expression was downregulated in the model group compared with their expression in the PQR group, which was consistent with

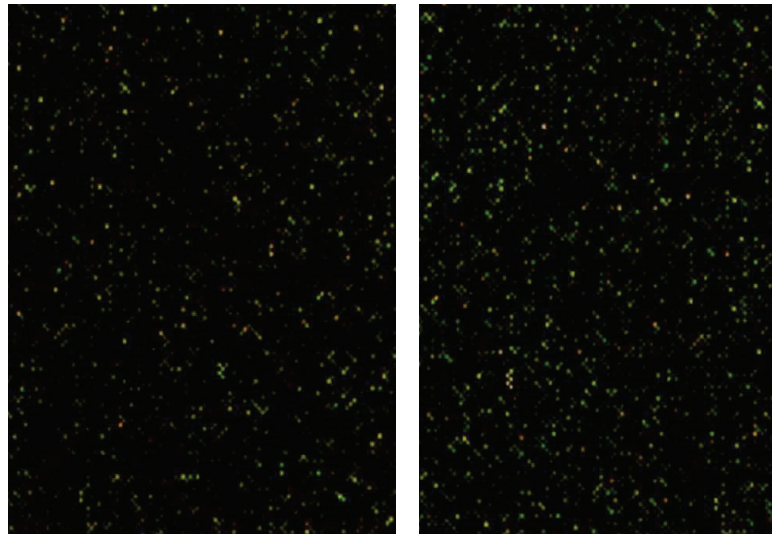

(a) (b)

Figure 4: Detection of miRNA by microarray analysis. Total RNA extracted from three groups of rat aortic tissue were covalently labeled with Cy3 (green) and Cy5 (red) and hybridized to the array. The microarray slides contained two replicate subarrays. (a) Normal group and model group; (b) model group and PQR group.

the microarray results. Thus, the miRNA expression profiles obtained by qRT-PCR fully support the results of miChip analysis (Figure 5).

3.6. Results of miR-20a Target Gene Prediction. We also performed a predicted target analysis for miRNA-20a, which was chosen because it was highly expressed in the model group and downregulated in the PQR group. Potential target genes were predicted using four software programs (miRanda, TargetScan, PicTar and DIANA-microT). To reduce false positive results, genes predicted by at least three of these four databases were selected as differentially expressed miRNA targets for subsequent analysis. Screening resulted in the selection of 38 target genes (Table 3). The target genes of miR-20a may be involved in the etiology of vascular remodeling through cell proliferation, apoptosis, migration, and differentiation.

4. Discussion

The observations reported here indicate that the underlying mechanism of PQR treatment for essential hypertension does not mediate vascular remodeling but strictly regulates miRNA expression. Our previous studies have shown that TCM (traditional Chinese medicine) treatment not only reduces high blood pressure in hypertension but also reverses both cardiac and vascular smooth muscle cell hypertrophy [18]. In the present study, we demonstrated that PQR treatment fully prevented the development of hypertension, as well as cardiac hypertrophy and aorta remodeling. It has been argued that excessive use of PQR in hypertension might interfere with some anatomical and/or functional parameters that are necessary to prevent blood pressure increase.

A range of evidence has demonstrated that miRNAs could be used as clinical biomarkers in essential hypertension [19]. The most robust multicenter study that provided such evidence was conducted in Ghent, Belgium, and focused on miRNA analysis of potential prognostic biomarkers in 500 neuroblastoma patients [20]. Although different technological platforms have been used for miRNA profiling, there is significant overlap between prognostic signatures described in previous work and several miRNAs that were later identified by more than three independent studies as being downregulated in essential hypertension or associated with vascular remodeling (e.g., miR-221, miR-26a, miR-21, miR-296-5p, and miR-204) [21–24].

In the present study, a microarray assay was applied to obtain miRNA expression profiles for thoracic aorta in three groups of SHR, and qRT-PCR was used to verify the microarray data. A total of 32 miRNAs in SHR (18 upregulated and 14 downregulated) and 17 miRNAs in the PQR treatment group (7 upregulated and 10 downregulated) were successfully identified. Furthermore, we also found differentially expressed miRNA-20a, with 38 potential target genes in rats, which demonstrated that miRNA expression might be significant in PQR treatment for rats with essential hypertension. In our studies, the most frequently observed and the most promising miRNAs as potential treatment targets are miR-145 [11] and miR-208 [25]. We found that miR-208 is upregulated in insulin-mediated proliferation of vascular smooth muscle cells and may promote a switch from the G0/G1 phase of the cell cycle to the S phase. The direct target of miR-208 has been shown to be p21 [25], and p21 expression in vascular smooth muscle cells has been shown to be crucial in limiting vascular proliferation in vascular remodeling, which is strongly associated with essential hypertension [26]. Interestingly, some studies [27–29]

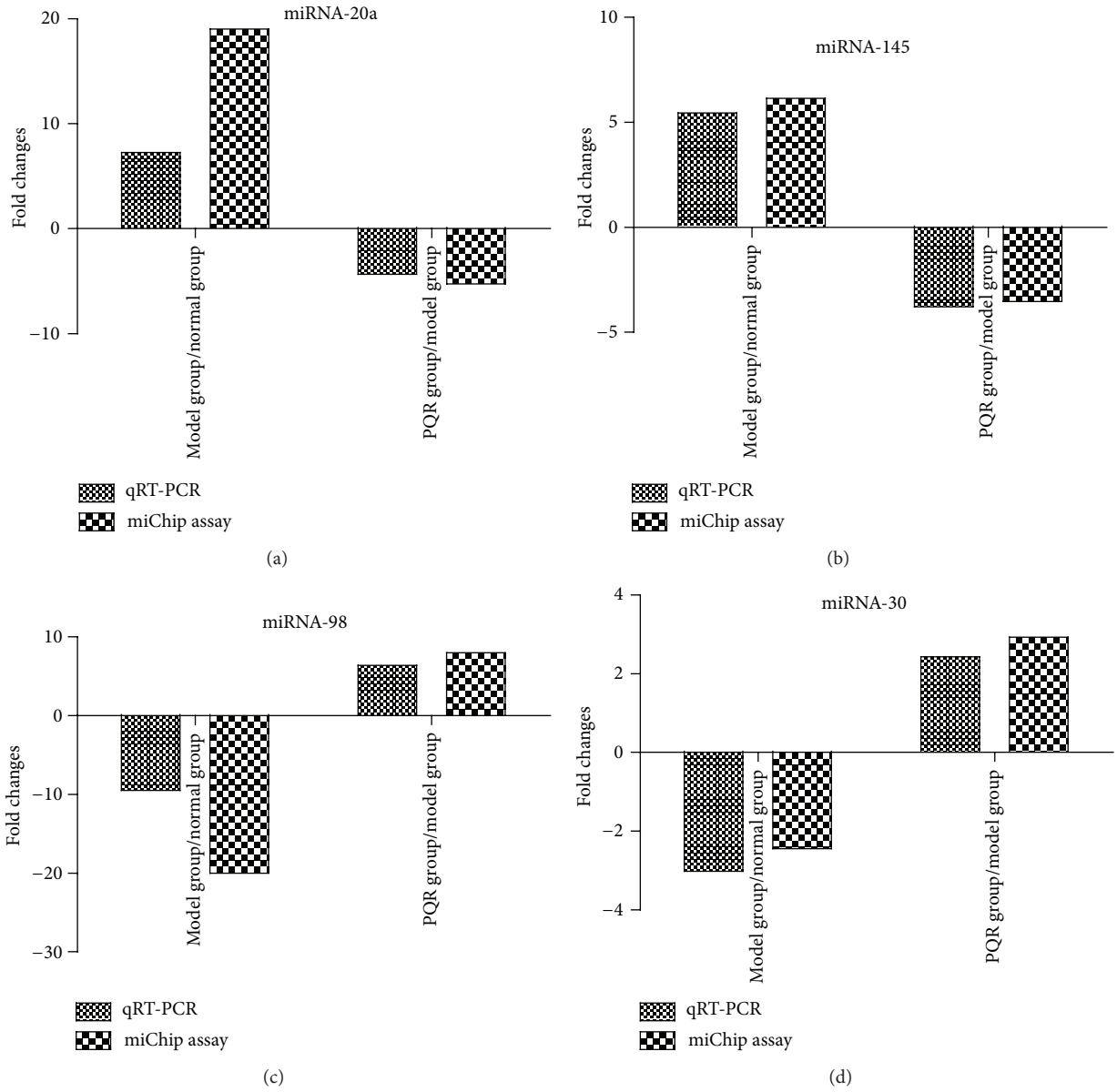

Figure 5: Validation of miRNA microarray data by qRT-PCR. (a) *miR-20a;* (b) *miR-145*; (c) *miRNA-98;* (d) *miR-30*. The relative expression of four miRNAs was normalized to the expression of the internal control gene (*U6*).

have shown that miR-143 and miR-145 play an important role in switching the phenotypes of smooth muscle cells during vascular remodeling. The function of these miRNAs is likely mediated by the degradation of many transcription factors, including KLF4, KLF5, Elk-1, and other transcription factors involved in Jagged-1/Notch signaling [30], which have been linked to the inhibition of differentiation of smooth muscle cells. MiR-20a, a member of the miR-17–92 cluster, is a highly conserved miRNA within a noncoding RNA encoded by the c13 or f25 host gene localized on chromosome 13 [31]. The functions of each cluster member in essential hypertension have not been clearly established. Recently, Pin et al. found that miR-20a can inhibit the expression of MKK3 and downregulate p38 pathway-mediated and VEGF-induced endothelial cell migration and angiogenesis [32]. miR-20a has also been shown to play an important role in vascular remodeling [33]. In contrast, several functionally well-characterized miRNAs that had previously been observed in other diseases were later identified in SHR for the first time with a high level of statistical significance, indicating their potential involvement in essential hypertension pathogenesis. These included miR-20a, miR-18b, miR-375, and miR-215 [34].

In conclusion, our study demonstrates that PQR has beneficial effects in reducing blood pressure and vascular remodeling in SHR. The underlying mechanism might be related to the modulation of 18 upregulated and 14 downregulated miRNAs, in particular, miR-20a, miR-145,

Table 3: Predicted target genes of miRNA-20a.

Target gene	Accession no.	Target gene name
ZNFX1	NM_021035	Zinc finger, NFX1-type containing 1
IL25	NM_022789	Interleukin 25
MAP3K2	NM_006609	Mitogen-activated protein kinase kinase kinase 2
AMPD3	NM_001025390	Adenosine monophosphate deaminase 3
GPR137C	NM_001099652	G protein-coupled receptor 137C
ACTBL2	NM_001017992	Actin, beta-like 2
MFAP3L	NM_001009554	Microfibrillar-associated protein 3-like
TRIP11	NM_004239	Thyroid hormone receptor interactor 11
DGUOK	NM_080918	Deoxyguanosine kinase
MFN2	NM_001127660	Mitofusin 2
VPS36	NM_004755	Vacuolar protein sorting 36 homolog
PLS1	NM_001145319	Plastin 1
ARHGAP12	NM_018287	Rho GTPase activating protein 12
FZD3	NM_017412	Fizzled family receptor3
PDK4	NM_002612	Pyruvate dehydrogenase kinase, isozyme 4
KIF23	NM_004856	Kinesin family member 23
VLDLR	NM_003383	Very low density lipoprotein receptor
FBXO4B	NM_001024680	F-box protein 4B
ZNF652	NM_014897	Zinc finger protein 652
RASD1	NM_016048	RAS, dexamethasone-induced 1
RS1	NM_000330	Retinoschisin 1
TNFRSF21	NM_014452	Tumor necrosis factor receptor superfamily, member 21
FGL1	NM_004467	Fibrinogen-like 1
CCND2	NM_001759	Cyclin D2
TMEM133	NM_032021	Transmembrane protein 133
LPGAT1	NM_014873	Lysophosphatidylglycerol acyltransferase 1
IPO7	NM_006391	Importin 7
GUCY1A3	NM_000856	Guanylate cycle 1, souble, alpha 3
TSPAN9	NM_001168320	Tetraspanin 9
KLF12	NM_007249	Kruppel-like factor 12
SMOC2	NM_001166412	SPARC related modular calcium binding 2
MAP3K3	NM_002401	Mitogen-activated protein kinase kinase kinase 3
NRP2	NM_018534	Neuropilin 2
SOCS6	NM_004232	Suppressor of cytokine signaling 6
SLC16A6	NM_001174166	Solute carrier family 16, member 6 (monocarboxylic acid transporter 7)
PRR14L	NM_173566	Proline rich 14-like
ANO6	NM_001025356	Anoctamin 6
ZBTB43	NM_001135776	Zinc finger and BTB domain containing 43

miR-30, and miR-98. We suggest that the target genes of miR-20a may be involved in the etiology of vascular remodeling through cell proliferation, apoptosis, migration, and differentiation. However, the underlying mechanisms should be further investigated through basic research and well-controlled clinical trials.

5. Conclusion

Taken together, our findings indicated that PQR could exert its antihypertensive effect through deterioration of the vascular remodeling process. The mechanism might be associated with regulating differentially expressed miRNAs in aorta tissue.

Conflict of Interests

The authors claim no conflict of interests involved in the study.

Acknowledgments

This work was supported by research grants from the National Natural Science Foundation of China (30506644

and 30407125) and Chinese Medicine and Pharmacy Planned Project of Hunan Province, P. R. China (2009047 and 201245). The authors thank Dr. Joen-Rong Sheu for critical reading of this paper.

References

[1] D. Lloyd-Jones, R. Adams, M. Carnethon et al., "Heart disease and stroke statistics—2009 update. A report from the American heart association statistics committee and stroke statistics subcommittee," *Circulation*, vol. 119, no. 3, pp. 480–486, 2009.

[2] F. H. Messerli, B. Williams, and E. Ritz, "Essential hypertension," *The Lancet*, vol. 370, no. 9587, pp. 591–603, 2007.

[3] Y.-J. Lv, G.-L. Liu, X.-M. Ji et al., "Qindan capsule changes adventitial collagen synthesis in spontaneously hypertensive rats," *Chinese Journal of Integrative Medicine*, vol. 19, no. 9, pp. 689–695, 2013.

[4] G.-W. Zhong, M.-J. Chen, Y.-H. Luo et al., "Effect of Chinese herbal medicine for calming Gan and suppressing hyperactive yang on arterial elasticity function and circadian rhythm of blood pressure in patients with essential hypertension," *Chinese Journal of Integrative Medicine*, vol. 17, no. 6, pp. 414–420, 2011.

[5] G. W. Zhong, Y. H. Luo, L. L. Xiang et al., "Clinical efficacy study on calming liver and restraining Yang formula in treating patients with mild or moderate degree of essential hypertension," *China Journal of Chinese Materia Medica*, vol. 16, no. 9, pp. 776–778, 2010.

[6] G. W. Zhong, W. Li, M. J. Chen et al., "Effeets on the vascular remodeling and adiponectin expression in aorta in the spontaneously hypertensive rats by Chinese herb mixture method," *Chinese Journal of Hypertension (China)*, vol. 16, no. 9, pp. 812–816, 2008.

[7] D. P. Bartel, "MicroRNAs: genomics, biogenesis, mechanism, and function," *Cell*, vol. 116, no. 2, pp. 281–297, 2004.

[8] H.-W. Hwang and J. T. Mendell, "MicroRNAs in cell proliferation, cell death, and tumorigenesis," *British Journal of Cancer*, vol. 94, no. 6, pp. 776–780, 2006.

[9] T. Kunej, I. Godnic, S. Horvat, M. Zorc, and G. A. Calin, "Cross talk between MicroRNA and coding cancer genes," *Cancer Journal*, vol. 18, no. 3, pp. 223–231, 2012.

[10] D. Catalucci, P. Gallo, and G. Condorelli, "Advances in molecular genetics, genomics, proteomics, metabolomics, and systems biology: microRNAs in cardiovascular biology and heart disease," *Circulation: Cardiovascular Genetics*, vol. 2, no. 4, pp. 402–408, 2009.

[11] K. R. Cordes, N. T. Sheehy, M. P. White et al., "MiR-145 and miR-143 regulate smooth muscle cell fate and plasticity," *Nature*, vol. 460, no. 7256, pp. 705–710, 2009.

[12] S. K. Gupta, C. Bang, and T. Thum, "Circulating MicroRNAs as biomarkers and potential paracrine mediators of cardiovascular disease," *Circulation: Cardiovascular Genetics*, vol. 3, no. 5, pp. 484–488, 2010.

[13] S. Li, J. Zhu, W. Zhang et al., "Signature microRNA expression profile of essential hypertension and its novel link to human cytomegalovirus infection," *Circulation*, vol. 124, no. 2, pp. 175–184, 2011.

[14] D. Torella, C. Iaconetti, D. Catalucci et al., "MicroRNA-133 controls vascular smooth muscle cell phenotypic switch in vitro and vascular remodeling in vivo," *Circulation Research*, vol. 109, no. 8, pp. 880–893, 2011.

[15] X.-P. Li, Y.-H. Luo, G.-W. Zhong, L.-L. Xiang, and Y.-H. Li, "Pharmacodynamic studies on formula for calming the liver and suppressing yang in treating spontaneous hypertension rats," *China Journal of Traditional Chinese Medicine and Pharmacy*, vol. 26, no. 4, pp. 710–715, 2011.

[16] E. L. Schiffrin, "Remodeling of resistance arteries in essential hypertension and effects of antihypertensive treatment," *American Journal of Hypertension*, vol. 17, no. 12, pp. 1192–1200, 2004.

[17] A. Krek, D. Grün, M. N. Poy et al., "Combinatorial microRNA target predictions," *Nature Genetics*, vol. 37, no. 5, pp. 495–500, 2005.

[18] G.-W. Zhong, W. Li, Y.-H. Luo et al., "Effects of the calming liver and suppressing yang method on proliferation and the expression of heat shock protein 27 in vascular smooth muscle cells of spontaneously hypertensive rats," *Chinese Journal of Gerontology*, vol. 29, no. 2, pp. 385–388, 2009.

[19] Y. D'Alessandra, P. Devanna, F. Limana et al., "Circulating microRNAs are new and sensitive biomarkers of myocardial infarction," *European Heart Journal*, vol. 31, no. 22, pp. 2765–2773, 2010.

[20] J. Bienertova-Vasku, P. Mazanek, R. Hezova et al., "Extension of microRNA expression pattern associated with high-risk neuroblastoma," *Tumor Biology*, vol. 34, no. 4, pp. 2315–2319, 2013.

[21] N. J. Leeper, A. Raiesdana, Y. Kojima et al., "MicroRNA-26a is a novel regulator of vascular smooth muscle cell function," *Journal of Cellular Physiology*, vol. 226, no. 4, pp. 1035–1043, 2011.

[22] H. Kang, B. N. Davis-Dusenbery, P. H. Nguyen et al., "Bone morphogenetic protein 4 promotes vascular smooth muscle contractility by activating microRNA-21 (miR-21), which down-regulates expression of family of dedicator of cytokinesis (DOCK) proteins," *The Journal of Biological Chemistry*, vol. 287, no. 6, pp. 3976–3986, 2012.

[23] X. Liu, Y. Cheng, J. Yang, L. Xu, and C. Zhang, "Cell-specific effects of miR-221/222 in vessels: molecular mechanism and therapeutic application," *Journal of Molecular and Cellular Cardiology*, vol. 52, no. 1, pp. 245–255, 2012.

[24] R.-R. Cui, S.-J. Li, L.-J. Liu et al., "MicroRNA-204 regulates vascular smooth muscle cell calcification *in vitro* and *in vivo*," *Cardiovascular Research*, vol. 96, no. 2, pp. 320–329, 2012.

[25] Y. Zhang, Y. Wang, X. Wang et al., "Insulin promotes vascular smooth muscle cell proliferation via microRNA-208-mediated downregulation of p21," *Journal of Hypertension*, vol. 29, no. 8, pp. 1560–1568, 2011.

[26] E. M. Jeon, H. C. Choi, K. Y. Lee, K. C. Chang, and Y. J. Kang, "Hemin inhibits hypertensive rat vascular smooth muscle cell proliferation through regulation of cyclin D and p21," *Archives of Pharmacal Research*, vol. 32, no. 3, pp. 375–382, 2009.

[27] B. N. Davis-Dusenbery, M. C. Chan, K. E. Reno et al., "Down-regulation of Krüppel-like Factor-4 (KLF4) by microRNA-143/145 is critical for modulation of vascular smooth muscle cell phenotype by transforming growth factor-β and bone morphogenetic protein 4," *The Journal of Biological Chemistry*, vol. 286, no. 32, pp. 28097–28110, 2011.

[28] M. Xin, E. M. Small, L. B. Sutherland et al., "MicroRNAs miR-143 and miR-145 modulate cytoskeletal dynamics and responsiveness of smooth muscle cells to injury," *Genes & Development*, vol. 23, no. 18, pp. 2166–2178, 2009.

[29] Y. Cheng, X. Liu, J. Yang et al., "MicroRNA-145, a novel smooth muscle cell phenotypic marker and modulator, controls

vascular neointimal lesion formation," *Circulation Research*, vol. 105, no. 2, pp. 158–166, 2009.

[30] J. M. Boucher, S. M. Peterson, S. Urs, C. Zhang, and L. Liaw, "The miR-143/145 cluster is a novel transcriptional target of Jagged-1/Notch signaling in vascular smooth muscle cells," *Journal of Biological Chemistry*, vol. 286, no. 32, pp. 28312–28321, 2011.

[31] C. Doebele, A. Bonauer, A. Fischer et al., "Members of the microRNA-17-92 cluster exhibit a cell-intrinsic antiangiogenic function in endothelial cells," *Blood*, vol. 115, no. 23, pp. 4944–4950, 2010.

[32] A.-L. Pin, F. Houle, M. Guillonneau, É. R. Paquet, M. J. Simard, and J. Huot, "miR-20a represses endothelial cell migration by targeting MKK3 and inhibiting p38 MAP kinase activation in response to VEGF," *Angiogenesis*, vol. 15, no. 4, pp. 593–608, 2012.

[33] D. Frank, J. Gantenberg, I. Boomgaarden et al., "MicroRNA-20a inhibits stress-induced cardiomyocyte apoptosis involving its novel target Egln3/PHD3," *Journal of Molecular and Cellular Cardiology*, vol. 52, no. 3, pp. 711–717, 2012.

[34] J. Song, D. Kim, C.-H. Chun, and E.-J. Jin, "MicroRNA-375, a new regulator of cadherin-7, suppresses the migration of chondrogenic progenitors," *Cellular Signalling*, vol. 25, no. 3, pp. 698–706, 2013.

Hindawi Publishing Corporation
Evidence-Based Complementary and Alternative Medicine
Volume 2015, Article ID 232789, 8 pages
http://dx.doi.org/10.1155/2015/232789

Research Article

Antrodia camphorata Potentiates Neuroprotection against Cerebral Ischemia in Rats via Downregulation of iNOS/HO-1/Bax and Activated Caspase-3 and Inhibition of Hydroxyl Radical Formation

Po-Sheng Yang,[1,2] Po-Yen Lin,[2,3] Chao-Chien Chang,[4] Meng-Che Yu,[5] Ting-Lin Yen,[5] Chang-Chou Lan,[6] Thanasekaran Jayakumar,[5] and Chih-Hao Yang[2]

[1]*Department of Surgery, Mackay Memorial Hospital and Mackay Medical College, Taipei, Taiwan*
[2]*Department of Pharmacology, School of Medicine, Taipei Medical University, Taipei, Taiwan*
[3]*Cardiovascular Division, Department of Surgery, Yuan's General Hospital, Kaohsiung, Taiwan*
[4]*Department of Cardiology, Cathay General Hospital, Taipei, Taiwan*
[5]*Graduate Institute of Medical Sciences, College of Medicine, Taipei Medical University, Taipei, Taiwan*
[6]*Sheen Chain Biotechnology, Co., Ltd., Taipei, Taiwan*

Correspondence should be addressed to Thanasekaran Jayakumar; tjaya_2002@yahoo.co.in
and Chih-Hao Yang; chyang@tmu.edu.tw

Received 28 August 2014; Accepted 20 October 2014

Academic Editor: Joen-Rong Sheu

Antrodia camphorata (*A. camphorata*) is a fungus generally used in Chinese folk medicine for treatment of viral hepatitis and cancer. Our previous study found *A. camphorata* has neuroprotective properties and could reduce stroke injury in cerebral ischemia animal models. In this study, we sought to investigate the molecular mechanisms of neuroprotective effects of *A. camphorata* in middle cerebral artery occlusion (MCAO) rats. A selective occlusion of the middle cerebral artery (MCA) with whole blood clots was used to induce ischemic stroke in rats and they were orally treated with *A. camphorata* (0.25 and 0.75 g/kg/day) alone or combined with aspirin (5 mg/kg/day). To provide insight into the functions of *A. camphorata* mediated neuroprotection, the expression of Bax, inducible nitric oxide synthase (iNOS), haem oxygenase-1 (HO-1), and activated caspase-3 was determined by Western blot assay. Treatment of aspirin alone significantly reduced the expressions of HO-1 ($P < 0.001$), iNOS ($P < 0.001$), and Bax ($P < 0.01$) in ischemic regions. The reduction of these expressions was more potentiated when rats treated by aspirin combined with *A. camphorata* (0.75 g/kg/day). Combination treatment also reduced apoptosis as measured by a significant reduction in active caspase-3 expression in the ischemic brain compared to MCAO group ($P < 0.01$). Moreover, treatment of *A. camphorata* significantly ($P < 0.05$) reduced fenton reaction-induced hydroxyl radical ($OH^{\bullet}$) formation at a dose of 40 mg/mL. Taken together, *A. camphorata* has shown neuroprotective effects in embolic rats, and the molecular mechanisms may correlate with the downregulation of Bax, iNOS, HO-1, and activated caspase-3 and the inhibition of $OH^{\bullet}$ signals.

1. Introduction

Stroke denotes to a rapid worldwide neurological impairment that victims may grieve paralysis and speech disorder, as well as loss of cognizance due to either ischemia or hemorrhage. It is considered as one of the leading causes of death and disability worldwide [1]. Currently, intravascular techniques and thrombolytic agents have remarkably decreased functional deficits. Although there are good improvements established in treatment, there is still little that can be done to prevent stroke-related brain damage. Therefore, active prevention and control of stroke are of great clinical value. Aspirin is the most widely used drug for the prevention of secondary stroke. However, the incidence of cerebral haemorrhage and other

bleeding events are major issues, while recurrent stroke is controlled by this treatment [2]. Thus, research has been focused on finding alternative drugs that may act on different pathways that have been used to recover them from the group of inflammation, necrosis, and apoptosis, all of which are associated in ischemic stroke [3]. Natural products are a prolific source of bioactive agents of different structure and varying biological activities. In the search for neuroprotective agents from natural sources, a number of plant extracts and several natural products isolated from them have been reported to provide neuroprotection against ischemic stroke [4].

Antrodia camphorata is being used as the complementary and alternative medicines, and it grows only on the inner heartwood wall of the endangered species *Cinnamomum kanehirai* Hay (Lauraceae) [5–7]. *A. camphorata* has long been used in Taiwanese folk medicine for abdominal pain, chemical intoxication, diarrhea, hypertension, itchy skin, and hepatoma [8]. Studies have demonstrated that *A. camphorata* induces significant apoptosis of human promyelocytic leukemia (HL-60) cells [9] and its extracts may be used as an adjuvant antitumor agent for human hepatoma cells, which are resistant to most other antitumor agents. Our previous study had shown that *A. camphorata* possesses antioxidant effects against carbon tetrachloride- (CCl_4-) induced hepatic injury *in vivo*, via mediating free radical scavenging activities [10]. *A. camphorata* also has shown to reduce H_2O_2-induced lipid peroxidation and enhance hepatic glutathione-dependent enzymes upon protecting CCl_4-induced damage on rat liver [11]. Despite the fact that our very recent study has demonstrated that *A. camphorata* has neuroprotective effect against ischemic stroke in rats through reducing infarct volume and improves neurobehavioral scores and regulating blood perfusion without increasing hemorrhagic transformation [12], the molecular mechanism of action of *A. camphorata* in this effect is remained obscured. Thus, in this study, we investigated the effects and possible mechanisms of action of *A. camphorata* on ischemic stroke in rats.

2. Materials and Methods

2.1. Plant Material. Well Shine Biotechnology Development Co., Pvt. Ltd., Taipei, Taiwan, provided the extracts of *A. camphorata* for this study.

2.2. Animals. Male Wistar rats (250–300 g) were used to determine the effects of *A. camphorata* alone or in combination with aspirin against MCAO induced brain damage. Animal care and the general protocols for animal use were approved by the Institutional Animal Care and Use Committee (IACUC) of Taipei Medical University. All animals were clinically normal, free of apparent infection or inflammation, and showed no neurological deficits while they were checked before undergoing the experimental procedures.

2.3. MCAO-Induced Ischemia. As demonstrated in our previous studies, an autologous blood clot was administered in rats for MCAO-induced ischemia [13–15]. In brief, 0.6 mL of arterial blood was withdrawn from a femoral catheter by using 1-mL syringe and the blood was immediately injected into PE-10 tubes. The tubes were kept at 4°C for 22 h, and the thread-like clots were removed and placed in a saline-filled dish. The clots were then washed to remove blood cells. Washed clots were transferred to fresh dishes, and the washing process was continued until the saline remained clear. The cleared clot sections were cut into 30 mm long fragments and then drawn up with the saline solution into a PE-10 catheter.

At the time of surgical procedure, animals were anesthetized with a mixture of 75% air and 25% O_2 gases containing 3% isoflurane. The common carotid artery (CCA) was identified, and approximately 1 cm of the external carotid artery (ECA) was ligated and cut. Consequently, the pterygopalatine artery (PA) was clamped with a 10 mm microaneurysm clamp, and the CCA was similarly clamped before the carotid bifurcation. The internal carotid artery (ICA) was then clamped between the carotid bifurcation and the PA. After that, the PE-50 catheter containing the clot was introduced approximately 5 mm into the previously cut ECA and tied in place with sutures. The ICA clamp was removed, and the clot was flushed into the ICA over a period of approximately 5 s. The PA clamp was removed, and the rat was left in this condition for 1 h.

2.4. Experimental Procedure. Rats were randomly separated into six groups at 1 hr after MCA occlusion: (1) a sham-operated group; (2) a group orally treated with an isovolumetric solvent (distilled water) for 60 days, followed by thromboembolic occlusion; (3) and (4) groups orally treated with *A. camphorata* (0.25 and 0.75 g/kg/day) alone for 60 days, followed by thromboembolic occlusion, respectively; (5) and (6) groups treated with *A. camphorata* (0.25 and 0.75 g/kg/day) and aspirin (5 mg/kg/day), followed by thromboembolic occlusion, respectively. An observer blinded to the identity of the groups assessed the neurological deficits after reperfusion by forelimb akinesia test.

2.5. Immunoblotting Assay. Expressions of HO-1, iNOS, Bax, and active caspase-3 in the ischemic brain at 24 h after thromboembolic occlusion-reperfusion injury were analyzed by immunoblotting as described by our previous study [14]. Thromboembolic occlusion-insulted and sham-operated rats were anesthetized with chloral hydrate (400 mg/kg, i.p.), and then the apex of the heart was penetrated with a profusion cannula inserted through the left ventricle into the ascending aorta. Perfusion with ice-cold PBS was performed, and an incision was made in the right atrium for venous drainage. Brains were freshly removed and sectioned coronally into four sequential parts from the frontal lobe to the occipital lobe. The third of four parts of the right hemisphere was separately collected, snap-frozen in liquid nitrogen, and stored at −70°C. The frozen tissues were placed in homogenate buffer and homogenized and then sonicated for 10 s three times at 4°C. The sonicated samples were subjected to centrifugation (10,000 ×g).

The supernatant (50 μg protein) was subjected to sodium dodecylsulfate polyacrylamide gel electrophoresis (SDS-PAGE) and electrophoretically transferred to polyvinylidenedifluoride (PVDF) membranes (0.45 μm, Hybond-P, Amersham). After incubation in blocking buffer and being washed three times with TBST buffer (10 mMTris-base, 100 mMNaCl, and 0.1% Tween 20; pH 7.5), blots were treated with an anti-HO-1 polyclonal antibody (pAb, 1 : 1000; R&D, Minneapolis, MN), an anti-iNOS monoclonal antibody (mAb; 1 : 3000, BD Biosciences, San Jose, CA), an anti-BaxpAb (1 : 1000; Cell Signaling, Beverly, MA), and an anti-active caspase-3 pAb (1 : 250; Biovision, Mountain View, CA), or an anti-α-tubulin mAb (1 : 2000; Santa Cruz Biotechnology, Santa Cruz, CA) in TBST buffer overnight. Blots were subsequently washed with TBST and incubated with a secondary horseradish peroxidase- (HRP-) conjugated goat anti-mouse mAb or donkey anti-rabbit immunoglobulin G (IgG)(Amersham) for 1 h. Blots were then washed, and the immunoreactive protein was detected using film exposed to enhanced chemiluminescence (ECL) detection reagents (ECL$^+$ system; Amersham). The bar graph depicts the ratios of semiquantitative results obtained by scanning reactive bands and quantifying the optical density using video densitometry (Bio-1D vers. 99 image software).

2.6. Measurement of Hydroxyl Radical ($HO^\bullet$) Formation by Electron Spin Resonance (ESR) Spectrometry. The ESR method used a Bruker EMX ESR spectrometer (Billerica, MA, USA) as described previously [16]. In brief, a Fenton reaction solution (50 μM $FeSO_4$ + 2 mM H_2O_2) was pretreated with a solvent control (0.1% DMSO) or *A. camphorata* (20 and 40 mg/mL) for 10 min. The rate of hydroxyl radical-scavenging activity was defined by the following equation: inhibition rate = 1 − [signal height (*A. camphorata*)/signal height (solvent control)].

2.7. Data Analysis. Experimental results are expressed as the mean ± S.E.M. and are accompanied by the number of observations. The experiments were assessed by the method of analysis of variance (ANOVA). If this analysis indicated significant differences among the group means, then each group was compared using the Newman-Keuls method. A P value of <0.05 was considered statistically significant.

3. Results

3.1. A. camphorata Inhibits iNOS and HO-1 Expression in Thromboembolic Cerebral Tissues. To examine the effect of *A. camphorata* in the ischemic brain, we measured the expression of iNOS and HO-1 in thromboembolic occlusion-insulted cerebral tissues. As shown in Figure 1, iNOS was more evidenced in tissues of thromboembolic occlusion-reperfusion injury than the level obtained in the corresponding area of the sham-operated group. Treatment of *A. camphorata* and aspirin alone at a respective doses of 0.75 g/kg and 5 mg/kg significantly ($P < 0.001$) diminished iNOS expression compared to the MCAO-untreated rats. Moreover, a combined treatment of *A. camphorata* with aspirin apparently potentiated *A. camphorata* mediated suppression of iNOS expression.

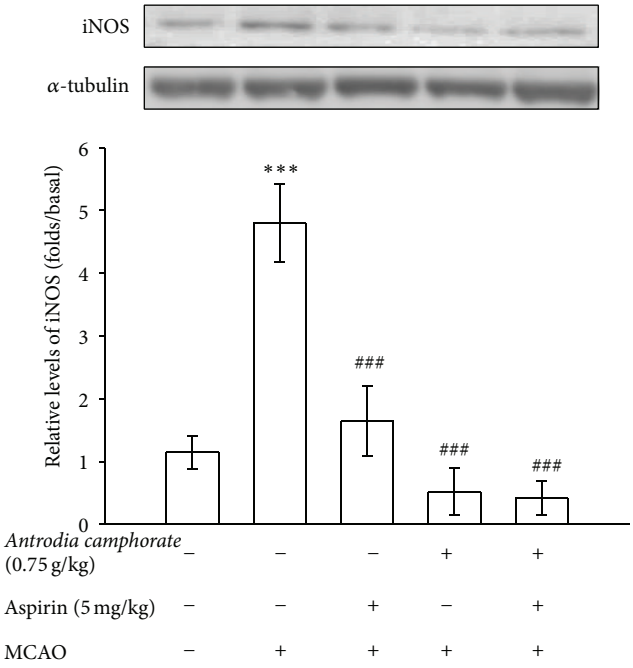

Figure 1: Effects of the extracts of *A. camphorata* combined with aspirin on the expressions of iNOS in cerebral homogenates 24 h after thromboembolic stroke in rats. Fresh brains from each group rats were removed and sectioned coronally into four sequential parts of the frontal lobe to the occipital lobe. The third of four sequential parts of the ischemic-injured hemisphere was separately collected, homogenized, and centrifuged. The supernatant (50 μg protein) was then subjected to SDS-PAGE and transferred onto membranes for analysis of iNOS expressions. Data are presented as the mean ± S.E.M. $^{***}P < 0.001$, compared to the sham-operated group, and $^{###}P < 0.001$, compared to the MCAO group.

A study has revealed that HO-1 is a key player for drugs upon neuroprotection in transient MCAO model [17]. In this study, Western blot was done to investigate whether *A. camphorata* affects the level of HO-1 expression. The results showed that *A. camphorata* and aspirin alone significantly ($P < 0.001$) reduced the expression of HO-1 protein in brain tissues of MCAO-induced rats (Figure 2). However, this protein expression was not changed when *A. camphorata* was treated with aspirin, since HO-1 expression seemed quite similar as appeared in their individual treatment.

3.2. A. camphorata Reduces Aspirin-Mediated Suppression of Bax-1 and Active Caspase-3 Expressions in Thromboembolic Cerebral Tissues. Bax is the proapoptotic member and caspase-3 is the most abundant cysteine protease in the brain and is acutely cleaved and activated in neurons in the early stages of reperfusion, leading to cell apoptosis. In this study, the expression levels of these apoptotic proteins, which are considered as the most important determining factors for the fate of cell and tissues in response to apoptotic stimulations were determined. We found a significant increase in the

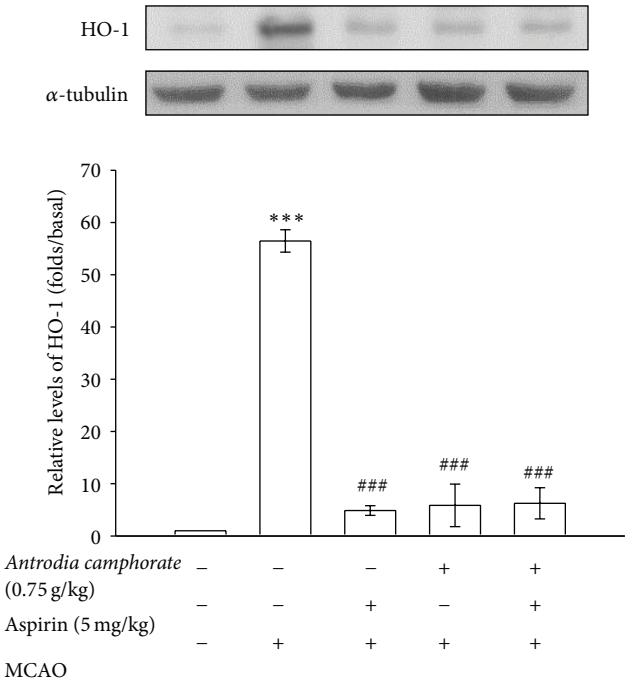

Figure 2: Effects of the extracts of *A. camphorata* combined with aspirin on the expressions of HO-1 in cerebral homogenates 24 h after thromboembolic stroke in rats. Data are presented as the mean ± S.E.M. $^{***}P < 0.001$, compared to the sham-operated group, and $^{\#\#\#}P < 0.001$, compared to the MCAO group.

expressions of Bax ($P < 0.01$) and active caspase-3 ($P < 0.01$) in the injured hemisphere of the MCAO rats as compared to the level obtained in the corresponding area of the sham-operated group (Figures 3(a) and 3(b)). Despite the fact that the individual treatment of aspirin suppresses both the expressions of Bax and activated caspase-3 proteins, the rate of inhibition was potentiated when the treatment was combined with *A. camphorata*.

3.3. A. camphorata Reduces In Vitro OH• Formation. To determine the efficacy of *A. camphorata* upon inhibiting fenton reaction-induced OH• formation *in vitro*, a cell-permeative ROS-sensitive dye, DCFDA (nonfluorescent in a reduced state but fluorescent upon oxidation by ROS) was used [16]. In this study, we found that OH• was produced during the fenton reaction very obviously. Interestingly, treatment with *A. camphorata* (40 mg/mL) markedly inhibited the fenton reaction induced OH• (Figure 4); however no effects were observed when *A. camphorata* is treated at a concentration of 20 mg/mL.

4. Discussion

Our recent study has demonstrated that *A. camphorata* shows neuroprotective effect against ischemic insults in MCAO model through a mechanism of blood perfusion regulation without increasing hemorrhagic transformation. This treatment also reduced infarct volume in the focal ischemic brain injury and improves neurological outcomes. In this study, we investigated the possible molecular mechanisms of *A. camphorata* on the observed neuroprotective effect. The results were found that an extract of *A. camphorata* possesses neuroprotective effect via antiapoptotic and anti-inflammatory effects and reduces OH radical formation in rat thromboembolic stroke.

Recently, researchers have been attracted to notice the hypothesis that secondary brain damages from hemoglobin as well as its byproducts such as ferrous iron released after heme degradation [18]. Heme or hemin released from hemoglobin accumulates in intracerebral hemorrhage (ICH) [19] and the increased hemin induces HO-1, the rate-limiting enzyme in the oxidative degradation of free heme [20]. High levels of heme metabolites such as ferrous iron resulted in neuronal cell death. Although HO-1 serves a cytoprotective function [21], reports of protective effects of HO-1 inhibitors in experimental ICH models support the idea that HO-1 is a mediator of neurotoxicity in ICH [22, 23] and an attractive therapeutic target for ICH.

In this study, we found that *A. camphorata* exerted neuroprotective effects by reducing the MCAO-induced expression of HO-1. As reported by Chen et al. [24], the induction of HO-1 has been correlated with an experimental model of MCAO and HO-1 knockout mice are reported to be protected from brain injury and functional impairment by ICH [25]. Our results showed that reduced expression of HO-1 by *A. camphorata* protects the MCAO-induced ischemic brain injury. Several reports proposed that a decrease of HO-1 expression by HO-1 inhibitor may provide a protective effect against stroke in various animal models [26, 27]. Recently, Huang et al. reported that treatment of vitamin C offers neuroprotection via reducing HO-1 activity in methamphetamine-induced neurotoxicity in neuronal cells [28]. Combined with the current data, these reports suggest that modulation of HO-1 might have a potential as a new therapy for stroke.

A study demonstrated that iNOS knock-out mice showing reduced brain damage after ischemia, because of an increased expression of iNOS, may also contribute to enhanced neuronal injury [29] and there is an evidence that iNOS plays a role as a mediator in the reduction of infarct size via late preconditioning [30]. A recent study also suggests that iNOS may be involved in the inflammatory reaction that follows cerebral ischemia and iNOS mRNA and enzymatic activity are expressed in brain after permanent MCA occlusion [31]. Treatment with the selective iNOS inhibitor was reported to be reduced infarct volume, suggesting that iNOS activity contributes to ischemic brain damage [32]. A study reported that bioactive constituents of mycelium of *A. camphorata*, antroquinonol B, 4-acetyl-antroquinonol B, 2,3-(methylenedioxy)-6-methylbenzene-1,4-diol, and 2,4-dimethoxy-6-methylbenzene-1,3-diol along with antrodin D inhibit iNOS activity in lipopolysaccharide- (LPS-) activated murine macrophages [33]. In the present study, we demonstrated that treatment of *A. camphorata* in MCAO-induced embolic rats significantly reduced the expression of iNOS, is harmful to the postischemic brain, and may be of worth in the treatment of cerebral ischemia.

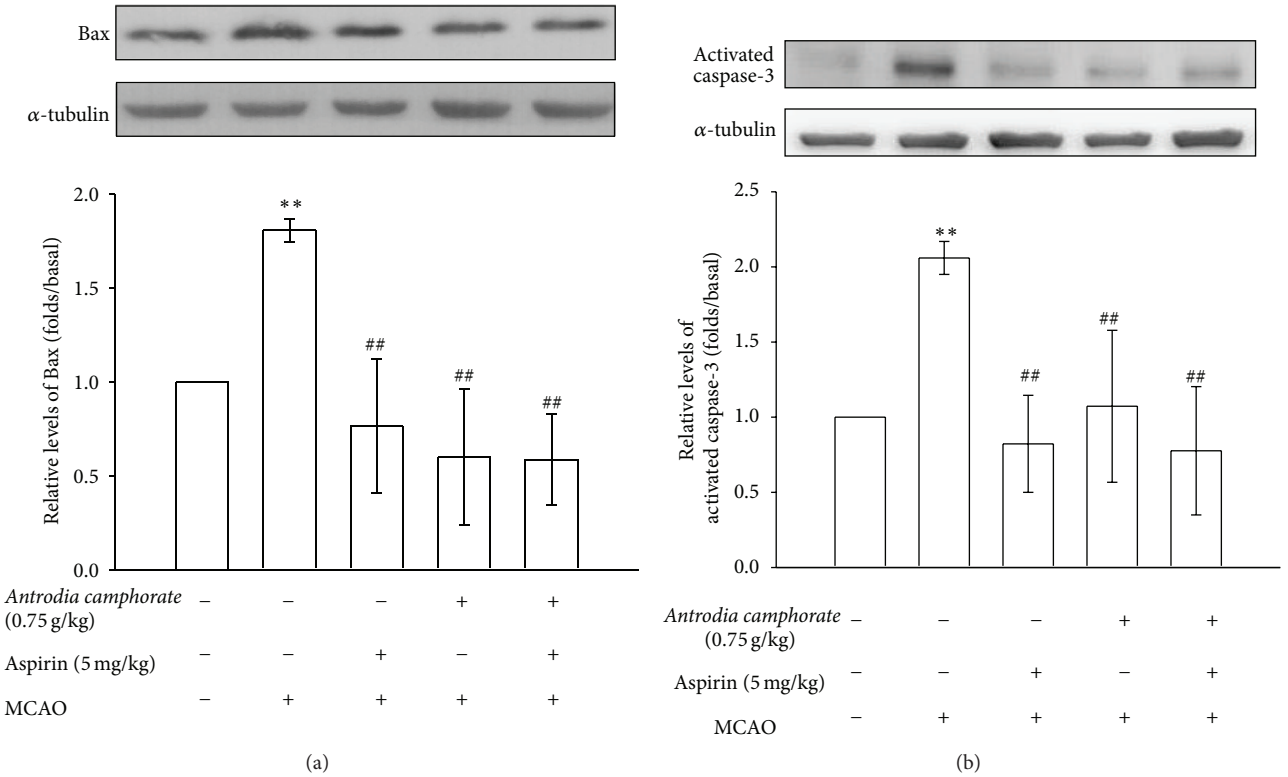

Figure 3: Effects of the extracts of *A. camphorata* combined with aspirin on the expressions of (a) Bax and (b) caspase-3 in cerebral homogenates 24 h after thromboembolic stroke in rats. Data are presented as the mean ± S.E.M. $^{**}P < 0.01$, compared to the sham-operated group, and $^{\#\#}P < 0.01$, compared to the MCAO group.

Apoptosis is also known as programmed cell death, which is an initiative suicide process after the cells receive a signal or stimulation with some other related gene. The Bcl-2 family proteins are key regulators of apoptosis, which include both antiapoptotic members such as Bcl-2 and the proapoptotic members such as Bax. It has been suggested that a slight change in the dynamic balance of Bcl2/Bax proteins may result either in inhibition or promotion of cell death [34]. Apoptosis has been reported to occur after transient cerebral ischemia and is regulated by the pro- and antiapoptotic proteins and it contributes to ischemic cell damage after stroke [35]. Caspase-3 is an essential protein for brain development, but it also serves as a crucial mediator of neuronal apoptosis [36]. During ischemia, caspase-3 is cleaved and activated whereupon it degrades multiple substrates in the cytoplasm and nucleus leading to cell death [37]. Caspase-3 deficient adult mice reported to be more resistant to ischemic stress both *in vivo* and *in vitro* [37]. Therefore, it is of great interest to control the activation of Bax and caspase-3 for the potential therapeutic treatment of neurological diseases. Several studies have demonstrated that treatment of caspase-3 inhibitors reduced ischemic-induced brain damage [38]. A recent study has suggested that inhibition of Bcl2/Bax ratio may be a novel target for the treatment of stroke [39], and these authors have shown that chemokine-like factor 1 (CKLF1), a novel C-C chemokine, with antibodies displays neuroprotective effects against cerebral ischemia via regulation of apoptosis-related protein expression in ischemic hemisphere. In the present study, it has been shown that *A. camphorata* has neuroprotective effects in MCAO-induced rats via inhibiting Bax and caspase-3 expressions.

Oxidative stress involves the formation of reactive oxygen/nitrogen species (ROS/RNS), which are causal factors in the neuropathology of stroke [40]. Abundant ROS are generated during an acute ischemic stroke through multiple injury mechanisms, such as mitochondrial inhibition, Ca_2+ overload and reperfusion injury [41]. Brain ischemia generates super oxide radical ($O_2^{\bullet}$), from which H_2O_2 is formed. H_2O_2 is the source of hydroxyl radical ($OH^{\bullet}$). An *in vivo* study has revealed that a dry matter of fermented filtrate (DMF) from *A. camphorata* in submerged culture shows antioxidant like effects against H_2O_2-induced cytotoxicity in HepG2 and carbon tetrachloride- (CCl_4-) induced hepatotoxicity [11]. They showed that DMF may play a role in preventing oxidative damage in living systems by upregulating hepatic glutathione-dependent enzymes to preserve the normal reduced and oxidized glutathione (GSH/GSSH) ratio and scavenging free radicals formed during CCl_4 metabolism.

A previous study was reported that polysaccharides extracted from fruiting bodies or cultured mycelia of *A. camphorata* exhibit an antihepatitis B virus effect [42]. In that study, the authors have specified that extracts from cultured mycelia of *A. camphorata* inhibit N-formyl-methionyl-leucyl-phenylalanine (fMLP) or phorbol 12-myristate 13-acetate- (PMA-) induced ROS production in peripheral human neutrophils (PMN) or mononuclear cells (MNC).

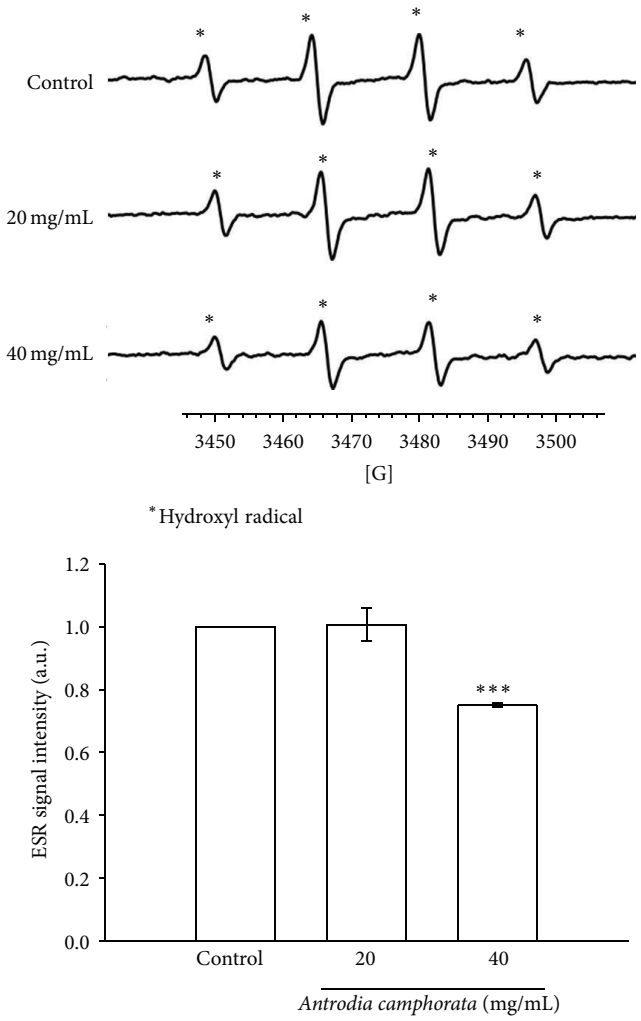

FIGURE 4: Effects of the extracts of *A. camphorata* on hydroxyl radical formation. ESR spectra show the effects of *A. camphorata* at 40 mg/mL and significantly inhibit hydroxyl radical formation in the fenton reaction. Data are presented as the mean ± S.E.M. $^{***}P < 0.001$, compared to the control group.

$OH^{\bullet}$ can be produced from O_2 under a variety of stress conditions and are involved in numerous cellular disorders such as inflammations, embryo teratogenesis, herbicide effects, cell death, and killing of microorganisms in pathogen-defense reactions. It is generally assumed that $OH^{\bullet}$ is generated in biological systems from H_2O_2 by the Fenton reaction [43, 44]. Therefore, in the present study, we used fenton reaction to evaluate the hydroxyl radical-scavenging activity of *A. camphorata* by the ESR experiment. We found that *A. camphorata* significantly inhibits $OH^{\bullet}$ formation at a higher concentration of 40 mg/mL. These results proposed that neuroprotection by *A. camphorata* may be involved, at least partly, in the inhibition of free radical formation.

In conclusion, our recent study was demonstrated that *A. camphorata* provides neuroprotection against MCAO-induced ischemic stroke via improved neurological functional scores and reduced infarct volume without causing hemorrhagic incidence when it is used in conjunction with aspirin therapy; nevertheless, the mechanisms underlying remained intricate. Therefore, we performed this study and found that the neuroprotective effect of *A. camphorata* is possibly via enhanced inhibition of HO-1, followed by the inhibition of inflammatory responses (i.e., iNOS) and apoptosis (Bax and activated caspase-3) in the ischemic brain. In addition, neuroprotection by *A. camphorata* may be involved, at least partly, by the inhibition of free radical formation.

Conflict of Interests

The authors declare that they have no conflict of interests to disclose.

Authors' Contribution

Po-Sheng Yang and Po-Yen Lin contributed equally to this work.

Acknowledgment

This work was supported by Grants from the National Science Council of Taiwan (NSC97-2320-B-038-016-MY3 and NSC100-2320-B-038-021-MY3) and Yuan's General Hospital-Taipei Medical University (103-YGH-TMU-01-3).

References

[1] A. Towfighi and J. L. Saver, "Stroke declines from third to fourth leading cause of death in the United States: historical perspective and challenges ahead," *Stroke*, vol. 42, no. 8, pp. 2351–2355, 2011.

[2] W. Hacke, M. Kaste, E. Bluhmki et al., "Thrombolysis with alteplase 3 to 4.5 hours after acute ischemic stroke," *The New England Journal of Medicine*, vol. 359, no. 13, pp. 1317–1329, 2008.

[3] P. H. Chan, "Reactive oxygen radicals in signaling and damage in the ischemic brain," *Journal of Cerebral Blood Flow & Metabolism*, vol. 21, no. 1, pp. 2–14, 2001.

[4] Z. A. Malik, M. Singh, and P. L. Sharma, "Neuroprotective effect of Momordica charantia in global cerebral ischemia and reperfusion induced neuronal damage in diabetic mice," *Journal of Ethnopharmacology*, vol. 133, no. 2, pp. 729–734, 2011.

[5] T. Y. Song, S. L. Hsu, C. T. Yeh, and G. C. Yen, "Mycelia from Antrodia camphorata in submerged culture induce apoptosis of human hepatoma HepG2 cells possibly through regulation of fas pathway," *Journal of Agricultural and Food Chemistry*, vol. 53, no. 14, pp. 5559–5564, 2005.

[6] Y. L. Hsu, Y. C. Kuo, P. L. Kuo, L. T. Ng, Y. H. Kuo, and C. C. Lin, "Apoptotic effects of extract from *Antrodia camphorata* fruiting bodies in human hepatocellular carcinoma cell lines," *Cancer Letters*, vol. 221, no. 1, pp. 77–89, 2005.

[7] P. C. Cheng, C. Y. Hsu, C. C. Chen, and K. M. Lee, "In vivo immunomodulatory effects of *Antrodia camphorata* polysaccharides in a T1/T2 doubly transgenic mouse model for inhibiting infection of *Schistosoma mansoni*," *Toxicology and Applied Pharmacology*, vol. 227, no. 2, pp. 291–298, 2008.

[8] H. Nakano, S. Ikenaga, T. Aizu et al., "Human metallothionein gene expression is upregulated by β-thujaplicin: possible

involvement of protein kinase C and reactive oxygen species," *Biological & Pharmaceutical Bulletin*, vol. 29, no. 1, pp. 55–59, 2006.

[9] Y.-C. Hseu, H.-L. Yang, Y.-C. Lai, J.-G. Lin, G.-W. Chen, and Y.-H. Chang, "Induction of apoptosis by *Antrodia camphorata* in human premyelocytic leukemia HL-60 cells," *Nutrition and Cancer*, vol. 48, no. 2, pp. 189–197, 2004.

[10] G. Hsiao, M.-Y. Shen, K.-H. Lin et al., "Antioxidative and hepatoprotective effects of *Antrodia camphorata* extract," *Journal of Agricultural and Food Chemistry*, vol. 51, no. 11, pp. 3302–3308, 2003.

[11] T. Y. Song and G. C. Yen, "Protective effects of fermented filtrate from *Antrodia camphorata* in submerged culture against CCl_4-induced hepatic toxicity in rats," *Journal of Agricultural and Food Chemistry*, vol. 51, no. 6, pp. 1571–1577, 2003.

[12] Y. M. Lee, C. Y. Chang, T. L. Yen et al., "Extract of *Antrodia camphorata* exerts neuroprotection against embolic stroke in rats without causing the risk of hemorrhagic incidence," *The Scientific World Journal*, vol. 2014, Article ID 686109, 8 pages, 2014.

[13] G. Hsiao, K. H. Lin, Y. Chang et al., "Protective mechanisms of inosine in platelet activation and cerebral ischemic damage," *Arteriosclerosis, Thrombosis, and Vascular Biology*, vol. 25, no. 9, pp. 1998–2004, 2005.

[14] T. Jayakumar, W.-H. Hsu, T.-L. Yen et al., "Hinokitiol, a natural tropolone derivative, offers neuroprotection from thromboembolic stroke *in vivo*," *Evidence-based Complementary and Alternative Medicine*, vol. 2013, Article ID 840487, 8 pages, 2013.

[15] J. J. Lee, W. H. Hsu, T. L. Yen et al., "Traditional Chinese medicine, Xue-Fu-Zhu-Yu decoction, potentiates tissue plasminogen activator against thromboembolic stroke in rats," *Journal of Ethnopharmacology*, vol. 134, no. 3, pp. 824–830, 2011.

[16] D.-S. Chou, G. Hsiao, M.-Y. Shen, Y.-J. Tsai, T.-F. Chen, and J.-R. Sheu, "ESR spin trapping of a carbon-centered free radical from agonist-stimulated human platelets," *Free Radical Biology and Medicine*, vol. 39, no. 2, pp. 237–248, 2005.

[17] S. Saleem, H. Zhuang, S. Biswal, Y. Christen, and S. Doré, "Ginkgo biloba extract neuroprotective action is dependent on heme oxygenase 1 in ischemic reperfusion brain injury," *Stroke*, vol. 39, no. 12, pp. 3389–3396, 2008.

[18] F.-P. Huang, G. Xi, R. F. Keep, Y. Hua, A. Nemoianu, and J. T. Hoff, "Brain edema after experimental intracerebral hemorrhage: role of hemoglobin degradation products," *Journal of Neurosurgery*, vol. 96, no. 2, pp. 287–293, 2002.

[19] A. H. Koeppen, A. C. Dickson, and J. Smith, "Heme oxygenase in experimental intracerebral hemorrhage: the benefit of tin-mesoporphyrin," *Journal of Neuropathology & Experimental Neurology*, vol. 63, no. 6, pp. 587–597, 2004.

[20] N. G. Abraham and A. Kappas, "Pharmacological and clinical aspects of heme oxygenase," *Pharmacological Reviews*, vol. 60, no. 1, pp. 79–127, 2008.

[21] Z.-P. Teng, J. Chen, L.-Y. Chau, N. Galunic, and R. F. Regan, "Adenoviral transfer of the heme oxygenase-1 gene protects striatal astrocytes from heme-mediated oxidative injury," *Neurobiology of Disease*, vol. 17, no. 2, pp. 179–187, 2004.

[22] Y. Gong, H. Tian, G. Xi, R. F. Keep, J. T. Hoff, and Y. Hua, "Systemic zinc protoporphyrin administration reduces intracerebral hemorrhage-induced brain injury," *Acta Neurochirurgica, Supplementum*, vol. 96, pp. 232–236, 2006.

[23] K. R. Wagner, Y. Hua, G. M. de Courten-Myers et al., "Tin-mesoporphyrin, a potent heme oxygenase inhibitor, for treatment of intracerebral hemorrhage: in vivo and in vitro studies," *Cellular and Molecular Biology*, vol. 46, no. 3, pp. 597–608, 2000.

[24] P. S. Chen, C.-C. Wang, C. D. Bortner et al., "Valproic acid and other histone deacetylase inhibitors induce microglial apoptosis and attenuate lipopolysaccharide-induced dopaminergic neurotoxicity," *Neuroscience*, vol. 149, no. 1, pp. 203–212, 2007.

[25] J. Wang and S. Doré, "Heme oxygenase-1 exacerbates early brain injury after intracerebral haemorrhage," *Brain*, vol. 130, no. 6, pp. 1643–1652, 2007.

[26] K. Kawaguchi, F. Lambein, and K. Kusama-Eguchi, "Vascular insult accompanied by overexpressed heme oxygenase-1 as a pathophysiological mechanism in experimental neurolathyrism with hind-leg paraparesis," *Biochemical and Biophysical Research Communications*, vol. 428, no. 1, pp. 160–166, 2012.

[27] Y. Guo, Q. Wang, K. Zhang et al., "HO-1 induction in motor cortex and intestinal dysfunction in TDP-43 A315T transgenic mice," *Brain Research*, vol. 1460, pp. 88–95, 2012.

[28] Y.-N. Huang, J.-Y. Wang, C.-T. Lee, C.-H. Lin, and C.-C. Lai, "L-Ascorbate attenuates methamphetamine neurotoxicity through enhancing the induction of endogenous heme oxygenase-1," *Toxicology and Applied Pharmacology*, vol. 265, no. 2, pp. 241–252, 2012.

[29] C. Iadecola, F. Zhang, R. Casey, M. Nagayama, and M. Elizabeth Ross, "Delayed reduction of ischemic brain injury and neurological deficits in mice lacking the inducible nitric oxide synthase gene," *Journal of Neuroscience*, vol. 17, no. 23, pp. 9157–9164, 1997.

[30] J. Imagawa, D. M. Yellon, and G. F. Baxter, "Pharmacological evidence that inducible nitric oxide synthase is a mediator of delayed preconditioning," *British Journal of Pharmacology*, vol. 126, no. 3, pp. 701–708, 1999.

[31] C. Iadecola, X. Xu, F. Zhang, E. E. El-Fakahany, and M. E. Ross, "Marked induction of calcium-independent nitric oxide synthase activity after focal cerebral ischemia," *Journal of Cerebral Blood Flow and Metabolism*, vol. 15, no. 1, pp. 52–59, 1995.

[32] C. Iadecola, F. Zhang, and X. Xu, "Inhibition of inducible nitric oxide synthase ameliorates cerebral ischemic damage," *American Journal of Physiology—Regulatory Integrative and Comparative Physiology*, vol. 268, no. 1, pp. R286–R292, 1995.

[33] S.-S. Yang, G.-J. Wang, S.-Y. Wang, Y.-Y. Lin, Y.-H. Kuo, and T.-H. Lee, "New constituents with iNOS inhibitory activity from mycelium of *Antrodia camphorata*," *Planta Medica*, vol. 75, no. 5, pp. 512–516, 2009.

[34] M. S. Ola, M. Nawaz, and H. Ahsan, "Role of Bcl-2 family proteins and caspases in the regulation of apoptosis," *Molecular and Cellular Biochemistry*, vol. 351, no. 1-2, pp. 41–58, 2011.

[35] S. I. Savitz, J. A. Erhardt, J. V. Anthony et al., "The novel β-blocker, carvedilol, provides neuroprotection in transient focal stroke," *Journal of Cerebral Blood Flow and Metabolism*, vol. 20, no. 8, pp. 1197–1204, 2000.

[36] A. G. Porter and R. U. Jänicke, "Emerging roles of caspase-3 in apoptosis," *Cell Death & Differentiation*, vol. 6, no. 2, pp. 99–104, 1999.

[37] D. A. Le, Y. Wu, Z. Huang et al., "Caspase activation and neuroprotection in caspase-3-deficient mice after in vivo cerebral ischemia and in vitro oxygen glucose deprivation," *Proceedings of the National Academy of Sciences of the United States of America*, vol. 99, no. 23, pp. 15188–15193, 2002.

[38] M. Sun and C. Xu, "Neuroprotective mechanism of taurine due to up-regulating calpastatin and down-regulating calpain

and caspase-3 during focal cerebral ischemia," *Cellular and Molecular Neurobiology*, vol. 28, no. 4, pp. 593–611, 2008.

[39] L. L. Kong, Z. Y. Wang, J. Hu et al., "Inhibition of chemokine-like factor 1 protects against focal cerebral ischemia through the promotion of energy metabolism and anti-apoptotic effect," *Neurochemistry International*, vol. 76, pp. 91–98, 2014.

[40] J. T. Coyle and P. Puttfarcken, "Oxidative stress, glutamate, and neurodegenerative disorders," *Science*, vol. 262, no. 5134, pp. 689–695, 1993.

[41] S. Cuzzocrea, D. P. Riley, A. P. Caputi, and D. Salvemini, "Antioxidant therapy: a new pharmacological approach in shock, inflammation, and ischemia/reperfusion injury," *Pharmacological Reviews*, vol. 53, no. 1, pp. 135–159, 2001.

[42] Y.-C. Shen, C.-J. Chou, Y.-H. Wang, C.-F. Chen, Y.-C. Chou, and M.-K. Lu, "Anti-inflammatory activity of the extracts from mycelia of *Antrodia camphorata* cultured with water-soluble fractions from five different *Cinnamomum* species," *FEMS Microbiology Letters*, vol. 231, no. 1, pp. 137–143, 2004.

[43] B. Halliwell and J. M. C. Gutteridge, "Biologically relevant metal ion-dependent hydroxyl radical generation. An update," *FEBS Letters*, vol. 307, no. 1, pp. 108–112, 1992.

[44] E. R. Stadtman, "Oxidation of free amino acids and amino acid residues in proteins by radiolysis and by metal-catalyzed reactions," *Annual Review of Biochemistry*, vol. 62, pp. 797–821, 1993.